GEOCHEMICAL ASSESSMENT AND RESOURCE POTENTIAL OF THE CRITICAL MINERALS IN SALT RANGE FORMATION, PUNJAB, PAKISTAN: AN INTEGRATED APPROACH USING AI AND ML FOR RENEWABLE ENERGY RESOURCES

ALI NAQI

09-262242-012

BAHRIA UNIVERSITY ISLAMABAD

GEOCHEMICAL ASSESSMENT AND RESOURCE POTENTIAL OF THE CRITICAL MINERALS IN SALT RANGE FORMATION, PUNJAB, PAKISTAN: AN INTEGRATED APPROACH USING AI AND ML FOR RENEWABLE ENERGY RESOURCES

A thesis is submitted in fulfillment of the requirement for the award of the degree of Master of Science (Geology)

ALI NAQI
09-262242-012

Department of Earth and Environmental Sciences

BAHRIA UNIVERSITY ISLAMABAD

JULY 2026

Bahria University

Department of Earth & Environmental Sciences
Islamabad Campus, Islamabad

Date: July 17, 2026

Certificate

A thesis submitted by **Mr. Ali Naqi** to the Department of Earth & Environmental Sciences, Bahria University, Islamabad in partial fulfillment of the requirements for the degree of **Master of Science in Geology** (Session **2024-2026**).

Committee Member	Name	Signature
Supervisor	Dr. Mumtaz Ali Khan	
Internal Examiner	Dr. Adeeb Ahmed	
External Examiner	Dr. Asghar Ali	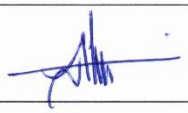
Post Graduate Coordinator	Dr. Muhammad Raiees Amjad	
Head of Department (E&ES)	Dr. Syed Umair Ullah Jamil	

APPROVAL OF EXAMINATION

Scholar's Name: "Ali Naqi" Registration No: "72004"

Program of Study: MS Geology

Thesis Title: "GEOCHEMICAL ASSESSMENT AND RESOURCE POTENTIAL OF THE CRITICAL MINERALS IN SALT RANGE FORMATION, PUNJAB, PAKISTAN: AN INTEGRATED APPROACH USING AI AND ML FOR RENEWABLE ENERGY RESOURCES"

It is to certify that the above scholar's thesis has been completed to my satisfaction and to my belief, its standard is appropriate for submission for examination. I have also conducted plagiarism test of this thesis using HEC prescribed software and found similarity index 2% that is within the permissible limit set by the HEC for the MS degree thesis. I have also found the thesis in a format recognized by the BU for the MS thesis.

NOTE: The Plagiarism report is attached at the end of thesis.

Principal Supervisor's
Signature:

Date:

Name: Dr. Mumtaz Ali Khan

AUTHOR'S DECLERATION

I, "Mr. Ali Naqi" is hereby state that my MS thesis titled "GEOCHEMICAL ASSESSMENT AND RESOURCE POTENTIAL OF THE CRITICAL MINERALS IN SALT RANGE FORMATION, PUNJAB, PAKISTAN: AN INTEGRATED APPROACH USING AI AND ML FOR RENEWABLE ENERGY RESOURCES" is my own work and has not been submitted previously by me of taking any degree from this university "Bahria University Islamabad Campus" or anywhere else in the country/world.

At any time if my statement is found to be incorrect even after my graduation, the University has the right to withdraw/cancel my MS degree.

Scholar Name: Ali Naqi

Sign: _____

Date:

PLAGIARISM UNDERTAKING

I solemnly declare that research work presented in the thesis titled "GEOCHEMICAL ASSESSMENT AND RESOURCE POTENTIAL OF THE CRITICAL MINERALS IN SALT RANGE FORMATION, PUNJAB, PAKISTAN: AN INTEGRATED APPROACH USING AI AND ML FOR RENEWABLE ENERGY RESOURCES" is solely my research work with no significant contribution from any other person. Small contribution/help wherever taken has been duly acknowledged and that complete thesis has been written by me.

I understand the zero-tolerance policy of HEC and Bahria University towards plagiarism. Therefore, I as an Author of the above titled thesis declared that no portion of my thesis has been plagiarized, and any material used as reference is properly referred/ cited.

I understand that if, I am found guilty of any formal plagiarism in the above titled thesis even after award of MS degree, the university reserves the right to withdraw, revoke my MS degree and that HEC and the University has the right to publish my name on the HEC/University website on which names of the scholars are placed who submitted plagiarized thesis.

Scholar/Author's

Sign: _____

Name of the Scholar: Ali Naqi

DEDICATION

Dedicated to my Father Mr. Muhammad Kazim

ACKNOWLEDGEMENT

All praise is due to Almighty Allah, the Most Gracious and the Most Merciful, whose countless blessings and guidance enabled me to successfully complete this research work. I would like to express my deepest gratitude to my supervisor Dr. Mumtaz Ali Khan Associate Professor, Earth and Environmental Sciences, Bahria University H11 Campus, for their invaluable guidance, continuous support, and insightful suggestions throughout the course of this study. Their encouragement and constructive feedback played a crucial role in shaping this thesis and enhancing my understanding of the subject. I am also sincerely thankful to Mr. Ishtiaq Noor, for providing a strong foundation and for their assistance during my postgraduate studies. Their knowledge and mentorship have greatly contributed to my academic and professional growth. Special thanks to Allama Iqbal open university for providing facilitations for sample analysis and guidance.

Above all, I express my heartfelt gratitude to my parents and family for their unconditional love, prayers, and unwavering support throughout my academic journey. Their encouragement has always been a source of strength and inspiration. Finally, I acknowledge all those who directly or indirectly contributed to the completion of this thesis.

ABSTRACT

The increasing demand for critical minerals required in renewable-energy technologies has encouraged the reassessment of underexplored sedimentary and evaporitic successions. This study evaluates the reconnaissance-level critical-element potential of the Salt Range Formation, Punjab, Pakistan, with emphasis on lithium and associated strategic elements in the Billianwala Salt, Sahwal Marl, and Bandarkas Gypsum members. A total of 23 representative samples were collected from salt, marl, and gypsum lithologies and analyzed through Inductively Coupled Plasma Mass Spectrometry (ICP-MS). The results are interpreted as aqua-regia-extractable geochemical concentrations where aqua regia digestion was used, rather than total-rock abundances, because this method mainly dissolves soluble salts, carbonates, sulfides, oxides, organic matter, clay-bound fractions, and weakly adsorbed phases, but may not completely dissolve resistant silicate minerals. The geochemical dataset was assessed through lithology-wise comparison, correlation analysis, principal component analysis, K-Means clustering, Isolation Forest anomaly detection, and integrated exploration-priority ranking. The results show that critical-element enrichment is not uniformly distributed across the evaporitic succession. Instead, enrichment is mainly controlled by lithology. Marl samples show the strongest relative enrichment in lithium, boron, rare earth elements, uranium, vanadium, and zinc, whereas rock salt and gypsum display more selective evaporite-related signatures, particularly for strontium, barium, and potassium. The highest aqua-regia-extractable lithium value is recorded in Marl-7, followed by other marl-dominated samples, indicating localized enrichment within fine-grained reactive facies rather than broad enrichment throughout the formation. The AI/ML component was used as an exploratory decision-support tool, not as definitive proof of mineralization. Because the dataset is limited and lacks independent mineralization labels, supervised model accuracy is not emphasized. Instead, multivariate and anomaly-detection methods are used to recognize geochemical patterns and identify priority samples for follow-up work. The results do not establish an economically viable critical-mineral deposit. Future work should include denser sampling, total digestion, XRD, SEM-EDS, petrography, and mineral-host validation to assess the true resource significance of the identified anomalies.

TABLE OF CONTENT

DEDICATION **IV**

ACKNOWLEDGEMENT **V**

ABSTRACT **VI**

CHAPTER 1 **1**

1 Introduction **1**

1.1 General Statement 1

1.2 Problem Statement 7

1.3 Aims and Objectives 8

1.4 Significance of Research 8

1.5 Literature Review 9

CHAPTER 2 **16**

2 Geology and Tectonics **16**

2.1 Regional Geological Settings 16

2.1.1 Structural Framework 17

2.2 Tectonic Setting and Its Influence on Mineral Deposition 18

2.3 Tectonic Evolution 19

2.3.1 Passive Margin Development and Neo-Tethyan Opening 19

2.3.2 Subduction and Arc Development 19

2.3.3 Neogene–Recent Deformation 20

2.3.4 Sedimentological Features 20

2.4 Stratigraphy of Salt Range 21

2.4.1 Precambrian Basement 21

2.4.2 Stratigraphic context of the Salt Range 22

2.4.3 Salt Range Formation (Pre-Cambrian) 23

2.4.4 Depositional environment and basin evolution 25

2.4.5 Structural role of the Salt Range Formation 26

2.4.6 Regional Stratigraphic Synthesis 27

CHAPTER 3 **30**

3 Methodology **30**

3.1 Field Sampling Strategy and Sample Collection 30

3.2 Laboratory Sample Preparation 33

3.2.1 Drying, Crushing and Pulverization 33

3.2.2 Acid Digestion Procedures 34

3.3 Inductively Coupled Plasma Mass-Spectrometry 38

CHAPTER 4 **42**

4 Results and Interpretation **42**

4.1 Introduction 42

4.2 General Character of the Analytical Dataset 43

4.3 Lithology-Wise Geochemical Distribution 45

4.3.1 Marl 45

4.3.2 Rock Salt 46

4.3.3 Gypsum 47

4.4 Critical Minerals 49

4.4.1 Lithium (Li) 49

4.4.2 Copper (Cu) 50

4.4.3 Nickel (Ni) and Cobalt (Co) 51

4.4.4 Zinc (Zn) 52

4.4.5 Vanadium (V) and Uranium (U) 53

4.4.6 Antimony (Sb), Niobium (Nb), Tantalum (Ta), Tungsten (W), and Other Critical Element 54

4.5 Rare Earth Elements (REEs) and Yttrium 54

4.6 Economically Important Minerals and Industrial Elements 56

4.6.1 Halite and Sodium (Na) 56

4.6.2 Potash and Potassium (K) 57

4.6.3 Gypsum and Sulfate Components 57

4.6.4 Boron (B) 58

4.6.5 Strontium (Sr) 58

4.6.6 Barium (Ba) 59

4.6.7 Magnesium (Mg) 59

4.6.8 Phosphorus (P), Iron (Fe), Manganese (Mn), Silicon (Si), Aluminum (Al), and Titanium (Ti) 60

4.7 Element Associations and Geochemical Controls 61

4.8 Interpretation of Enrichment Mechanisms 62

4.9 Resource implications and economic viability 64

4.10 Summary of Chapter 66

CHAPTER 5 67

5 AI & ML BASED PREDICTIVE MINERAL PROSPECTIVITY MODELING OF THE SALT RANGE FORMATION 67

5.1 Introduction 67

5.2 Data Pre-Processing and Feature Engineering 68

5.2.1 Treatment of Censored Values 68

5.2.2 Feature Selection and Normalization 69

5.3 Unsupervised geochemical pattern recognition 70

5.3.1 Model Architecture and Training 71

5.3.2 Prospectivity Scores and Spatial Distribution 71

5.3.3 Feature Importance Analysis 74

5.4 Composite Evidence Index 75

5.4.1 Cluster Number Determination 76

5.4.2 Geochemical Cluster Characterization 77

5.5 CEI-based target ranking 78

5.5.1 Variance Structure 79

5.5.2 Interpretation of Principal Components 80

5.5.3 Lithological Discrimination 81

5.6 Model limitations and uncertainty 81

5.7 Chapter Conclusions 82

CHAPTER 6 **84**

6 DISCUSSIONS **84**

6.1 Discussions 84

Conclusions **90**

RECOMMENDATIONS **91**

7 REFERENCES **92**

LIST OF FIGURES

Figure 1.1: Location map of Salt Range (Ghazi et al., 2014) 7
Figure 2.1: Generalized geological map of the Salt Range, northern Pakistan, illustrating the regional position of the study area along the southern margin of the Potwar Basin. The map shows the distribution of Precambrian, Palaeozoic–Mesozoic, Palaeocene, and Neogene rock units, together with the trace of the Salt Range Thrust (SRT), which marks the major structural boundary of the range. Key towns, localities, and drainage systems, including the Indus and Jhelum rivers, are shown for geographic reference. The study area lies in the eastern Salt Range near Ara, Tatral, and Khewra, where well-exposed stratigraphic sections and thrust-related deformation provide important evidence for interpreting the geological evolution of the region. An inset map shows the location of the Salt Range within Pakistan and its broader regional context 17
Figure 2.3: Structural cross-section of the Salt Range showing the Salt Range Formation as an evaporitic décollement and its relationship with the Salt Range Thrust. Redrawn/adapted after Ghani et al. (2021). 28
Figure 2.4: Generalized Stratigraphic Column of Salt Range (Ghazi et al., 2015) 29
Figure 3.1: Sample Collection Map 30
Figure 3.2: Sample Collected from Bandarkas Gypsum for Geochemical analysis 32
Figure 3.3: Sample collection from Salt Range Formation (Sahwal Marl Member) for geochemical analysis. 33
Figure 3.4: Sample Digestion Process 36
Figure 3.5: Sample Filtration Process 37
Figure 3.6: Digested Samples 37
Figure 3.7: Schematic Diagram of ICP-MS (Kashani & Mostaghimi, 2010) 41
Figure 4.1: Lithology-Element Enrichment Heatmap 45
Figure 4.2: Geochemical Profile for Sahwal Marl Member 46
Figure 4.3: Geochemical Profile for Billianwala Salt Member 47
Figure 4.4: Geochemical Profile for Bandarkas Gypsum 48
Figure 4.5: Critical Minerals Concentrations 49
Figure 4.6: Lithium Enrichment in Samples 50
Figure 4.7: Copper Abundance across sample 51
Figure 4.8: Abundance of V and Ni across the samples 52

Figure 4.9: Abundance of Zinc across the samples 52
Figure 4.10: Abundance of V and U across samples 53
Figure 4.11: Critical Minerals Variation across Samples 54
Figure 4.12: REE Variations in collected Samples 55
Figure 4.13: Industrial Mineral Variance Spider Diagram 56
Figure 4.14: Strontium Variation in three members of Salt Range Formation 59
Figure 4.15: Comparison of Al, Fe and Rb across different lithologies 60
Figure 4.16: Element Associations and Geochemical Controls 62
Figure 4.17: Enrichment Mechanism, three phase interpretive Model 64
Figure 4.18: Potential Critical minerals vs Industrial mineral 66
Figure 5.1: RF, Mineral Prospectivity Scores Salt Range Formation n=23 70
Figure 5.2: Prospectivity Scores 74
Figure 5.3: Features Analysis 75
Figure 5.4: PCA factor loadings for PC1 and PC2 in the Salt Range dataset 80
Figure 5.5: PCA biplot for PC1 and PC2 explaining 64.3% of the total variance 80

LIST OF TABLES

Table 4.1: Critical Mineral Results, whereas BDL shows the Below Detection Limit, ADL shows the Above Detection Limit, Li is Lithium, B is for Boron, K is Potassium, Sr is Strontium, Cu is Copper, Zn is Zinc, Ni is Nickel, Co is for Cobalt, V is for Vanadium, U is showing the uranium and REE is representing the Rare Earth Element. 44
Table 5.1: RF, Mineral Prospectivity Scores Salt Range Formation n=23 72
Table 5.2: Components used in the Composite Evidence Index 76
Table 5.3: Summary geochemical statistics for K-Means clusters (Cluster A, B, and C) geometric means of key critical mineral elements (ppm) 78
Table 5.4: CEI-based exploration-priority ranking 79

CHAPTER 1

Introduction

1.1 General Statement

The dynamic shift in the world system to the low-carbon energy system has provided a fundamental redefinition of the strategic value of mineral resource in the twenty first century. Greater interest in the accelerated use of renewable energy and grid infrastructure, electrification of transport, grid-scale storage, and the digital energy management systems have increased the need to focus on a set of mineral commodities that are currently defined as critical minerals (International Energy Agency, 2024). Such minerals are the basis of the technological infrastructure of decarbonization, and are co-elements of lithium-ion batteries, wind turbines, photovoltaic systems, high-efficiency motors, transmission networks, and hydrogen technologies. According to the International Energy Agency (IEA, 2024), the mineral intensity, which is used per unit of energy-generating clean technologies, is much greater than the standard fossil-fuel systems, therefore increasing the overall resource demand trajectories.

Critical minerals refer to mineral commodities that are non-fuel but that are critical to economic and national security as well as highly vulnerable to disruption of supplies because of geological concentrations and geopolitical and technological bottlenecks or limitations on processing (USGS, 2022). The title is not evidence of crustal profuseness, but the sophisticated system of geologic availability, extractability, processing ability, trade requirements, environmental limits and socio-political solidarity (USGS, 2022). The notion of criticality is thus dynamic by nature, and it changes with technological advancements, shifting to new market conditions, and changing geopolitical dynamics. Strategic minerals are now taking a leading role in the focus of strategic discussion because of the intensification of energy transition policies (IEA, 2024; Müller, 2025).

Specifically, lithium has become an essential component of energy storage systems in the world because it has electrochemical property, low atomic mass, and a large energy density in rechargeable batteries (Munk et al., 2016). Nevertheless, the geographical location of many of these mineral's supply is still geographically concentrated, and production is concentrated around a few jurisdictions to produce structural supply weaknesses (IEA, 2024). Also, the weakened ore grades, limited mine life and depletion of traditionally fruitful resources add to the worries over the sustainability of resources in the long-term perspective (Müller, 2025). All these trends bring about the need to reevaluate less explored geological provinces and update mineral systems models that can help point at the new frontiers of resources.

In geological perspective, the changing need in the critical minerals demands a revisit to the sedimentary basins, which were historically studied with the involvement of the industrial minerals. One such frontier that has not been sufficiently well explored is represented by evaporite-dominated systems. Conventionally as the source of halite, gypsum, and potash, evaporitic basins have lately been identified as a dynamic geochemical reactor, which may concentrate several elements through progressive evaporation, hydrological isolation, and sustained water-rock contact (Munk et al., 2016). Geochemical enrichment of lithium, boron, strontium, bromine, magnesium, and potassium is possible in the geochemical evolution of brines in closed or semi-closed basins than are found in average crusts (Yu et al., 2022; Yu et al., 2024).

Such a creation of lithium-bearing brine regimes proves that the process of enrichment is dictated by a complicated interplay of source lithology, hydrothermal investment, climatic regime, basin hydrodynamics, redox state, and diagenetic modification (Munk et al., 2016). Prolonged evaporation in closed-basin environments in the continent causes more total dissolved solids to be produced, which can be divided into trace elements partitions into late evaporation brines. In good structural and hydrological circumstances, lithium can become economically viable and evaporite-hosted brines can become one of the main classes of lithium resources in the world (Munk et al., 2016; Economic Geology, 2025). These processes emphasize the fact that evaporate systems are not only passive accumulations of sediment but living geochemical concentration systems and mineralogical and fluid records of histories of multi-stage green enrichment.

The systematic multi-element geochemical evaluation of most evaporitic provinces has been limited despite this appreciation. Traditionally, geological studies have pointed at bulk industrial mineral description and significant ion chemistry as opposed to detailed trace element assemblages in terms of current critical mineral theories and methods (USGS, 2022). Such an analytical gap is especially important because trace element partitioning in evaporitic systems can be indicative of nuances in depositional controls, fluid-rock deformation processes, diagenetic redistribution processes, fluid migration processes induced by the tectonic effect. In this regard, evaporite basins should be conceptualized as consolidated mineral systems where stratigraphy, geochemistry, hydrology and structural development co-exist to control the potential of resources.

In this worldwide setting, the Salt Range located in the state of Punjab in Pakistan is a scientifically interesting and unexploited exception study. The Salt Range is the southernmost element that makes up the frontal portion of the Potwar Plateau foreland fold-and-thrust belt that is structurally supported by Infra-Cambrian evaporites which as a detachment horizon are mechanically weak (Lillie et al., 1987; Gee and Gee, 1989). These evaporites have provided a chance of massive thin-skinned tectonic deformation linked with Indo-Eurasian collision which has made it possible to translate regions and to segment with thrusts and implicate the structures (Gee and Gee, 1989; Qayyum et al., 2015). Due to this, the Salt Range, Potwar Plateau system forms one of the best-investigated foreland thrust belts in the region of South Asia.

The exposed evaporitic succession, stratigraphically, is a crystalline mass of halite overlaying the potash salts, gypsiferous marls and suitable classic interbeds and topped by younger cycles of sediment (Shah, 2009). Rare surface exposure of a large, continuous sequence of Precambrian evaporates on an actively overriding foreland is found in the tectonic exhumation of its own. This combination has never been observed before, and is stratigraphic completeness combined with structural modification to form a unique natural laboratory of interest to both primary depositional geochemistry studies and secondary studies of diagenetic alteration.

The past studies in the Salt Range largely focused on structural development, petroleum system, industrial salt mining, and potash mineralization (Lillie et al., 1987; Shah, 2009). This variability of anions and zoning of potassium in the sets of rock salts

regarding geochemistry have been recorded, which proves the complexity of evaporative processes and the changes in the salinity of the basin (Hussain et al., 2021). These results suggest dynamics in the evolution of brine in the process of deposition and initial diagenesis. However, multi-element trace analyses have not been extensively conducted with explicit reference to the paradigms of critical mineral exploration.

The scientific problem is to distinguish between the primary depositional signatures and the secondary redistribution of the depositional features caused by diagenetic processes and remobilization caused by tectonic forces. Element enrichment can occur in evaporitic systems due to progressive events of evaporation, compaction of burial, recrystallization, fluid–rock interaction or structural fluid migration pathways (Munk et al., 2016; Yu et al., 2022). Structural re-evocation can also induce additional gas circulation as well as element redistribution, especially where there exists fold and thrust. To unravel this set of controls, analytical models that can combine stratigraphic, geochemical and structural data into coherent models of mineral systems are necessary (Carranza, 2009).

Data-driven approaches have become increasingly important in modern mineral exploration because geological and geochemical datasets are commonly multivariate, non-linear, and spatially heterogeneous. Conventional univariate interpretation can identify individual anomalies, but it may fail to detect complex associations among elements, lithologies, and geological processes. Multivariate statistics and AI/ML methods provide a structured way to recognize hidden geochemical patterns, classify samples, detect anomalies, and rank exploration targets. In mineral prospectivity studies, such methods are most effective when they are used together with geological reasoning rather than as purely statistical outputs. Therefore, in reconnaissance-scale studies with limited sample numbers, AI/ML results should be interpreted as decision-support tools for target ranking and hypothesis generation, not as definitive proof of economic mineralization.

The increasing dimensionality of geoscientific data is also one more explanation why innovation is also needed. Univariate or linear statistical analysis tends not to be considered with a non-linear interaction between multivariate predictors where there may be a complex geological setting. New opportunities in Artificial Intelligence (AI) and

Machine Learning (ML) have demonstrated how the high-dimensional mineral exploration data modeling can be prospectively and probabilistically mapped and anomalies detected as well as quantify uncertainties (Zuo and Carranza, 2011; Cracknell and Reading, 2014). The recent ML models can form geochemical, mineralogical, structural and spatial predictors that reveal latent patterns which are not possible in the traditional simplistic methods.

Predominantly applicable to workflow scenarios with any geological constraints in their application, AI/ML solutions can service interpretative enriching of service and defensibility of science (Li et al., 2021; Sun et al., 2024). Explainable AI systems also ensure openness in the model prediction; this will lessen the fear associated with prediction by the black-box models. They can have a particularly beneficial role in evaporitic landscapes, which have multi-staged geochemistry and geology, and where they have been overprinted structurally. They may also be applicable to the systematic evaluation of enrichment mechanisms and patterns of distribution in space where there is a sample density or spatial resolution constraint.

Meanwhile, the strategic environment of the world shows the urgency of the global integrated investigations of such type. Battery storage methods and renewable energy technologies will help ensure the long-term increase in the demand for lithium and other elements, which will further increase (IEA, 2024; World Bank, 2023). In geopolitical concentrated, environmental permit, and technological constraint however, geopolitical supply chains are vulnerable. Thus, the reconsideration of previously underestimated geologic provinces through process-based and data-driven approaches have become one of the primary priorities of current studies about mineral exploration (USGS, 2022; Balaram et al., 2024).

Under this research agenda most apparent place of occurrence is of evaporite dominated basins. They are natural geochemical ad-hoc rates in which cycles of evaporation, growing brines, redox change, and diagenetic realignment may profoundly enhance the trace elements in concentrations that are highly higher than the background (Munk et al., 2016; Yu et al., 2022). The Salt Range is a geologic system due to its stratigraphic thickness, how it maintains itself as evidence of evaporation, and how its

later behavior because of tectonic deformation is able to control the trace constituent's distribution.

Therefore, a systematic multi-factorial geochemical re-appraisal of Salt Range Formation, followed by AI/ML informed analysis modeling, is going to be a scientifically sound, as well as a strategically relevant, research project. The paper will integrate the traditional stratigraphic-tectonic experience with the recent data analytics to examine the evaporite-hosted systems as the providers of industrial mineralization, as well as the potential repository of the elements that are vital in technology as applied to the sustainable development of the resources.

These types of integrative studies are particularly essential at the time when mineral resource security has become incapable of being addressed outside of the notion of climate policy, economic enduring, and technological autonomy (USGS, 2022; IEA, 2024; World Bank, 2023). The objectives of the current study are thus to put the Salt Range in the global discourse of critical mineral on a new platform by giving significance to national resource strategy and the global scientific knowledge to the multi-element system, which is hosted by evaporites.

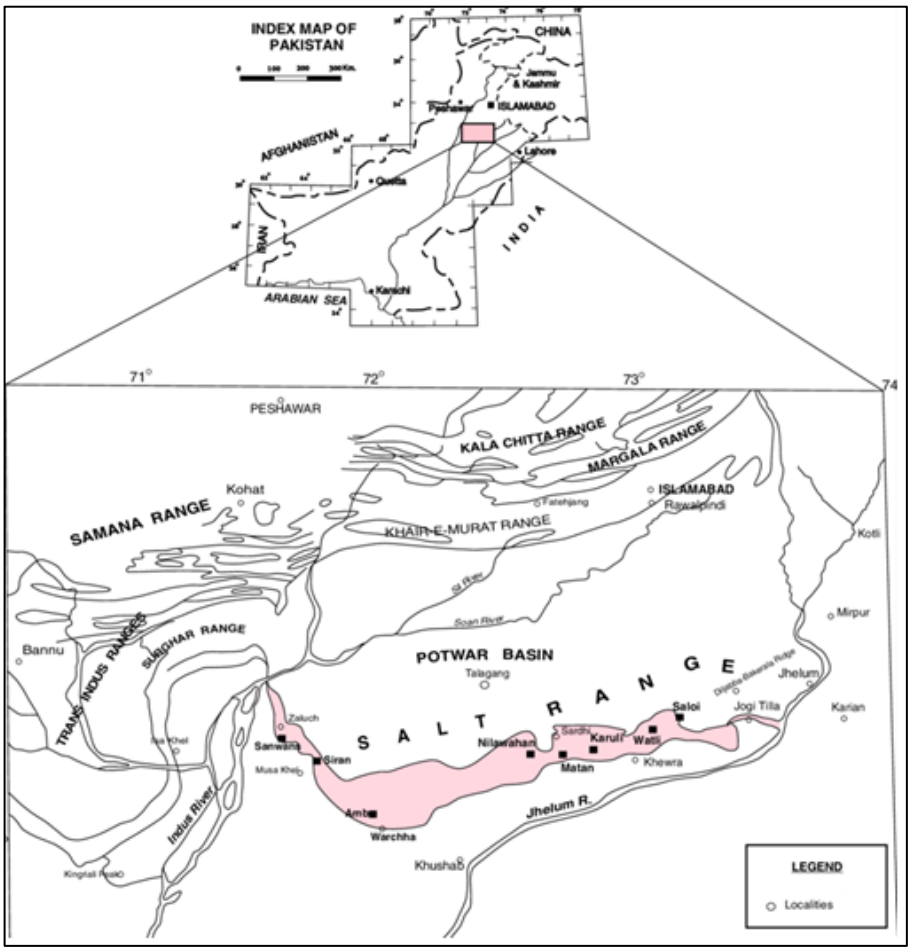

Figure 1.1: Location map of Salt Range (Ghazi et al., 2014)

1.2 Problem Statement

The Salt Range of Punjab, Pakistan, has been widely studied for its stratigraphy, structural evolution, evaporite deposits, industrial salt, gypsum, and potash resources. However, comparatively limited work has been carried out on the systematic multi-element geochemical assessment of its Salt, Marl, and Gypsum members in relation to modern critical-mineral exploration. Previous studies have mainly emphasized regional geology, tectonic development, industrial evaporite resources, and major-ion geochemistry, whereas the distribution, association, and enrichment behavior of lithium, boron, rare earth elements, uranium, vanadium, zinc, copper, and related strategic elements remain insufficiently constrained.

A further limitation is that the geochemical behaviors of critical elements within different lithological members of the Salt Range has not been adequately evaluated using integrated statistical and data-driven methods. It remains unclear whether critical-element enrichment is uniformly related to evaporitic concentration, preferentially hosted by specific members such as marl, or influenced by post-depositional processes such as diagenesis, fluid movement, and structural reactivation. This creates a scientific gap in understanding both the geochemical fertility and the preliminary exploration potential of the Salt Range evaporitic succession.

This study addresses this gap by combining ICP-MS-based multi-element geochemistry with multivariate statistical analysis and exploratory AI/ML methods. The aim is not to establish an economically proven deposit, but to identify lithology-controlled enrichment patterns, elemental associations, anomalous samples, and priority zones that can guide future detailed exploration and mineralogical validation.

1.3 Aims and Objectives

The general objective of the study is to numerically measure and visualize the critical mineral potential of the Salt Range Formation using an incidentally geochemical workflow for exploration of critical minerals to support an emerging renewable-energy mineral policy in Pakistan. The objectives of this research are as follows:

1. Geochemical evaluation and distribution of critical minerals in the Salt Range Formation at Khewra Gorge.
2. To evaluate the resource potential and identify priority exploration targets

1.4 Significance of Research

The study corresponds to the fact that it gives an evaluation of the critical mineral potential of the Salt Range Formation (Punjab, Pakistan) at formation scale, based on the evidence gathered and combined with the AI/ML modelling to solve the complex, non-

linear relationships at high-dimensional datasets that is not easily accessible through traditional univariate methods. Making a clear contribution to close the existing gap of systematic evaluation of energy-essential aspects in this evaporite-based stratigraphic system both contributes to the scientific underpinning of variability in geochemistry and would offer potential avenues of enrichment in the formation itself, at the very same time providing practical screening products (e.g., ranking zones/targets) that can provide a solid guide to cost-efficient follow-up, as well as supporting wider renewable-energy resource planning and sustainable development strategies.

1.5 Literature Review

Geological knowledge of the Salt Range, and ranges neighboring the Salt Range, the Potwar Plateau, have undergone the stage of continuous development through different periods of structural, stratigraphic, geochemical, and methodological analysis. The initial tectonic models put into place the Infra-Cambrian evaporites as a mechanically weak base of extraction horizon, which was easily broken through to spread during the Indo-Eurasian ordeal (Lillie et al., 1987). Balanced cross-sections and seismic reflection data permitted establishing that much shortening on a regional scale was accommodated along this layer of evaporites, and through this layer, the underlying sedimentary cover was able to slide southwards significantly. These discoveries placed the Salt Range Formation as a structural component rheologically significant in the Himalayan foreground fold-and-thrust system and aided the determination of the structural importance in the framework of accommodating crustal shortening.

Further stratigraphic syntheses further eliminated depository interpretation of the Salt Range Formation into extended evaporitic succession of successive layers of crystalline halite overlaying a base of potash salts, gypsiferous marls, and minor clastic aggregates being deposited under some unusual conditions of entities in arid climate (Gee and Gee, 1989; Shah, 2009). Depositional cyclicity was explained in terms of basin compression, climatic cycles as well as salinity gradients such that vertically layered evaporite-marl cycles occurred. These foundational studies made basin architecture and sedimentary evolution much clearer, but they were largely descriptive in extent, focusing

on lithostratigraphic subdivision and structural construction but a multi-element geochemical interrogation thereof was nonexistent.

Recent thermochronological work by Ghani et al. (2021) provides an important temporal constraint on the tectonic evolution of the Salt Range. Using low-temperature thermochronology, including apatite (U–Th–Sm)/He and fission-track analysis, they identified major cooling episodes associated with Late Palaeozoic regional exhumation and later Pliocene activity along the Salt Range Thrust. Their study demonstrates that the Salt Range has experienced both inherited tectonic development and younger structural reactivation. This is relevant to the present research because tectonic uplift, exhumation, thrusting, and fracture development may influence exposure patterns, fluid pathways, and post-depositional modification of evaporitic units. Although Ghani et al. (2021) did not directly investigate critical-mineral geochemistry, their work strengthens the structural framework required for interpreting possible geochemical redistribution within the Salt, Marl, and Gypsum members.

Through further developments in both thermochronology and structural segmentation, progressive southward movement of deformation and augmented the mechanical contribution of evaporitic detachments to the operations of the folds-and-thrust belts (Qayyum et al., 2015). But, although the timing and kinematics of the deformation process became better understood, little was done to consider the geochemical consequences of structural reactivation-most notably, whether it may affect the circulation of fluids and the volume of brine and redistribution of trace elements in evaporitic units. This omission is important as the salt tectonic and thrust-related fracturing can amplify permeability differences and designate pathways of fluid-rock communication which are progressively acknowledged as elemental controls in element motions in sedimentary basin.

The geochemical studies in the Salt Range have in the past focused on the industrial mineral assay, particularly, halite and potash deposits. The evaporative histories and anionic variation studies have shown evolutionary patterns of brine chemistries and major-ion chemistry during the deposition process (Hussain et al., 2021). These studies affirm the Salt Range Formation as a chemically active evaporitic system, although there is scanty trace-element data that can be used to assess critical mineral potential of the

system. The lack of high-resolution multi-element ICP-MS analyses has been consistent with current models of mineral systems to make an evaluation of whether the evaporitic members can be economically relevant sources of lithium or other critical minerals.

Carranza (2009) developed a probabilistic workflow of the sample mining prospectivity map by using weights-of-evidence and Bayesian methods, which facilitate quantitative combination of various geological predictors. This research study improved predictive targeting of structurally complex geographies by statistically assessing spatially related occurrences of known minerals and the variables of exploration. The model provided a significant methodological basis to future models of data-driven mineral exploration.

(Li et al., 2021) have shown optimization of multivariate geochemical and geospatial datasets fully integrating with the recent technologies of advanced artificial intelligence (including ensemble learning, deep neural networks, etc.) to conduct mineral exploration. Their outcome depicted better predictive ability than standard statistical training, especially in non-homogenous geologic environments where non-linear relations exist between factors governing the same. This paper also confirmed that AI-based mineral systems modeling is an effective exploration approach.

By proposing explainable artificial intelligence methods, (Sun et al., 2024) posed the issue of machine learning application to geoscience to be interpretable. The analysis allowed the study to have feature-importance values and clear model structures to make the predictive results compatible with geological interpretations. This development boosts the belief in AI-assisted mineral prospectivity mapping through the association of computational prediction with relevant geological processes.

The study by (Hussain et al., 2021) examined the geochemistry of major ions and evolutional evolution of the Salt Range deposits to reconstruct the trends on brine chemistry by performing detailed ionic study. They found progressive evaporative concentration and chemical differentiation in the basin to be true. The research, however, was confined to bulk chemical characterization and not as far as high-resolution trace-element or critical mineral analysis.

The surveys of the International Energy Agency (2024) and the World Bank (2023) made a point about the growing pace of global demand towards critical minerals due to renewable energy technologies, electrification and energy storage systems. According to these reports, the vulnerability of supply-chains was given its weight, and the strategic role of diversifying the resources base using rigorous geological evaluation. Through their analyses, it can be affirmed that the underexplored evaporite basins should be assessed in a much larger critical mineral approach globally.

(Balaram et al., 2024) focused on the combination of mineral systems theory and the high-resolution multi-element geochemical in modern critical mineral exploration. The paper claimed that subtle enrichment signatures in complex sedimentary basins can only be well discovered with advanced analytic solutions with solid data analytics. This view is consistent with new exploration paradigms which couple geological process knowledge with computer modeling methodologies.

Conversely, the international studies of evaporite-hosted mineral systems have experienced tremendous conceptual growth in the last decade. Lithium brine resources are now understood as the output of the complex mineral systems which are controlled by the source material, tectonic subsidence, hydro-isolated phases, long evaporation periods, and the long-term interaction between water and rock (Munk et al., 2016). Sequential precipitation of carbonates, sulfates, halite, and, eventually, potash-magnesium salts occur by progressive evaporation and partitioning of all the elements occurs, under varying ionic substitution mechanisms, partition coefficients, and changing physicochemical conditions.

Aridification South American Lithium Triangle Case studies reveal that under hyper-arid climatic conditions, lithium brines accumulate in the repeated evaporative concentration process under overshoot of tectonic basin conditions to be commercially important (Munk et al., 2016). In a similar way, the studies on the Tibetan Plateau brines indicate that the trace-element enrichment is additionally controlled by geothermal human contributions, hydro-dynamic changes in the basin, and redox evolution (Yu et al., 2022). In the totality of these studies, the conceptualization of evaporitic basins as multi-stage reactors of geochemical reactions in lasting operation into which multi-stage evaporation,

diagenesis, and structural overprinting of elemental mobility control elemental mobility are established.

Much of the more recent work has contributed to improved knowledge of the residence of trace-elements in the evaporite systems. Within fluid entrusted halite, lattice replacements on sulfate minerals, and clay/marl intermediaries, critical elements can occur with the ability to adsorb and exchange ions, as well as in residual brines. It has been shown using experimental and field-based research that basin-fill sediments vindicate possible basin sinks and secondarily contribute to lithium, which emits during its diagenesis and burial heating (Coffey et al., 2021). Geochemical estimates on a larger scale have shown that lithium enrichment is often due to the halite equilibrated brines undergoing further enhancement due to the process of fluid-rock interaction and mixing over some time (Dugamin et al., 2023). Such results imply that evaporite systems need to be considered as a complex unit of sediment-brine systems, not as a depositional product lying in the volatile state. The thick evaporitic members of the Salt Range that include structural reactivation and may involve fluid movement along thrust faults and interior features provide environments that favor such multistage modes of enrichment in the Salt Range.

Critical minerals hosted by evaporites have also increased interest in the strategic global environment. The accelerated development of renewable energy technologies, transport electrification, and wide-scale use of storage solutions have become a significant demand on lithium, copper, nickel, the rare earths, and other trace metals (IEA, 2024; World Bank, 2023). The concentrations of supply chains and geopolitical hazard have also led to conventionalizing unproven sedimentary basins and relying on processes-based mineral system examination (USGS, 2022). Modern models focus on reaching out to geological process knowledge and high-resolution data on geochemical to recognize elusive enrichment signals occurring in intricate basins (Balaram et al., 2024). Under this paradigm, evaporite provinces that have long been considered as sources of primarily industrial salt are also under growing consideration as a source of critical minerals.

The methodological advances have changed how the mineral exploration strategy is done in parallel ways. The weights-of-evidence and Bayesian based early probabilistic methods were used to establish statistical theoretical frameworks in mineral prospectivity

mapping (Carranza, 2009). Following introduction of logistic regression, multivariate statistical analysis increased predictive ability (Zuo & Carranza, 2011), whereas addition of remote sensing and geospatial data set boosted spatial targeting of deviations (Cracknell and Reading, 2014). In more recent studies, nonlinear relationship modeling of multivariate geochemical, structural, mineralogical, and spatial data is possible by use of Artificial Intelligence and Machine Learning (AI/ML) (Li et al., 2021). Significantly, explainable AI methodology development targets the issue of interpretability, so predictive results can be geological (Sun et al., 2024). These methods are especially useful in evaporitic systems of multistage geochemical evolution and with complex structure where more delicate forms of enrichment can be missed by more conventional linear statistical techniques.

Regardless of these global developments, the integration of AI/ML-driven mineral systems models with evaporite-hosted multi-element datasets is underrepresented and none of the studies have implemented an approach of that kind to Salt Range Formation. The Pakistani researchers in recent works show that coal and phosphate systems are examples of sedimentary deposits present with elevated levels of essential elements when evaluated using integrated geochemical and mineralogical techniques (Khan et al., 2022; Abubakar et al., 2024). But the same methodologies are yet to be applied on evaporitic sequences within Salt Range. Therefore, regional studies today are largely descriptive in nature, not predictive about the spatial model and multi-element integration on a broad foundation.

A chronological overview of the research lineage would be descriptive stratigraphic paradigms of the 1970s, consisting of structural-tectonic synthesis of the 1980s and 1990s, followed by the development of models of evaporites with evolving geochemistry's of the 2000s, and finally scrutinizing approaches of strategic critical mineral (and information-based) discourse exploration in the 2010s and 2020s. However, a systematized, procedural, geochemical evaluation of the Salt Range Formation that will fully integrate high-resolution datasets of trace elements in an AI/ML-powered framework that organizes mineral systems has never been conducted despite this progressive progress.

The current research is thus a nexus in an interdisciplinary field when it comes to structural geology, evaporite geochemistry and modeling of remnants of the mineral systems using computers. This study aims to develop beyond descriptive geological knowledge through the multi-element ICP-MS geochemical characterization and stratigraphic interpretations as well as the structural interpretation and application of sophisticated AI/ML tools to detect nonlinear patterns of enrichment and promising areas. By so doing, it has added to both regional and worldwide geological understanding as well as to the overall interests of the world in assessing the critical mineral systems in evaporites that are being predetermined in tectonically active foreland basins.

CHAPTER 2

Geology and Tectonics

2.1 Regional Geological Settings

The Salt Range area is situated in Punjab, Pakistan and is the oldest frontal expression of the Himalayan foreland belt and is a structurally significant zone of the Plate margin of the north-western Indian Plate (Gee, 1989; Lillie et al., 1987). The region is at a central tectonic location between the active deformation front, the North Main Boundary Thrust (MBT) to the North, and the Salt Range Thrust (SRT) to the South (Jaume and Lillie, 1988). Its geological structure is symptomatic of a prolonged and intricate tectono-sedimentary history beginning with the division of Gondwana and the Neo-Tethys Ocean as well as the ultimate collision between India and Asia (Powell et al., 1988; Yin, 2006).

Locally, the Salt Range belongs to the Himalayan foredeep which is a flexural basin that results because of lithospheric loading as the Himalayan thrust sheets advance towards each other in their Cenozoic collision of India with Eurasia (Beck et al., 1995; Najman et al., 2010). This basin system of the foreland stretches westward into the Kohat and Bannu basins and eastward into the Potwar Plateau making it one of the best-preserved systems of the foreland basin systems in the world (Kazmi & Jan 1997; Shah, 2009). The fill of accretion includes thick molasse type sediments formed by erosion of the uplifting Himalayan hinterland and over older marine and evaporitic sequences.

A pre-Cambrian evaporite succession of the Salt Range Formation is the basic controller of the regional geological set-up and it acts as a mechanically weak detachment horizon that provides the mechanism of thin-skinned tectonics (Gee, 1989). This layer of the evaporite is what gives the Salt Range a structural difference between other sections of the Himalayas and its primary focus in thrust propagation and the geometry of folds (Jaume & Lillie, 1988). The important aspect of this structural framework is its implication on the fluid migration, and diagenetic process, and concentration of mineral in the sedimentary sequences.

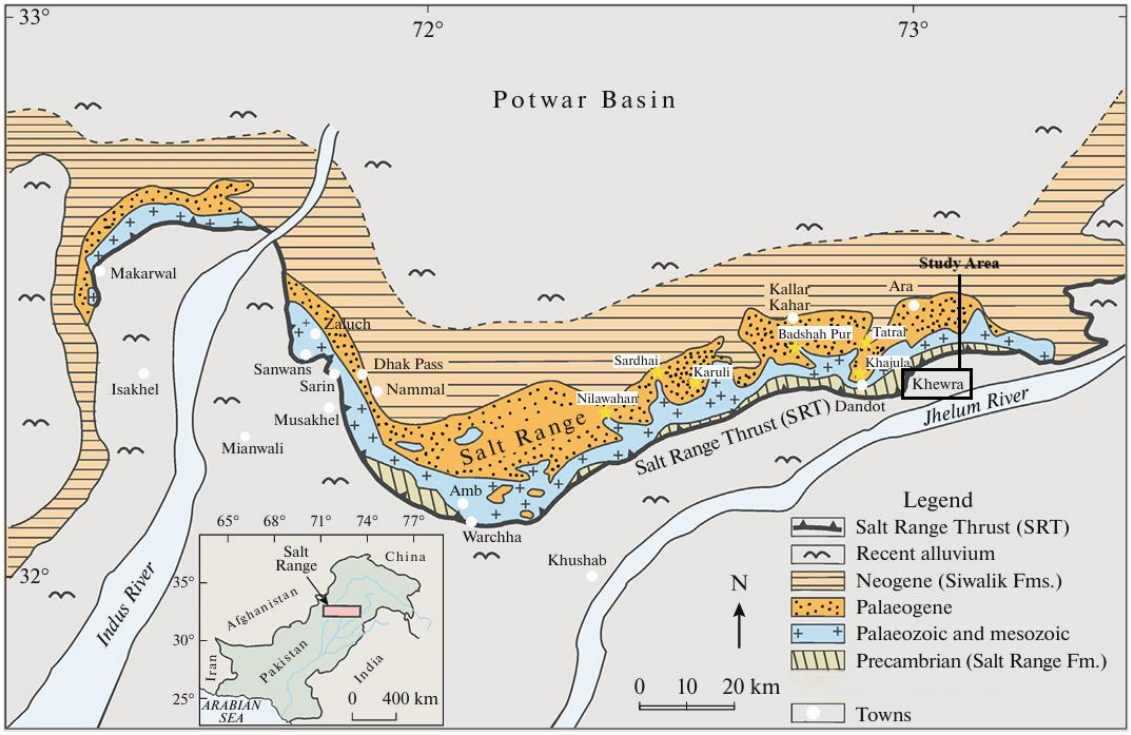

Figure 2.1: Generalized geological map of the Salt Range, northern Pakistan, illustrating the regional position of the study area along the southern margin of the Potwar Basin. The map shows the distribution of Precambrian, Palaeozoic–Mesozoic, Palaeocene, and Neogene rock units, together with the trace of the Salt Range Thrust (SRT), which marks the major structural boundary of the range. Key towns, localities, and drainage systems, including the Indus and Jhelum rivers, are shown for geographic reference. The study area lies in the eastern Salt Range near Ara, Tatral, and Khewra, where well-exposed stratigraphic sections and thrust-related deformation provide important evidence for interpreting the geological evolution of the region. An inset map shows the location of the Salt Range within Pakistan and its broader regional context

2.1.1 Structural Framework

The stratigraphy of the Salt Range also exhibits a nearly uninterrupted sedimentary record of Late Proterozoic to Recent days, which helps the Salt Range to provide one of the most classic sections of reference in the Himalayan foreland basin (Shah, 2009). The lowest unit is the Salt Range Formation, which majorly comprises of halite, gypsum, marl and few traces of clastics and was deposited in a confined shallow marine environment to evaporitic conditions during the Early Cambrian (Gee, 1989). The evaporitic deposition suggests dry weather conditions and tectonic subsidence of the left of the Gondwanian near, which is a passive deposition (Powell et al., 1988).

The clastics of Cambrian such as Khewra Sandstone are superimposing in the feature of movement of the more open sea conditions to the shallow-shelf conditions. The Wargal and Chhidru formations are carbonate platforms, which are stable marine deposition, and in which the initiation of the Neo-Tethyan subduction was preceded (Kazmi and Jan, 1997). Sedimentation of the Mesozoic continues recording the marine influence in successively switching between carbonate and clastic sedimentation, they may fluctuate sea level and the action of the active plates along the passive margin.

The Cenozoic succession is dominated by thick formations of molasses of the Siwalik Group which were formation of fluvial sandstones, tawny silt and/or rocky conglomerates which were deposited in a constantly evolving Himalayan foreland basin (Najman et al., 2010). These canyons were acquired due to sudden decay of the surging Himalayas and an all-time movement to the south of the deformation frontier (Lillie et al., 1987). It can be stated that the change between the active foreland basin subsidence to the passive margin stability is recorded in the sedimentary structure whenever the collision occurs along continents.

2.2 Tectonic Setting and Its Influence on Mineral Deposition

Basic tectonic environment in the Salt Range is governed by the constant convergence between the Indian and the Eurasian plate that started in the Paleocene-Eocene and remains to this day in the rates of about 4-5 cm/year (Powell et al., 1988; Beck et al., 1995). Such a collision brought about crustal thickening, uplifting of the hinterland of the Himalayas and flexural subsidence of the Indian Plate to become the foreland basin system (Najman et al., 2010).

The compression process of tectonics creates networks of fractures, thrust faults, and fold-based anisotropy of permeability which act as fluid movement pathways (Yin, 2006). Through these structural breaks deep-rooted basinal brines and hydrothermal fluids can circulate through the sedimentary sequences and generate geochemical redistribution of any of the trace elements uranium, lithium and rare earth elements. Evaporitic de-compartmentation also controls further fluid compartmentalization and

increases the growth of redox boundaries that are highly required in sediment-hosted minerals precipitation.

Compressional tectonics together with clastic deposition and evaporates, form favorable conditions of stratiform mineralization in foreland basin systems found around the planet and specifically in porous sandstones that are topped by impermeable shales (Beck et al., 1995). The Salt Range possesses those features, indicating high structural control of the flow of fluids and possible mineral enrichment.

2.3 Tectonic Evolution

2.3.1 Passive Margin Development and Neo-Tethyan Opening

In the Paleozoic and the early Mesozoic periods, the Indian Plate had its northern margin as a passive continent cognizant to the Neo-Tethys Ocean (Powell et al., 1988). This period was dominated by marine sedimentation as underlain tectonic quiescence, large carbonate platforms together with evaporitic basins were established. The Cambrian evaporites are an indicator of limited marine factors that probably were caused by eustatic variations and local subside (Gee, 1989).

2.3.2 Subduction and Arc Development

Eventually, at Jurassic-Cretaceous the subduction process triggered the arc magmatism and accretionary history in which it initiated developing the Kohistan Island Arc by the subduction of the Neo-Tethyan oceanic lithosphere under the Eurasia (Kazmi & Jan, 1997). Further oceanic feeding caused the ocean basin to be narrowed which resulted in the collision of the continents. The process of collision between India and Eurasia and the formation of Foreland Basin happened.

The first collision between the continents took place around 5550 Ma resulting in crustal thickening and uplift of the Himalayan orogenic belt (Najman et al., 2010). Bending forces of the Indian lithosphere created the Himalayan foreland basin where the Salt Range formed as a structural emanation (Lillie et al., 1987). The series of sedimentary

sequences moved south along the evaporitic detachment by the progressive thrust propagation.

2.3.3 Neogene–Recent Deformation

The convergence that continued into the Miocene-Pliocene led to the Salt Range Thrust becoming active along with uplifting the Salt Range anticlinorium (Jaume & Lillie, 1988). This type of thin-skinned structural style was also prevalent because of mechanical decoupling along horizons that were rich in halite. The current seismicity indicates the continuous compression of the strains along these structures (Ying, 2006).

2.3.4 Sedimentological Features

The Salt Range is marked by superimposition of marine, marginal marine, and continental depositional systems as recorded in the sedimentology (Shah, 2009). The presence of Cambrian evaporites shows that there was an arid and constrained environment in the seas and the formation of the Permian carbonates signifies the fact of stable shelf deposition (Gee, 1989). The Siwalik Group of records fluvial sediments in the systems of a braided river that relates to an active foreland subsidence (Najman et al., 2010).

The data has shown that the molasse sequence has high-energy depositional environments, as shown by the grain size distribution, sedimentary structures, and paleocurrent. These coarse clastics are mixed with fine grained flood plain shales which may act as geochemical traps in conditions of reducing environments. Shales contain intervals that are rich in organic matter, which increases the adsorption capacity of uranium and other redox elements.

Redox stratification of the sedimentary sequences is central in uranium precipitation. Uranium that is dissolved in the form of U6 + complex could be reduced to insoluble U4 + in reducing conditions in the presence of organic matter or presence of

sulfide and become stratiform mineralized in porous sandstones (Yin, 2006). Sedimentology and basin architecture therefore have a strong impact on the critical mineral accumulation.

2.4 Stratigraphy of Salt Range

2.4.1 Precambrian Basement

Though the Precambrian crystalline basement rocks are not seen on the surface of the Salt Range itself, deep drilling of the area and other geophysical surveys indicate that the whole succession of sediments lie unconformably above a basement complex of igneous and metamorphic rocks, as seen in the Kirana Hills of the Sargodha High (Gee, 1989) itself. The relationship between the basement and the cover was confirmed by drilling a borehole at Karampur, which drilled about 900 m of the Salt Range Formation that was at a depth of about 2,100 m, directly above Precambrian crystalline basement (Gee, 1989)

In geological perspective, such basement is the northern passive margin of the Indian crust that existed before the disintegration of Rodinia and the further formation of Gondwana. Several cratonic margins formed a lengthy intracratonic sag basin through the action of different thermal subsidence regions along this cratonic margin plastic zone, which offered ample accommodation space to permit the thick deposition of evaporitic formations. This arrangement of basins is in line with the evolution of passive margins with attenuation of the crust and localized subsidence.

The relative hiatus of the original stratigraphy between Late Cambrian and Carboniferous periods indicates prolonged uplift and peneplanation (Gee, 1989) which had significant impacts on the later stratigraphic and deposit patterns of the Permian period. Therefore, whether in regulating basin architecture and sediment dispersal over time, the Precambrian basement is the structural basis of the Salt Range in addition to being a vital factor.

2.4.2 Stratigraphic context of the Salt Range

The Salt Range exposes a long and well-preserved stratigraphic succession that records multiple phases of basin development, marine transgression, evaporite deposition, glaciation, carbonate-platform development, and foreland-basin sedimentation (Kazmi & Jan, 1997; Shah, 2009). The basal Salt Range Formation is overlain by Cambrian siliciclastic and carbonate units, Permian glacial to shallow-marine deposits, and younger Mesozoic to Cenozoic formations. However, because the present research focuses exclusively on the Salt Range Formation, detailed descriptions of the overlying formations are not necessary.

The overlying formations are important only because they provide the regional geological context for the evaporitic succession. The Cambrian units, including the Khewra Sandstone, Kussak Formation, Jutana Formation, and Baghanwala Formation, record the transition from restricted evaporitic deposition to shallow-marine siliciclastic and carbonate sedimentation (Gee & Gee, 1989; Shah, 2009). The Permian succession, including the Tobra, Warchha, Sardhai, Amb, Wargal, and Chhidru formations, records a later phase of glacial, post-glacial, siliciclastic, and carbonate-platform development along the northern Gondwanan margin (Kazmi & Jan, 1997; Shah, 2009).

These younger formations are not the subject of the present geochemical investigation. Their relevance is mainly stratigraphic and structural: they show that the Salt Range Formation forms the basal evaporitic unit beneath a thick sedimentary cover and later acted as a weak décollement during Himalayan deformation (Lillie et al., 1987; Gee & Gee, 1989). Therefore, the detailed geological discussion in this chapter is restricted to the Salt Range Formation and its Salt, Marl, and Gypsum members.

2.4.3 Salt Range Formation (Pre-Cambrian)

2.4.3.1 Stratigraphic position and age

The Salt Range Formation is the basal evaporitic unit of the Salt Range succession and is generally considered late Neoproterozoic to early Cambrian in age, although it has also been described in earlier regional literature as Infra-Cambrian or Eocambrian (Gee & Gee, 1989; Shah, 2009). The formation occurs beneath the Cambrian siliciclastic succession and consists mainly of halite, gypsum, marl, anhydrite, and subordinate dolomitic or clastic material (Gee & Gee, 1989; Hussain et al., 2021). Its position at the base of the exposed sedimentary sequence makes it essential for understanding both the depositional history and structural evolution of the Salt Range.

The formation records deposition in a restricted evaporitic basin developed along the northern margin of the Indian Plate before widespread Cambrian marine sedimentation. Such evaporitic successions commonly form in arid to semi-arid settings where evaporation exceeds inflow, causing progressive brine concentration and precipitation of carbonate, sulphate, halite, and locally potash-bearing minerals (Warren, 2016; Munk et al., 2016). In the Salt Range, the repeated association of halite, gypsum, and marl suggests fluctuating salinity, periodic restriction, and episodic influx of detrital or marine waters during basin evolution (Gee & Gee, 1989; Hussain et al., 2021).

2.4.3.2 Lithological members of the Salt Range Formation

The Salt Range Formation is commonly divided into three principal lithological members: the Billianwala Salt Member, the Bandarkas Gypsum Member, and the Sahwal Marl Member (Gee & Gee, 1989; Shah, 2009). These members are central to the present study because the collected samples and geochemical interpretations are based on their lithological differences. Each member represents a different evaporitic or mixed evaporitic-siliciclastic environment and therefore has a different capacity to host or retain critical and economically important elements.

2.4.3.2.1 Billianwala Salt Member

The Billianwala Salt Member represents the halite-dominated part of the Salt Range Formation. It consists mainly of massive to crystalline rock salt, locally associated with marl, gypsum, and potash-bearing intervals (Gee & Gee, 1989; Shah, 2009). The dominance of halite indicates deposition from highly concentrated brines under restricted evaporitic conditions. Such conditions develop when evaporation progressively increases the total dissolved solids of basin waters, eventually leading to halite precipitation after earlier carbonate and sulphate phases (Warren, 2016).

From a geochemical perspective, the Billianwala Salt Member is important because halite-rich facies can preserve evidence of brine evolution, evaporation intensity, and possible trace-element incorporation within fluid inclusions or insoluble residues (Warren, 2016; Munk et al., 2016). However, pure halite commonly dilutes many lithophile trace elements because it contains relatively low proportions of clay, oxide, carbonate, and detrital components. For this reason, the Salt Member provides an important comparison with the more geochemically reactive Marl Member and the sulphate-rich Gypsum Member.

2.4.3.2.2 Bandarkas Gypsum Member

The Billianwala Salt Member represents the halite-dominated part of the Salt Range Formation. It consists mainly of massive to crystalline rock salt, locally associated with marl, gypsum, and potash-bearing intervals (Gee & Gee, 1989; Shah, 2009). The dominance of halite indicates deposition from highly concentrated brines under restricted evaporitic conditions. Such conditions develop when evaporation progressively increases the total dissolved solids of basin waters, eventually leading to halite precipitation after earlier carbonate and sulphate phases (Warren, 2016).

From a geochemical perspective, the Billianwala Salt Member is important because halite-rich facies can preserve evidence of brine evolution, evaporation intensity, and possible trace-element incorporation within fluid inclusions or insoluble residues (Warren, 2016; Munk et al., 2016). However, pure halite commonly dilutes many

lithophile trace elements because it contains relatively low proportions of clay, oxide, carbonate, and detrital components. For this reason, the Salt Member provides an important comparison with the more geochemically reactive Marl Member and the sulphate-rich Gypsum Member.

2.4.3.2.3 Sahwal Marl Member

The Sahwal Marl Member consists mainly of red to brown gypsiferous marl, locally associated with dolomitic, clay-rich, and evaporitic intervals (Gee & Gee, 1989; Shah, 2009). Compared with halite and gypsum, marl contains a higher proportion of fine-grained detrital and chemically reactive material. This makes the Marl Member particularly important for critical-mineral assessment because clay minerals, iron oxides, carbonates, and insoluble residues can adsorb or retain trace elements more effectively than pure evaporite minerals (Munk et al., 2016; Yu et al., 2022).

In the context of this study, the Sahwal Marl Member is the most important target unit because marl-rich facies are more likely to preserve multi-element enrichment signatures. Fine-grained sediments in evaporitic basins can act as sinks for elements introduced during primary deposition, brine evolution, early diagenesis, or later fluid movement (Munk et al., 2016; Yu et al., 2022). Therefore, the Marl Member provides a suitable lithological host for evaluating the distribution of Li, B, REEs, U, V, Zn, Cu, and related strategic elements within the Salt Range Formation.

2.4.4 Depositional environment and basin evolution

The Salt Range Formation was deposited in a restricted evaporitic basin where evaporation, water inflow, salinity variation, and sediment supply controlled mineral precipitation. Evaporitic basins typically develop when hydrological restriction limits water exchange and evaporation exceeds recharge, producing progressive brine concentration and sequential mineral precipitation (Warren, 2016; Munk et al., 2016). The presence of halite, gypsum, anhydrite, and marl in the Salt Range Formation indicates repeated evaporitic cycles rather than a single uniform depositional event (Gee & Gee, 1989; Hussain et al., 2021).

The alternation of salt, gypsum, and marl suggests that the basin experienced repeated changes in salinity, detrital input, and chemical conditions. Halite-rich intervals reflect highly concentrated brines, gypsum-rich intervals indicate sulphate saturation, and marl-rich intervals reflect increased fine-grained siliciclastic or mixed evaporitic-siliciclastic input (Warren, 2016; Hussain et al., 2021). These lithological variations are directly relevant to critical-mineral exploration because trace elements partition differently among brines, evaporite minerals, clay minerals, carbonates, and insoluble residues (Munk et al., 2016; Yu et al., 2022).

Evaporite-hosted critical mineral systems are controlled by several processes, including source-rock composition, evaporation intensity, brine residence time, water-rock interaction, adsorption onto clay-rich phases, redox variation, and post-depositional fluid movement (Munk et al., 2016; Yu et al., 2022; Yu et al., 2024). In the Salt Range Formation, these processes may have contributed to lithology-controlled geochemical variation among the Salt, Marl, and Gypsum members. However, such interpretations must remain cautious unless supported by mineralogical, petrographic, and isotopic evidence.

2.4.5 Structural role of the Salt Range Formation

The Salt Range Formation played a fundamental role in the structural development of the Salt Range because its halite-rich intervals acted as a weak basal detachment during Himalayan compression. Thin-skinned deformation in the Salt Range–Potwar Plateau region is widely attributed to southward movement of the sedimentary cover above the evaporitic décollement (Lillie et al., 1987; Jaume & Lillie, 1988; Gee & Gee, 1989). This detachment controlled the geometry of thrusting, folding, and uplift along the Salt Range front.

The structural evolution of the Salt Range is also relevant to geochemical interpretation. Thrusting, folding, salt movement, and fracture development can influence fluid pathways and may promote local redistribution of mobile elements during burial, deformation, or uplift (Ghani et al., 2021). Nevertheless, the available geochemical data alone cannot prove hydrothermal enrichment. Therefore, any interpretation of structurally

controlled element mobility should be presented as a possibility that requires further testing through petrography, mineral chemistry, SEM-EDS, XRD, fluid-inclusion work, or isotope analysis.

2.4.6 Regional Stratigraphic Synthesis

The stratigraphy of the Salt Range indicates recurrent periods of:

1. Passive margin subsidence **(Precambrian -Cambrian)**
2. Extensive elevation and wear **(Late Cambrian-Carboniferous)**
3. Glacial-postglacial continental sedimentation **(Early Permian)**
4. Tropical carbonate platforms development **(Late Permian)**
5. Marine and continental cycles (**Later Mesozoic- Cenozoic)**

There are major unconformities at the base of the Permian, Paleocene, Miocene and late Pliocene-Pleistocene units which indicate episodic tectonic reactivation (Gee, 1989), the Eo-cambrian evaporates were critical in late Cenozoic Himalayan tectonics as they were able to concentrate the thrusting movements along a regional detachment. The mobility of salt formed the complicated anticlinorium, overfolds, and thrust repetitions of the Salt Range presently.

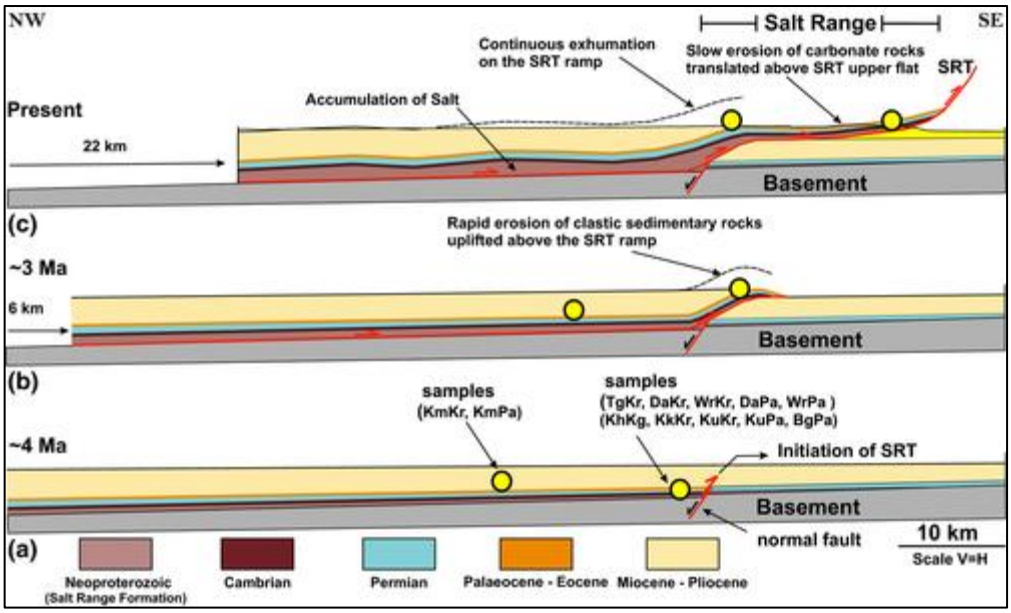

Figure 2.2: Structural cross-section of the Salt Range showing the Salt Range Formation as an evaporitic décollement and its relationship with the Salt Range Thrust. Redrawn/adapted after Ghani et al. (2021).

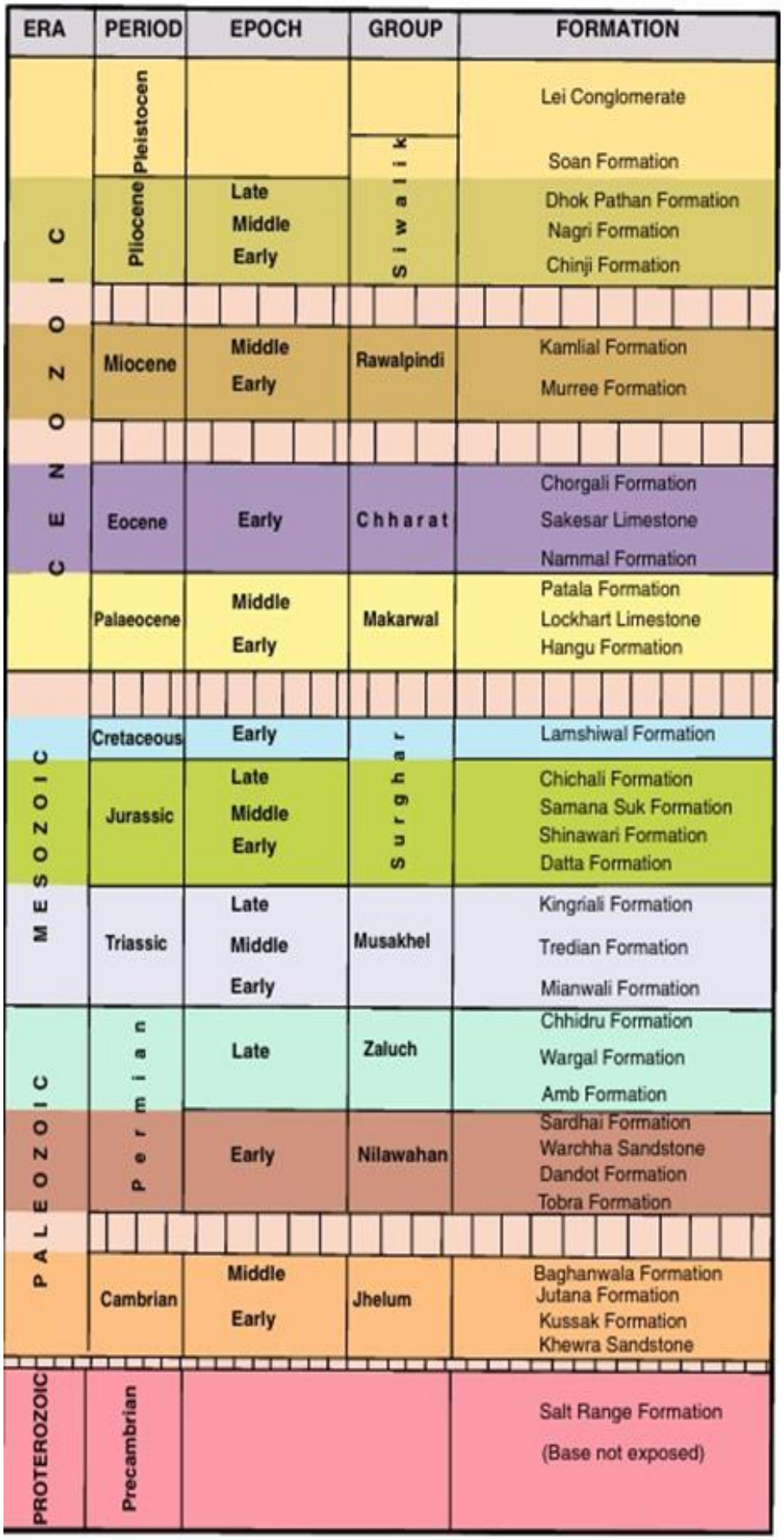

Figure 2.3: Generalized Stratigraphic Column of Salt Range (Ghazi et al., 2015)

CHAPTER 3

Methodology

3.1 Field Sampling Strategy and Sample Collection

Figure 3.1: Sample Collection Map

The Salt Range in Punjab, Pakistan was sampled stratigraphically through the systematic and controlled field sampling campaign with a focus on the three main members of the Salt Range Formation: the Billianwala Salt Member, the Sahwal Marl Member and the Bandarkas Gypsum Member. The choice of these members was based on their disparate mineralogical composition, evaporitic nature, and possible ability to contain important trace elements, which are related to the process of concentrating brine and to the process of fractionation of sediments.

The sampling design was a stratified probability sampling that was based on lithology to achieve representativity of the evaporitic, clastic and sulfate-dominated facies. It is assumed that stratified sampling should be used in non-homogeneous geological environments to reduce the bias and achieve a high geochemical quality (Rollinson, 2014). Selection of Field sites relied on the comprehensive stratigraphic logging, transitions in lithofacies, and accessibility, structural location, and minimum weathering surface of field sites.

Twenty-two (22) solid rock were sampled and there was one water sample collected. New, pure rock had been targeted to prevent supergene effects of alteration, which can be very influential in changing the distribution of primary trace elements (Reimann and Garrett, 2005). Extraction was done after removing weathered crusts with a geological hammer and chisel. All the samples had weight such that each was about 500-900 gram to be crushed, tested twice, and stored in an archival place.

The samples were placed in clean and high-density polyethylene (HDPE) sample bags after labelling with special alpha numerical (sample number) codes based on lithology and stratigraphic position. Chain of custody and proper labeling was followed, and documentation was done to ensure traces and analytical integrity. The shape of the containers is non-metallic, which minimizes the risk of contamination during the trace metal analysis (USGS, 2007).

A single brine based liquid sample was sampled in an HDPE bottle that was pre-washed with acid. Before this was used, the bottle was washed three times with distilled deionized water. The bottle was immediately tightly sealed to avoid evaporation and contamination by the atmosphere. To preserve the trace metals, the sample was acidified

to pH less than 2 with the use of ultrapure nitric acid, which is consistent with the standard procedures used to stabilize the dissolved metal (APHA, 2017).

Each sample was measured using GPS coordinates, stratigraphic height, lithological description, mineralogical observations, the orientation, and field photographs.

Figure 3.2: Sample Collected from Bandarkas Gypsum for Geochemical analysis

Figure 3.3: Sample collection from Salt Range Formation (Sahwal Marl Member) for geochemical analysis.

3.2 Laboratory Sample Preparation

3.2.1 Drying, Crushing and Pulverization

Solid samples on receipt in the laboratory were dried under room temperature in air to eliminate any left-over moisture. To preserve original mineralogical characteristics, the process of thermal drying was avoided which could lead to loss of volatile elements.

The samples were first cut down with the help of a steel jaw crusher. The samples were adequately separated by cleaning the crusher between samples with compressed air and ethanol. An agate mortar and pestle were used to perform secondary pulverization

and obtain fine homogeneous powder. Agate was chosen because it has a low background of the trace elements and it is non-reactive (Potts, 2012).

Definite grain sizes of the powder were taken by sieving the sample using stainless steel sieves (30–200 mesh; ~75–600 μm). Uniformity of grain size increase generalizability and efficacy of digesting (Jarvis and Jarvis, 1992). The mass of each homogenate sample of the samples was measured on a digital analytical balance with known weights with a margin of error of 0.0001 grams. All the laboratory work done on the samples was done in a clean laboratory with minimum contamination.

3.2.2 Acid Digestion Procedures

3.2.2.1 Rationale for Acid Digestion

Geological minerals are important in determining trace elements using ICP-MS. When these minerals are not completely dissolved, they may be underestimated and this underestimation may occur because of the refractory elements being trapped in silicate lattices (Totland et al., 1992). Thus, protocols of digestion were chosen by lithological composition and target analytes.

3.2.2.2 Aqua Regia Digestion

Aqua regia digestion was used in this study as a partial geochemical extraction method prior to ICP-MS analysis. Aqua regia is a highly reactive acid mixture, commonly prepared by combining concentrated hydrochloric acid and concentrated nitric acid in a 3:1 ratio. The mixture produces strong oxidizing and chlorinating species that are effective in dissolving many metals, sulfides, carbonates, evaporitic salts, organic matter, and exchangeable or weakly bound trace-element phases. The simplified reaction involved in the formation of reactive species is expressed as:

$$HNO_3 + 3HCl \rightarrow NOCl + Cl_2 + 2H_2O$$

In the present study, aqua regia digestion was considered appropriate because the analyzed samples were mainly derived from evaporitic and carbonate-dominated lithologies, including rock salt, gypsum, and marl. These lithologies commonly contain soluble salts, carbonate phases, sulfate minerals, clay-rich fractions, and weakly bound trace elements that can be effectively attacked by aqua regia. Therefore, aqua regia digestion provides a useful basis for evaluating the readily extractable or geochemically mobile fraction of lithium and associated critical elements within the Salt Range Formation.

However, it is important to clarify that aqua regia digestion does not represent a total digestion method. Although aqua regia is suitable for the extraction of many metals and can release lithium present in soluble, carbonate-associated, clay-bound, oxide-associated, or exchangeable forms, it may not completely dissolve lithium locked within resistant silicate minerals or refractory aluminosilicate lattices. Complete digestion of such phases normally requires more aggressive total digestion procedures, such as hydrofluoric acid-based multi-acid digestion or lithium metaborate fusion. Therefore, the elemental concentrations reported in this study should be interpreted as aqua-regia-extractable concentrations rather than absolute total-rock concentrations.

This distinction is particularly important for lithium because its recovery depends strongly on the mineralogical host phase. If lithium occurs in soluble salts, adsorbed phases, carbonates, clays, or fine-grained reactive material, aqua regia may extract a significant proportion of it. In contrast, if lithium is structurally incorporated within resistant silicate minerals, aqua regia may underestimate the true bulk lithium content. For this reason, the digestion method used in this research is most suitable for reconnaissance-level geochemical screening, lithology-wise comparison, anomaly detection, and identification of priority samples for further investigation.

3.2.2.3 Four-Acid Total Digestion

On silicate-laden marl samples and the potential presence of refractory mineral phases, a complete digestion procedure with the use of a mixture of HF/HCl/HNO 3/HCl was undertaken. The silicate minerals are dissolved by hydrofluoric acid (HF) which breaks the SiO bonds:

$$SiO_2+6HF \rightarrow H_2SiF_6+2H_2O$$

Perchloric acid ($HClO_4$) is a powerful oxidizing agent that is used to break down recalcitrant organic and oxide phases. Sulfuric acid is oxidized by nitric acid and metal ions in chloride complex are stabilized by hydrochloric acid (Hall et al., 1996).

The method of digestion provides full breakdown of silicate matrices therefore tracing back to accurate determination of elements which are trace and rare earth elements (REEs). Each of their digestion processes was conducted in a fume hood and relevant personal protective equipment (PPE) was used.

Figure 3.4: Sample Digestion Process

Figure 3.5: Sample Filtration Process

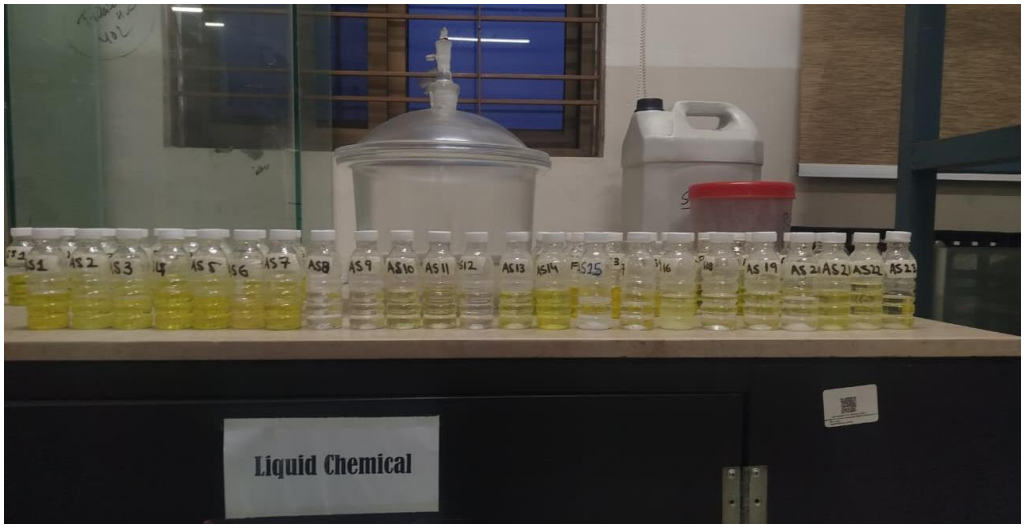

Figure 3.6: Digested Samples

3.3 Inductively Coupled Plasma Mass-Spectrometry

Inductively Coupled Plasma–Mass Spectrometry (ICP–MS) is a very sensitive and powerful analytical method that is used in the determination of major, minor, and trace elements in geological samples. The ICP-MS analysis were carried out in Allama Iqbal Open University, Islamabad, Geochemical Lab. The method is especially appropriate to geochemical studies comprising of elements of importance and strategy by virtue of the exceptionally low detection thresholds, high accuracy, and multi-elements (Hou and Jones, 2000). To assess the critical minerals geochemical distribution and potential resource in the Salt Range Formation, ICP-MS measurements of elemental concentrations in acid-digested rock samples were performed on the Salt Range Formation.

The principle of the analytical ICP-MS is sequential, aerosol generation, ionization of the plasma, ionic extraction, separation of mass and charge, and ionic determination. A digested liquid sample is injected into the instrument with the help of a nebulization system through which it is turned into a fine mist of aerosols. This aerosol is directed to an argon plasma that has been inductively coupled and maintained by a radiofrequency electromagnetic field at the normal frequencies of 27 or 40 MHz. The temperature of the plasma is between 6,000 and 10,000 K, which is high enough to guarantee the total desolvation, vaporization, atomization, and ionization of the sample (Thomas, 2013). That is because chemical bonds are easily destroyed in such high temperatures and most elements transform into singly charged positives.

Thermodynamic equilibrium regulates ionization efficiency in the plasma, and it is the relationship between level of ionization and the temperature of the plasma and the first ionization potential of the element (Becker, 2007). The elements whose ionization potential is less will be ionized better and the refractory elements might have to be fully dissolved in the matrix before introduction of plasma, to ascertain their correct quantification. The extreme plasma temperature provides high peak for reducing the chemical interferences in comparison to other spectroscopic methods and provides greater reliability in analysis.

Plasma is produced by passing the argon gas through a quartz torch that is enclosed into a copper induction coil. A low ion density in a gas is heated by resistive heating, where an incoming spark ionizes the gas and a radiofrequency oscillating field produces circular currents in the gas creating a stable and hot plasma (Hou and Jones, 2000). In this plasma, there are various processes that take place one right behind the other and these are solvent evaporation, dissociation of the species in the gas, creation of atoms and creation of ions. This will produce ions that are directed to the interface part of the instrument.

The interface system comprises of a sampler cone and a skimmer cone that divides the high-vacuum of the mass spectrometer and the atmospheric-pressure plasma. These cones cause the steep drop in pressure to about 10 -6 torr in the mass analyzer chamber as the ions go through them (Becker, 2007). The high efficiency of ion extraction is vital in the process of retaining sensitivity and avoiding suppression effects of the matrix. It was necessary that the solutions that were filtered and free of particles to be produced during the digestion step to avoid congestion of the interface cones as well as to maintain the stability of the signal.

Most quadrupole ICP-MS devices employ a quadrupole mass filter provided with four parallel sacs to which radiofrequency and direct current voltages are applied as a means of performing mass separation. Only the ions with selected mass means to charge (m/z) ratios have stationary trajectories and are drawn through the quadrupole to the detector (Thomas, 2013). The instrument produces a complete elemental spectrum by scanning the instrument across a completely different range of m/z values, permitting multi-element analysis. This is especially beneficial in critical mineral analysis where many trace elements are typically needed, such as lithium, rare earth elements (REEs), cobalt, nickel, and transition metals, need to be determined simultaneously.

An electron multiplier detector is employed to detect the ion, and it can amplify the signal produced when the ions hit the detector facet. The voltage obtained depends on the concentrations of the element in the sample (Hou & Jones, 2000). ICP-MS devices can detect trace elements in the sub-parts-per-billion range which means that they are particularly appropriate in assessing low concentrations of critical trace elements of sedimentary and evaporative systems (Becker, 2007).

Independent of the high sensitivity of this analysis method, ICP-MS is prone to spectral and non-spectral interferences. Interferences that are spectral in nature are due to polyatomic ions that are formed in the plasma e.g. argon oxide species and those that are isobaric and those that are doubly charged (Jarvis and Jarvis, 1992). These interferences may have an impact on a particular isotope and need correction either by collision/reaction cell technology or mathematical correction algorithms. Other non-spectral interferences are suppression effects due to high total dissolved solids in the matrix and can lead to changes in the ion transmission efficiency. In the current research, internal standards were added to every sample to remove the notion of instrumental drift and signal variations attributable to the matrix effect (Thomas, 2013).

External calibration in certified multi-element standard solutions was used to do quantitative analysis. Calibration curves were obtained by creating graphs of the signal intensity verses the known concentrations keeping the correlation coefficients (R 2) at a level of 0.995 as an assurance of analytical linearity. The instrumental detection limits were determined using three standard deviations (SD) of the procedural blanks, which was in line with the acceptable analytical guidelines (Potts, 2012). The remainder of the analytical methods were applied to analytical blanks, duplicate substances, and certified reference materials to evaluate contamination, accuracy and precision. The values of the relative standard deviation were kept under 5 percent of trace elements, and the recovery values of reference materials were found to range between 90 and 110 percent, which means high values of analysis reliability.

The use of the ICP MS in this analysis has several benefits to critical mineral analysis in the Salt Range. These fine detection capabilities allow detection of traces of element enrichments as small as to sentinel element enrichments that could be indicating geochemical anomalies or mineralization trends. The multi-element capability enables the consideration of the elemental association and geochemical signatures approachable to lithium, the rare earth components and the other energy transition metals (Becker, 2007). Moreover, the production of quantitative data of high resolution can be followed by a following statistical analysis and incorporation into the artificial intelligence and machine learning models to predictive resource assessment (Hastie et al., 2009).

Overall, ICP-MS analysis is the focal elemental analysis of the study, as it offers high-precision and high-sensitivity elemental data that will be needed to characterize the geochemical of the Salt Range Formation and evaluate its potential as a critical mineral.

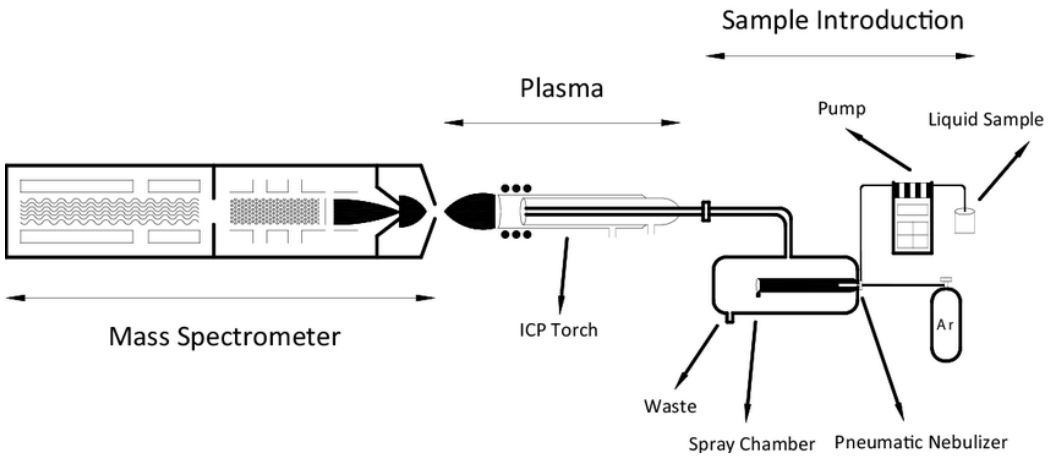

Figure 3.7: Schematic Diagram of ICP-MS (Kashani & Mostaghimi, 2010)

CHAPTER 4

Results and Interpretation

4.1 Introduction

The chapter documents the geochemical findings of the standard samples that were taken at the Salt Range Formation according to the ICP-MS analysis of some of the main lithological units of the marl, rock salt, and gypsum. The chapter aims at satisfying the key goals of the study: to determine the distribution of the critical minerals, to understand the occurrence of the economically significant mineral constituents, to determine the critical and economic mineral assemblages, and to use the results in the context of the depositional, diagenetic, and structurally controlled enrichment processes.

The Salt Range Formation has already been put into perspective, thick succession of evaporitic consisting primarily of salt, gypsum and marl, formed in a shallow basin and subsequently with Himalayan tectonics. The latter geological context is required in the explanation of the current findings since evaporite basins usually represent multistage geochemical systems wherein progressive evaporation, fluid segregation, mineral re-crystallization and structural directed fluid movement may enriched desired trace elements. Here the results of analysis as shown will be regarded as not the isolated concentrations indicated, but the manifestations of a more comprehensive behavior of minerals-systems. The interpretable solid samples included 22 solid and 1 liquid sample. These samples include 7 marl samples, 8 rock- salt samples and 8 gypsum samples. The dataset contained an approximation of 68 columns on the exclusion of identifiers showing the elemental concentrations. All the elements were not always found in all the samples and some of the elements had been reported as below detection limit. This aspect is relevant since an interpretation is to be weighed on the aspect of analytical completeness; those elements which are represented through one or few detections cannot be discussed, similarly as those that are regularly measured throughout the entire dataset.

4.2 General Character of the Analytical Dataset

By analyzing the results basically, they have shown that the Salt Range Formation is not competitively homogenous but geochemically heterogeneous. Such heterogeneity is manifested at two levels. The first one is an extreme difference among lithologies; marl samples are always enriched in most trace and key elements as compared to gypsum and salt samples. Second, some samples placed in a single lithology become strongly enriched in comparison with background and this suggests local concentration and not mere stratigraphic uniformity.

Throughout the whole data the lithium are within the range of 0.003 ppm to 4.111 ppm with a mean of approximately 0.731 ppm but a considerably smaller median of approximately 0.076 ppm. Potassium, where detected, ranges from about 0.452 ppm to 9.685 ppm; boron from about 0.009 ppm to 2.932 ppm; strontium from about 0.059 ppm to 3.129 ppm; uranium from about 0.024 ppm to 1.339 ppm; vanadium from about 0.005 ppm to 4.706 ppm; zinc from about 0.004 ppm to 1.142 ppm; and copper from about 0.003 ppm to 1.479 ppm. There is also the rare earth suite and La, Ce, Nd, Sm, Gd, Dy, Er, Y, and Yb are clearly enriched in the chosen samples.

While interpreting the results there are two general features of the dataset. To start with, the evaporitic system can concentrate economically and technologically significant aspects. Secondly, it seems that the marl facies is the main environment of trace-elements enrichment, whereas rock salt and gypsum hold more discriminating enrichments, in salty-brine-associated and sulfate-carbonate-equilibrium elements.

Table 4.1: Critical Mineral Results, whereas BDL shows the Below Detection Limit, ADL shows the Above Detection Limit, Li is Lithium, B is for Boron, K is Potassium, Sr is Strontium, Cu is Copper, Zn is Zinc, Ni is Nickel, Co is for Cobalt, V is for Vanadium, U is showing the uranium and REE is representing the Rare Earth Element.

Sample ID	Lab label	Member	Li	B	K	Sr	Cu	Zn	Ni	Co	V	U	ΣREE +Y
M1	AS1	Marl Member	0.093	0.067	4.076	0.188	0.058	0.072	BDL	BDL	0.069	0.089	0.166
M2	AS2	Marl Member	0.492	0.547	ADL	1.173	0.119	0.233	0.030	BDL	0.319	0.275	0.360
M3	AS3	Marl Member	0.302	0.349	ADL	0.679	0.059	0.124	0.010	BDL	0.155	0.182	0.268
M4	AS4	Marl Member	2.326	1.647	ADL	ADL	0.371	0.447	0.093	BDL	2.228	0.539	2.806
M5	AS5	Marl Member	3.879	2.932	ADL	ADL	0.651	0.869	0.215	BDL	4.129	1.339	3.327
M6	AS6	Marl Member	1.520	1.684	ADL	ADL	0.358	0.532	0.094	0.027	2.453	0.123	3.458
M7	AS7	Marl Member	4.111	1.994	ADL	ADL	0.722	1.142	0.341	BDL	4.706	0.690	3.172
S1	AS8	Salt Member	0.035	0.232	ADL	3.129	1.479	0.161	BDL	BDL	0.0052	0.060	0.046
S2	AS9	Salt Member	0.0030	0.029	ADL	0.483	0.150	0.083	BDL	BDL	BDL	BDL	0.0074
S3	AS10	Salt Member	0.593	1.349	ADL	2.319	0.113	0.216	0.011	BDL	0.363	0.093	0.301
S4	AS11	Salt Member	0.011	0.063	ADL	0.483	0.103	0.141	BDL	BDL	BDL	0.024	0.045
S5	AS12	Salt Member	0.0038	0.050	ADL	2.122	0.263	0.085	BDL	BDL	BDL	0.055	0.022
S6	AS13	Salt Member	0.076	0.672	ADL	ADL	0.096	0.022	BDL	BDL	0.045	0.049	0.049
S7	AS14	Salt Member	2.142	0.118	ADL	ADL	0.016	0.041	BDL	BDL	0.157	0.057	0.193
S8	AS15	Salt Member	0.076	0.013	5.320	ADL	0.0048	0.089	BDL	BDL	0.033	0.072	0.412
G1	AS16	Gypsum Member	0.951	0.078	ADL	ADL	0.043	0.240	BDL	BDL	0.164	0.101	0.933
G2	AS17	Gypsum Member	0.091	0.033	9.685	ADL	0.013	0.145	BDL	BDL	0.036	0.171	0.703
G3	AS18	Gypsum Member	0.012	BDL	0.631	0.153	0.0073	0.015	BDL	BDL	0.026	BDL	0.222
G4	AS19	Gypsum Member	0.0038	BDL	0.691	0.117	0.0032	0.0090	BDL	BDL	0.018	0.039	0.124
G5	AS20	Gypsum Member	0.0057	BDL	0.652	0.059	BDL	0.0094	BDL	BDL	BDL	BDL	0.147
G6	AS21	Gypsum Member	0.053	0.0094	4.239	0.245	0.0066	0.024	BDL	BDL	0.025	0.037	0.202
G7	AS22	Gypsum Member	0.018	BDL	0.507	0.136	BDL	0.018	BDL	BDL	BDL	BDL	0.135
G8	AS23	Gypsum Member	0.012	BDL	0.452	0.063	BDL	0.0041	BDL	BDL	BDL	BDL	0.293

4.3 Lithology-Wise Geochemical Distribution

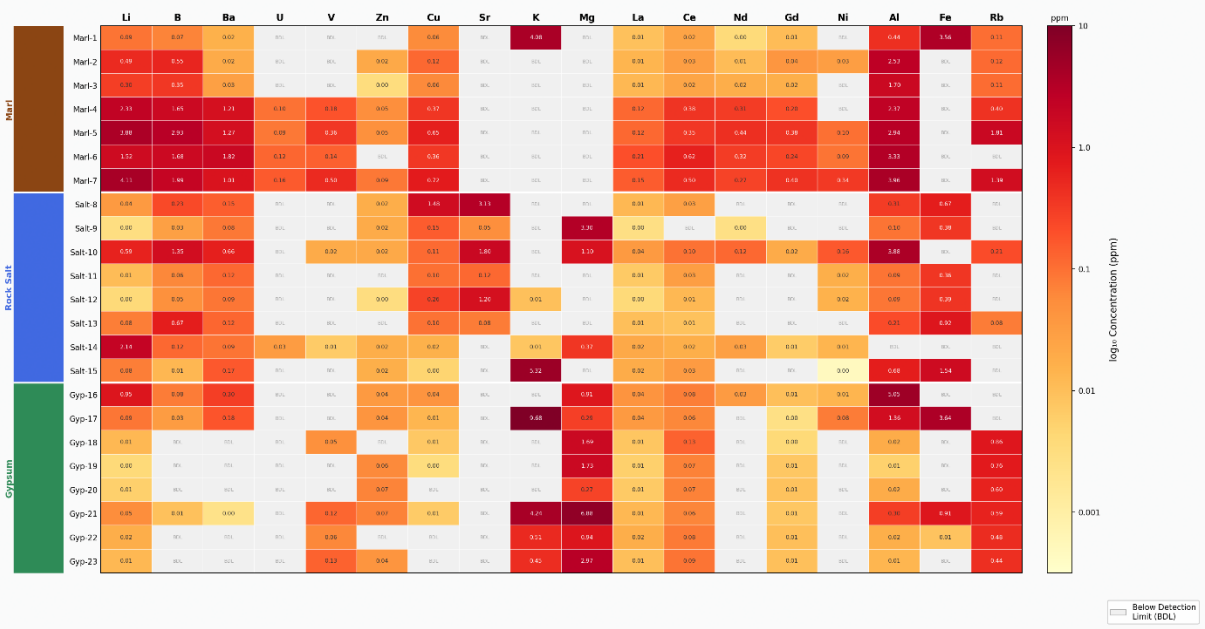

Figure 4.1: Lithology-Element Enrichment Heatmap

4.3.1 Marl

The marl samples are enriched and shows the most diverse concentrations of all the lithologies analyzed. Lithium, boron, barium, most of the REEs, uranium, vanadium, zinc, iron, manganese, titanium, and aluminum have the greatest mean concentrations at Marl. The lithium concentration of marl is about 1.818/ppm which is much higher than that of salt (0.368/ppm) and gypsum (0.143/ppm). On the same note, the primary average content of boron (1.317 ppm), barium (0.769 ppm), uranium, vanadium, zinc, and total REE are also highest in marl.

Marl is a more chemically reactive and texturally favorable host as compared to massive halite. Marl homogenous and fine-grained units rich in clay are capable of being adsorptive and exchange-active media of a large variety of trace elements. They smear signals of the early diagenetic pore fluids also than recrystallized salt. Marl can further play the role of a depositional sink and the post-depositional system of geochemical trapping in an evaporitic basin. The high values of marl are a very strong indication that it is not only pure evaporite minerals which are subject to the most significant trace-element enrichment in the Salt Range Formation, but to mixed sediment-brine interfaces

in the marl horizons. This agrees well with the larger mineral-system paradigm worked out in the previous chapters, in which the enhancement of trace-elements due to non-equilibrium between evaporation, diagenesis and structural remobilization was anticipated.

In the whole dataset the most enriched samples are mainly marl samples particularly Marl-4, Marl-5, Marl-6, and Marl-7. These recurrently are the top-ranking samples of lithium, REEs, uranium, vanadium, zinc, and boron and several other elements. This regularity implies that it is not an arbitrary analytical noise that enriches the signal but a real signal that is controlled by facies.

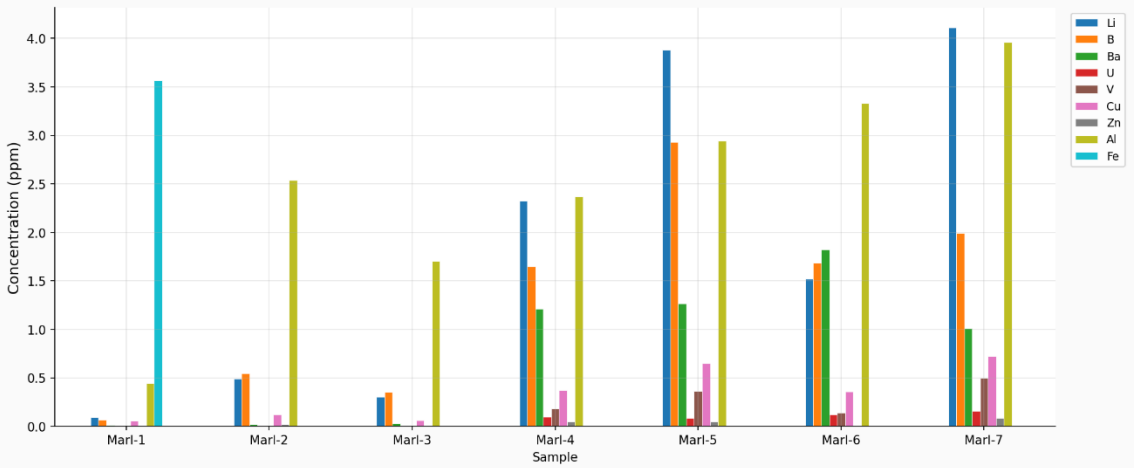

Figure 4.2: Geochemical Profile for Sahwal Marl Member

4.3.2 Rock Salt

The samples of salt have another geochemical nature. Overall, they are enriched in most trace elements compared to marl, although some of the elements that are compatible with evaporites are significantly enriched. Depending on importance, the peak of the mean strontium content is in salt, the average of which is 1.707 ppm compared to the average of marl 0.680 ppm and gypsum 0.129 ppm. Salt samples are also promising high potassium with one of the salt samples having high potassium level of 5.320 ppm, but the overall highest potassium level is found in gypsum.

This enrichment selectivity suggests that the salt facies documents a greater type of evaporative chemical progression, in which the concentration of saline preferred dissolvable ions and trace elements related to late-stage brines. The reality is that most salt samples are poor in lithium and REEs, however, point to the fact that pure halite was not the key host material in the larger scale multi-element enrichment that was recognized in the current study. Instead, it seems that the salt facies proves more helpful to make the identification of basin-scale evolution of brines and salinity history than the richest source of trace-elements.

Among other results that were particularly interesting was the large copper value in Salt-8 which is the largest copper concentration in the data. Since copper is not raised across all the salt samples, it is more likely to be an enrichment of localized fluids than a characteristic that was controlled by halite.

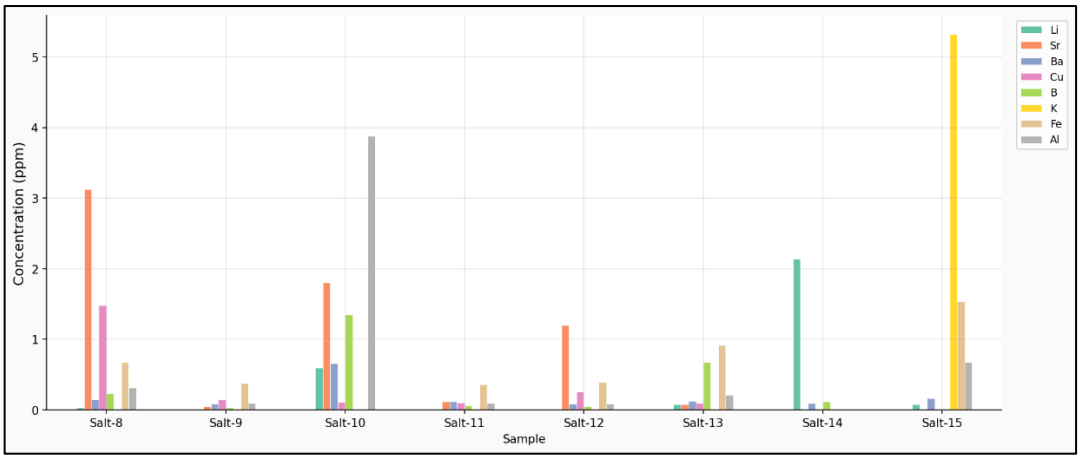

Figure 4.3: Geochemical Profile for Billianwala Salt Member

4.3.3 Gypsum

Generally, the gypsum samples are intermediate to low in trace-elements though not geochemically significant. Gypsum contains less average lithium and REE than marl, a few samples of gypsum contain high concentrations of potassium and moderate concentrations of rubidium and phosphorous. The maximum concentration of potassium in the dataset is found in one gypsum sample at approximately 9.685 ppm, which is significant as it could be a concentration of potassium during late evaporation or the

enrichment of certain areas with potassic compounds. Sulfate-rich fluid chemistry is normally sensitive when measured using gypsum units. Where the concentration of trace elements is moderate, even in those cases, gypsum may be able to preserve information on evaporative concentration, redox variation, and the composition of the brines. Consequently, the gypsum information must not be discounted as crazy, instead, this information indicates that the sulfate bearing horizons were involved in the geochemical development of the basin but was not the location of extensive wide scale critical element.

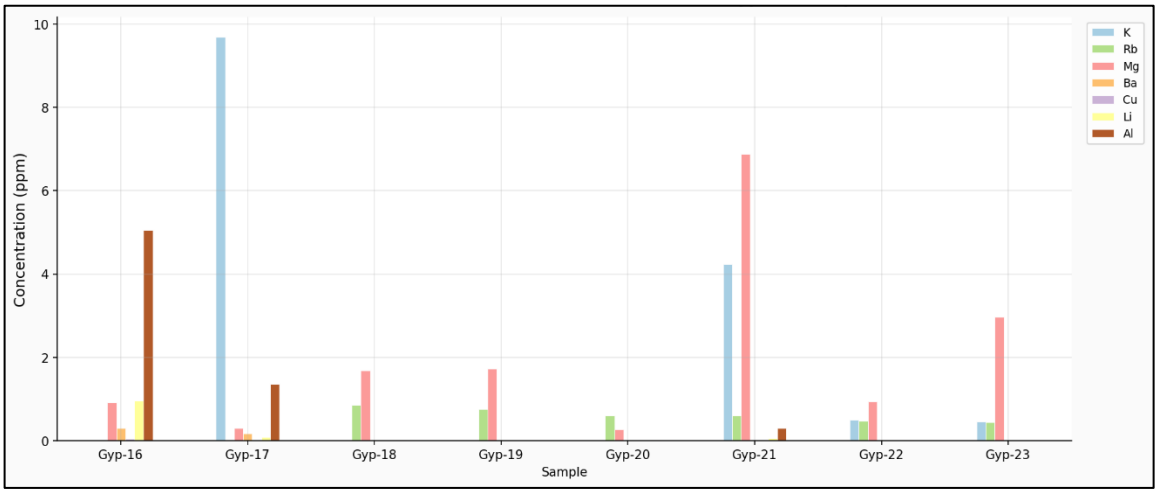

Figure 4.4: Geochemical Profile for Bandarkas Gypsum

4.4 Critical Minerals

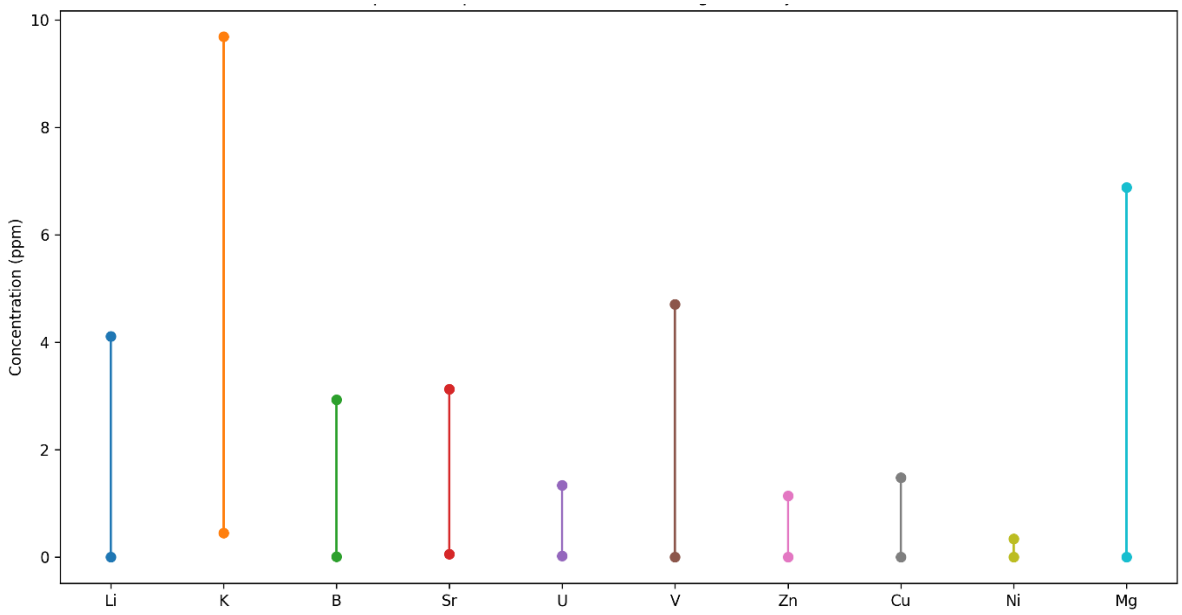

Figure 4.5: Critical Minerals Concentrations

4.4.1 Lithium (Li)

The most critical mineral in the case of this study is Lithium due to its strategic position in the battery technology of recharge, and the renewable energy systems, which are of concern in my proposal and introduction. The analytical results demonstrate that lithium occurs in all the three lithologies but heavily enriched in marl. The total maximum Lithium level has been measured in Marl- 7 (4.111 ppm), then its level is recorded in Marl-5 (3.879 ppm) and Marl-4 (2.326 ppm). The mean of marl is approximately 1.818 ppm which is many times more than means of salt and gypsum.

This distribution is very substantial. It reveals that the enrichment of lithium distribution within the Salt Range Formation cannot be explained solely by simple evaporative concentration. In case pure evaporative concentration only occurred in the halite rather than being only one of the controls, the salt samples should have dominated the lithium inventory. Rather, the findings indicate a preferential retention of lithium in those areas of the system where marl occurs, whereby clay-yielding or sediment-brine mixtures micro-environment may have promoted adsorption, exchange as well as late-

stage fixation. This is well in line with conceptual models of evaporite-hosted lithium systems as realized today, which realize that lithium can also be found not necessarily only as residual brines, but also as Fine-grained basin fill and diagenetically modified sediment.

The trend is also indicative of localized enhancement as opposed to the mineralization of the basin in uniformity. The severely skewed lithium pattern demonstrates that there are enriched intervals or areas in a lower ground geochemical pattern. This is promising by exploration standards since it means that there is a differentiation in the system and not a homogenous chemical system. However, the measured lithium concentrations should be interpreted only as reconnaissance-level geochemical indicators and not as evidence of an economically viable lithium resource as exploration values and indicators of enrichment deposition, not yet as indicators of an economically viable lithium ore system.

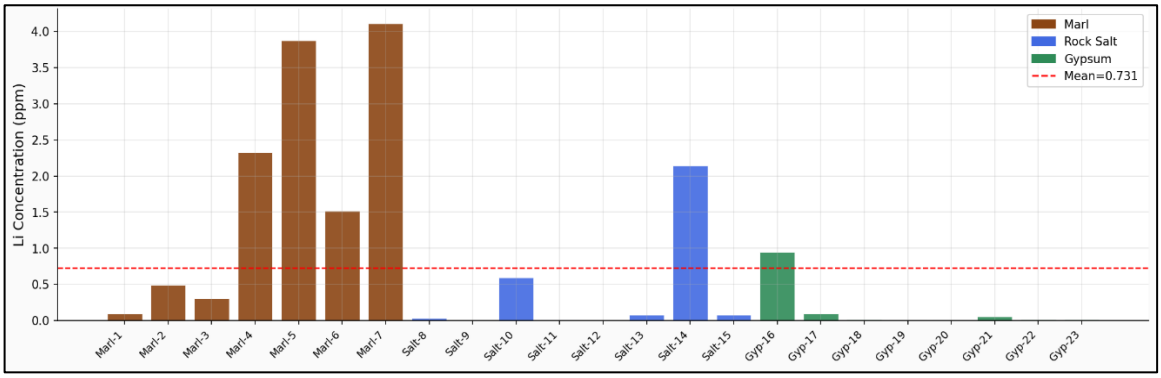

Figure 4.6: Lithium Enrichment in Samples

4.4.2 Copper (Cu)

Copper is a key industrial and energy-transition metal which is available in the dataset with a range of concentrations at about 0.003 ppm up to 1.479 ppm. The maximum is on Salt-8 then there is the marl samples like Marl-7 and Marl-5. The localization of copper is suggested by this trend because it is not as localized as lithium and does not correspond to one facies trend.

The enrichment of copper in evaporating or deposition systems may take place due to the movement of fluids, redox interfaces, as well as localized precipitation of sulfide. Given that highest copper values are found in salt and that highest values are found in enriched marble it would only be reasonable to propose that copper in the salt range formation was one that was modified by post-depositional fluid redistribution over the evaporitic stratigraphy. Its behavior is thus more structurally or diagenetically regulated or controlled rather than merely evaporite-compatible.

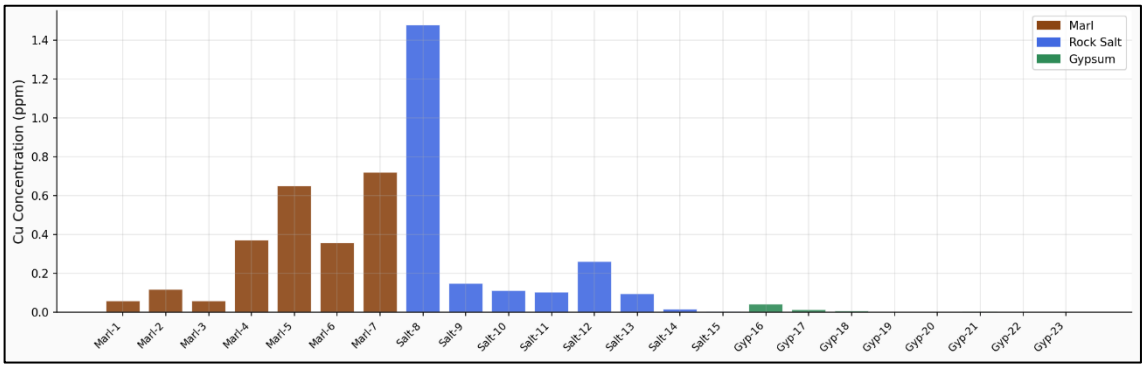

Figure 4.7: Copper Abundance across sample

4.4.3 Nickel (Ni) and Cobalt (Co)

Only a few samples contain nickel with a peak of (0.341 ppm) in Marl-7 and lesser levels in Marl-5 and Marl-6. Only one analytical detection of cobalt is available, and this is insufficient to give any good geochemical meaning. That is why nickel can be viewed with caution, but cobalt must be regarded as analytically inconclusive in the current dataset.

The enrichment of nickel which is hosted by the marl remains significant. The implication here is that it is also the case that transition-metal enrichment correlates with these chemically active marl intervals that are also lithium, vanadium, uranium and REEs. This reinforces the suggestion that units of marl were geochemical traps of a range of redox-sensitive and mobile fluid elements. But due to the low rate of detection, repeat verifications or an increased sample population would have to be made in regards to further validation of the detection before any wider metallogenic assertions could be made concerning the nickel and cobalt.

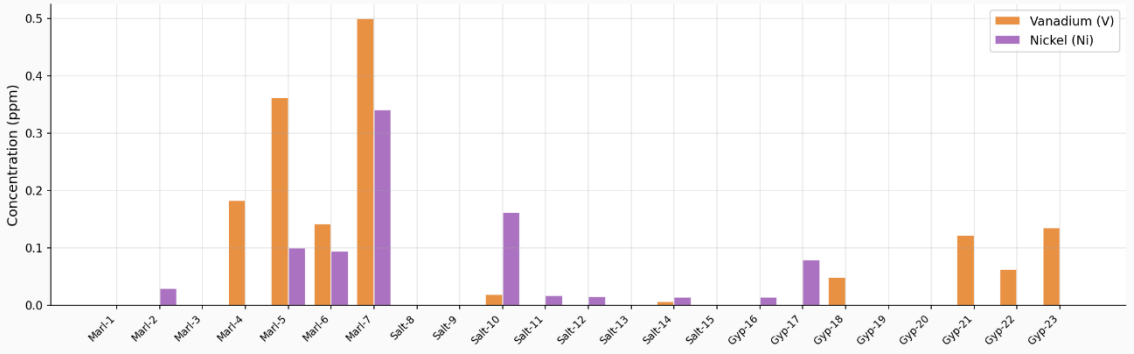

Figure 4.8: Abundance of V and Ni across the samples

4.4.4 Zinc (Zn)

One of the clearest critical/ base-metal indicators in the dataset is zinc since it was found in all valid samples. Zinc has a range of 0.004 ppm, 1.142 ppm and the most amount of the element is found in Marl-7, Marl-5 and Marl-6. The average (Zn) concentration is also evidently the highest in marl. This is very tight physical relationship with lithium, vanadium, uranium, boron and REEs viewing that zinc is a part of the same super-enrichment collection.

No less than three types of mobilization in evaporite-related basins can include: basinal brines and concentration by changing fluid chemistry or offering sorbent or precipitation sites with reactive sedimentary intervals. Its affinity towards marl in this dataset confirms the argument that mixed siliciclastic-evaporitic facilities, and not huge beds of pure evaporites, are the most favorable hosts to trace-element concentration.

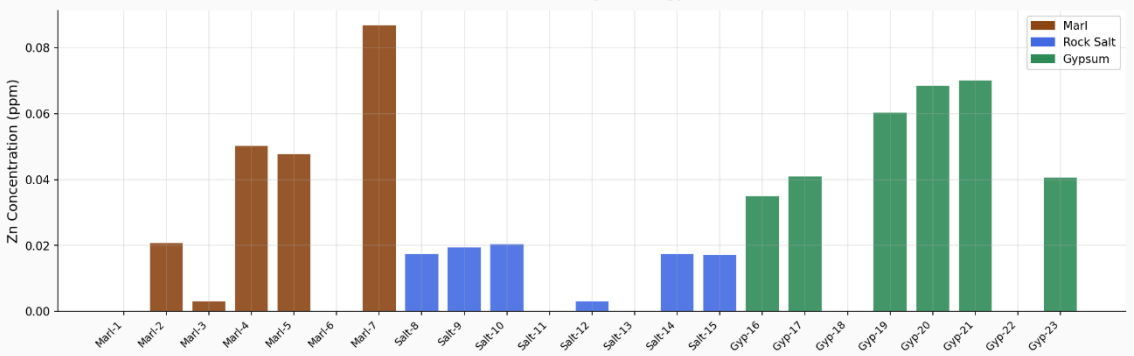

Figure 4.9: Abundance of Zinc across the samples

4.4.5 Vanadium (V) and Uranium (U)

Vanadium and uranium are especially significant since they are redox-sensitive and can tell both evolutional and depositional environment of fluids. The highest contents of vanadium and uranium are 4.706 ppm and 1.339 ppm respectively in Marl-7 and Marl-5 respectively. The two are highly concentrated in marl as compared to the other lithologies.

The pattern of enrichment is in keeping with geochemical trapping in a reducing or chemically reactive environment especially in fine-grained sedimentary intervals. In previous chapters, it was highlighted that tectonically affected evaporitic basins may form fluid pathways and redox boundaries that have the capability of redistributing trace elements. Results on uranium and vanadium can be well fitted in that model. They refer to a history of basin in which evaporation is not the only aspect, but also subsequent diagenetic and potentially structural control of fluid movement.

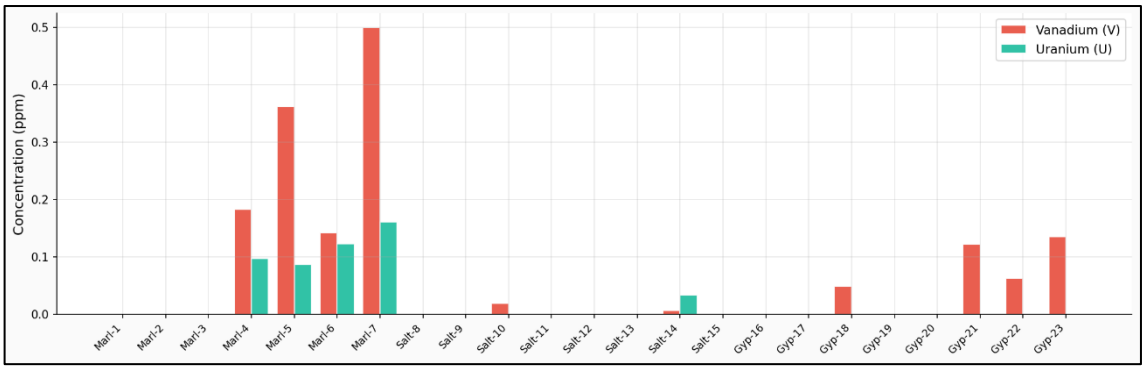

Figure 4.10: Abundance of V and U across samples

4.4.6 Antimony (Sb), Niobium (Nb), Tantalum (Ta), Tungsten (W), and Other Critical Element

The presence of antimony at low, yet measurable concentrations in several samples and only the occasional occurrence of niobium and tantalum and the absence of analytical limitations in the existing data of tungsten. These elements should therefore be discussed cautiously. Their existence contributes to the multi-element system, but the rate of detection does not provide enough material to elaborate on quantitative meaning. To the end of the research, the elements can be introduced as supplementary critical-element indicators instead of key mineralization targets at the current phase of exploration.

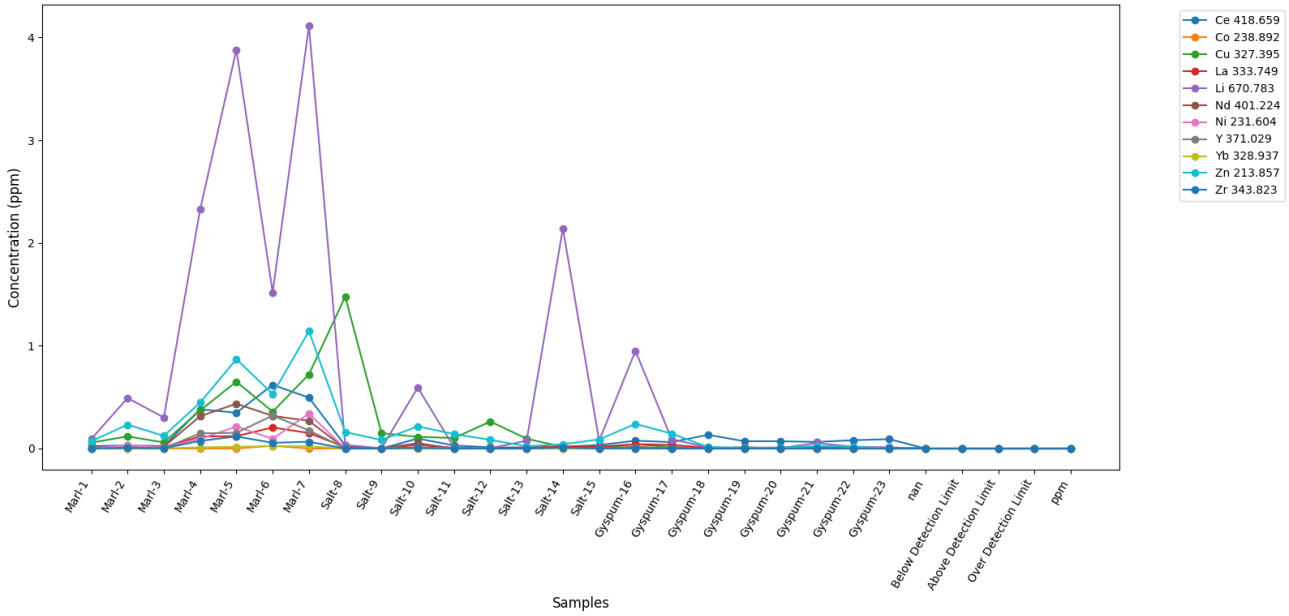

Figure 4.11: Critical Minerals Variation across Samples

4.5 Rare Earth Elements (REEs) and Yttrium

One of the strongest aspects of analytical findings is the REE dataset since virtually several REEs were detected repeatedly and exhibited consistent facies links. The suite at hand consists of La, Ce, Pr, Nd, Sm, Eu, Gd, Tb, Dy, Ho, Er, Tm, Yb, Lu, and Y. ENR enrichment is overpoweringly found in the marl samples, most notably in Marl-5, Marl-6 and Marl-7. Marl-6 (~3.458 ppm) has the highest total REE content, followed by

Marl-5 (~3.327 ppm) and Marl-7 (~3.172 ppm), as compared to the mean total REE content in marl, which is much higher than in gypsum and salt.

This lithological distribution is of great importance. It demonstrates that the distributions of REEs in the Salt Range Formation are not random and equally distributed to all the evaporitic units. Rather, they are selectively concentrated in marl-rich intervals which probably provided adsorption sites on clay minerals, fine detrital material and organic or diagenetically altered phases. This is typical of sedimentary systems in which REEs are not present as discrete ore minerals but are trapped in fine-grained matrices and authigenic phases.

There is a consistent pattern in the individual REEs. Light REEs, including La and Ce are not only more developed, in terms of absolute abundance, than the heavier REEs but also the same marl samples dominate the LREE and HREE populations. Y and Yb are also likewise peaked in the marl facies particularly the Marl-6 and Marl-7. This wide-spectrum REE enrichment is an indication that the marl layers have been an integrated trace-element trap, and not a host to a single, isolated mineralizing event.

Interpretively, the REEs have three conclusions. First, there was detrital or clay-rich marl which served as a substantial source of trace-elements in the formation. Second, the basin diagenesis must have increased redistribution and fixation of REEs. Third, the geochemically most promising aspect of the system is supported by data on the REE which indicates that the marl-bearing interval of evaporitic is the most promising rather than the pure endmember of either halite or gypsum.

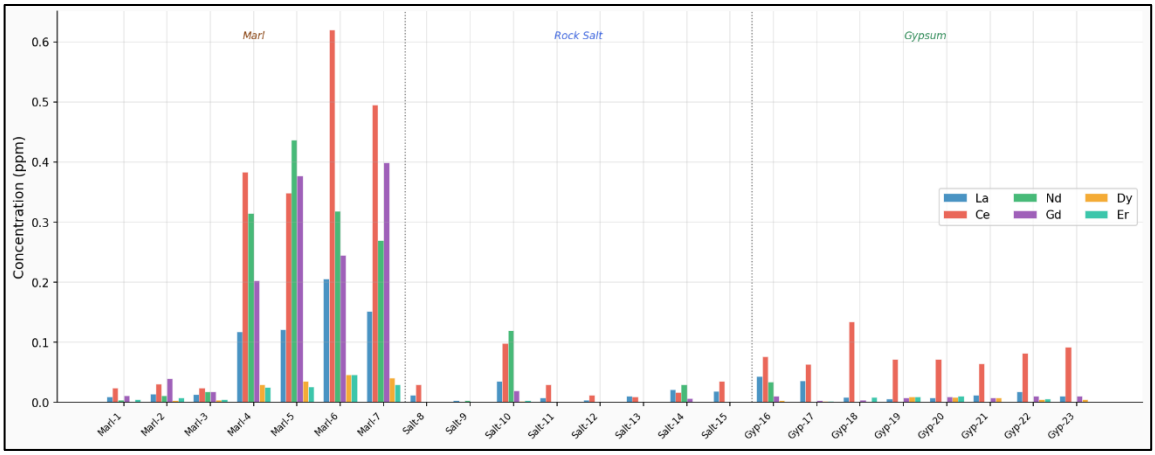

Figure 4.12: REE Variations in collected Samples

4.6 Economically Important Minerals and Industrial Elements

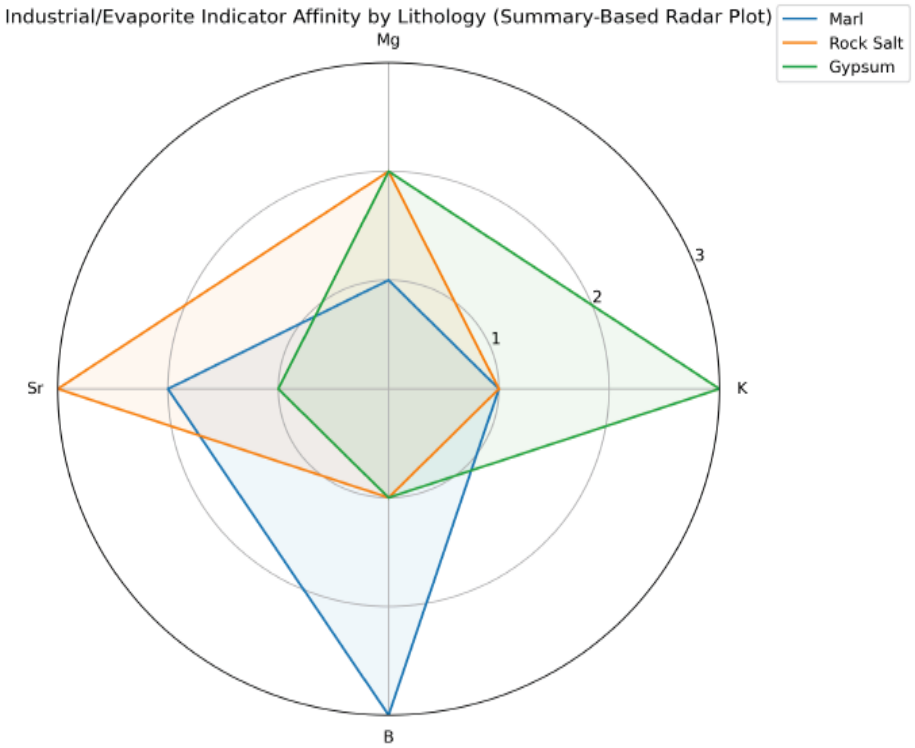

Figure 4.13: Industrial Mineral Variance Spider Diagram

4.6.1 Halite and Sodium (Na)

The Salt Range Formation has a long history of industrial salt and my proposal as well as the previous chapters acknowledge halite as one of the main economic commodities of the formation. Direct sodium measurements in the dataset are few, with just a handful of valid measurements and zero in the salt subset after cleaning the file. This is not to say that there is no sodium in the rock-salt samples. Instead, it is probably due to analytical constraints of detection conditions, dilution or behavior of the matrix in the ICP-MS process of this dataset.

Thus, the economic importance of halite is to be discussed mainly in terms of lithology and regional geology, and the analytical dataset must be viewed as additional evidence and not as the only one. By field identity, the samples of salt themselves attest that rock salt is one of the key economic elements of the sampled sequence. The

geochemical data however indicate that the halite facies is not as good as marl in holding on to many of the trace critical elements.

4.6.2 Potash and Potassium (K)

One of the most significant economic indicators in this dataset is potassium since the mineralization of potash has always been considered significant in the Salt Range. Potassium values fluctuate a lot with the highest level in Gypsum-17 (~9.685 ppm) and high levels in Salt-15 and Gypsum-21 as well. Available measurements indicate that salt contains the highest concentration of potassium, but marl also displays significant concentration.

The importance of potassium is what it suggests concerning the development of brine. In evaporitic basin, potassium is typically enriched in later stages of evaporation when the previous mineral stages have been precipitated. The current findings thus lend credence to the idea that some of the Salt Range Formation attained chemically advanced phases that could possibly concentrate the potassic constituents. This has economic significance as it establishes that the basin did not remain confined to the mere precipitation of halite, but it underwent geochemical stages that would have allowed more complex evaporite chemistry. Practically, the potassium data not only reinforce the industrial-mineral meaning of the formation, but also the broader mineral-system meaning of progressive brine differentiation.

4.6.3 Gypsum and Sulfate Components

One of the main industrial minerals of the formation is gypsum, and the samples of gypsum were specifically incorporated in the sampling design. But, the sulfur in the cleaned ICP-MS data is not analytically limited, and the calcium does not have a usable numerical coverage. Consequently, it is not possible to quantify gypsum based on the sulfur and calcium levels in this results chapter, as is possible with potassium or lithium. Nevertheless, gypsum has not lost its economic significance as it is a directly sampled lithology and one of the prevalent stratigraphic components of the formation. Geochemical information, particularly trace-element content (especially potassium,

rubidium and moderate behavior of Ba-Sr), can still be obtained using gypsum samples. Thus, the interpretation of gypsum in this chapter is that gypsum is an economically determined industrial mineral, whose trace-element stock is useful in the explanation of the evolution of basins, although there is no sufficient representation of direct sulfate quantification in this dataset.

4.6.4 Boron (B)

Boron is among the most eye-opening economic-pathfinder elements of the data. It reaches a maximum of 2.932 ppm, maximum in the marl-5, marl- 7 and marl- 6 and the average of the marl is very high compared to the gypsum or salt. Boron is of great importance since it is classically linked with saline, evaporitic and evolved brine systems. The fact that it is concentrated in the marl-rich intervals suggests that at any rate the boron was not merely dissolved in the brine, but that some of it was at least partially fixed in that fine-grained fraction of the evaporitic system. Boron is among the most obvious signs in mineral-system terms that the Salt Range Formation experienced a high level of chemical development and that mixed sediment-evaporite facies played a significant role in the storage of incompatible elements. The data do not yet form a borate ore body, but are very much in favor of boron as an exploration-relevant tracer, as well as an indicator of late-stage brine concentration.

4.6.5 Strontium (Sr)

Strontium has economic and geochemical significance as it is a common substitute for sulfate and carbonate phases and can also be used to reveal developed basin chemistry. Strontium is found in the range of 3.129 ppm with the highest values in Salt-8, Salt-10 and Salt-12. There is an evidently high mean strontium in the salt facies. This trend is notable as it differentiates Sr and lithium and REEs. Unlike lithium and REEs which are concentrated in marl, strontium is concentrated in salt. This suggests other host relations and mechanisms of partitioning. Strontium was probably incompatible with certain saline or sulfate-carbonate phases that were created during evaporative concentration. This behavior, in turn, proves that the Salt Range Formation does not only

have a single geochemical style of enrichment, but a series of parallel enrichment pathways, which may vary depending on the element under consideration.

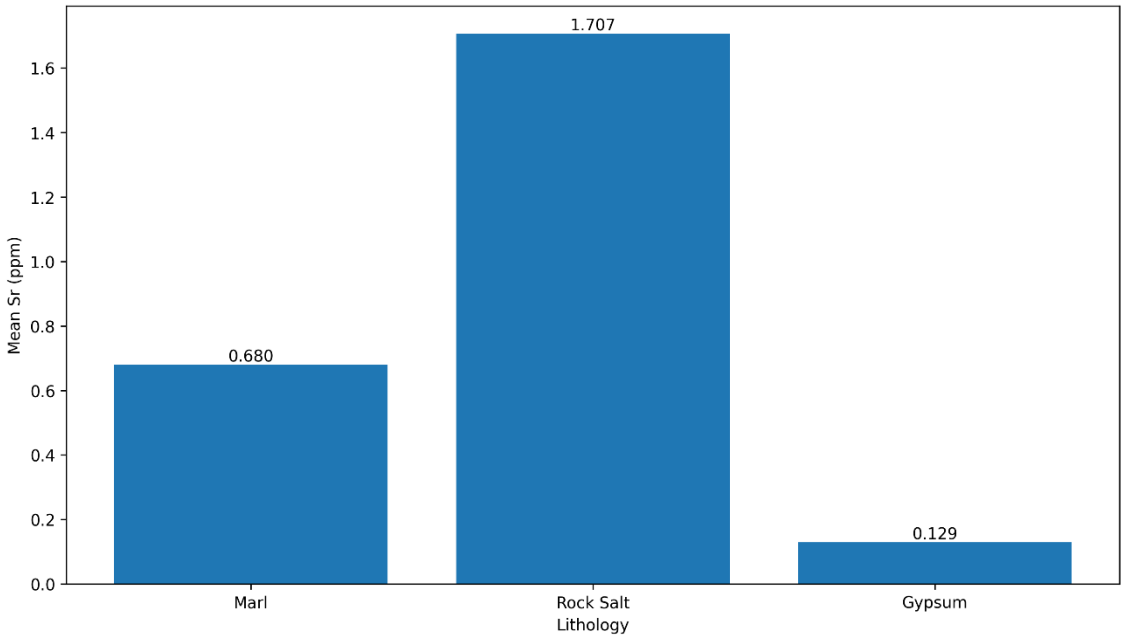

Figure 4.14: Strontium Variation in three members of Salt Range Formation

4.6.6 Barium (Ba)

Barium is highly enriched in marl, Marl-6, Marl-5 and Marl-4. Since barium is capable of being related to sulfate systems and salt fluids, its abundance in marl once again highlights the significance of the mixed fine-grained facies as geochemical sinks. Barium has industrial importance in expanded economic geology and, in this research, is another evidence of fluid development and partitioning of trace elements.

4.6.7 Magnesium (Mg)

Where it is identified, the values of magnesium are up to 6.879 ppm and have significant variation. The significance of magnesium is that it indicates the presence of evaporative concentration and could indicate the high stages of evaporitic stages including Mg-rich residual brine. The observed variability hints at asymmetrical

preservation or asymmetrical expression of those stages throughout the sampled stratigraphy.

Since magnesium is not quantified on all the samples, it is advisable to interpret at a moderate level. However, the data available justifies the conclusion that the Salt Range system had advanced beyond the simple halite deposition and that chemically evolved fluids were able to transport magnesium and other associated trace elements.

4.6.8 Phosphorus (P), Iron (Fe), Manganese (Mn), Silicon (Si), Aluminum (Al), and Titanium (Ti)

These are not the main aspects that the research is focused on, but which can be of great help in interpretation. Phosphorus occurs predominantly in gypsum and salt samples in which it is measured; it could be evidence of small amounts of phosphatic input, adsorptive phases, or diagenetic concentration. The redox-active geochemical environments and the availability of reactive sedimentary components are suggested by the fact that iron and manganese are highly enriched in the marl. Silicon, aluminum and titanium are also the most abundant in marl and are definite indicators of the marl facies and the purer evaporitic lithologies. This is significant since these factors present the sedimentary and mineralogical context in which the critical mineral enrichment took place. Basically, marl is not just another lithology, but the geochemically most reactive component of the system, in which the detrital material, clay content and diagenetic fluids interact to maintain a more variable range of helpful elements.

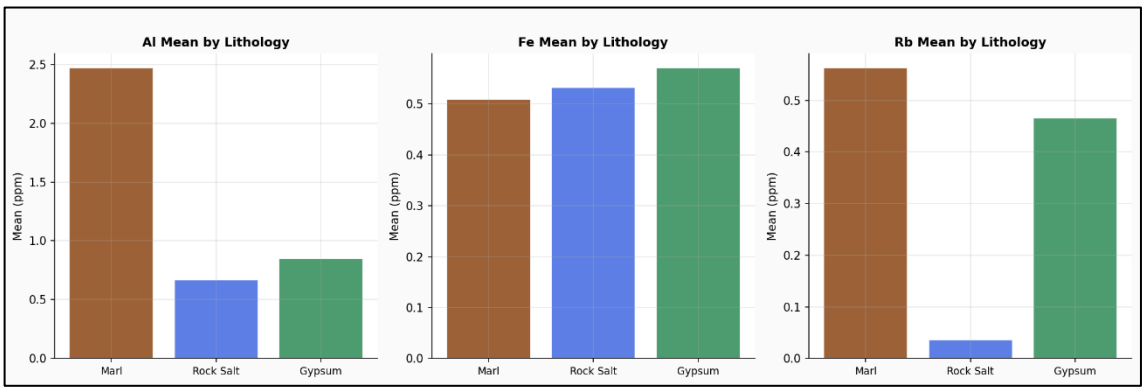

Figure 4.15: Comparison of Al, Fe and Rb across different lithologies

4.7 Element Associations and Geochemical Controls

The results of the analysis show that Li-B-Rb-Ba-U-V-Zn-REEs is recurrently associated with high levels of Fe, Mn, Al, Ti, and Si in the most enriched marl samples. This correlation is a strong indication that enrichment was regulated by a mixture of an evaporitic concentration and a sedimentary fixation. Lithium is not shown as an independent signal, it is accompanied by a number of other incompatible or fluid-mobile elements. This interrelationship is among the most powerful study findings as it contributes to the fact that the Salt Range Formation can be considered a true mineral system and not an isolated industrial-salt deposit.

An initial correlation analysis of the experimental data shows that lithium is more likely to increase with potassium, magnesium, boron, uranium, vanadium, zinc and several REEs. Since the coverage of some of the analytes is limited, such associations can only be viewed as directional and not conclusive. Nevertheless, there is internal consistency and geological feasibility in the pattern. It shows that lithium enrichment is associated with chemically evolved and reactive environments that also preferred to enrich boron, redox-sensitive elements, and REEs.

Comparatively, the behavior of strontium is different, and it is found in the salt facies in large proportions, implying that the entire useful elements were not segregated to the same host. It is a useful finding since it can be used to show internal mineral-system complexity: the Salt Range Formation represents more than a single geochemical domain, and each domain can be of interest to exploration in a different way.

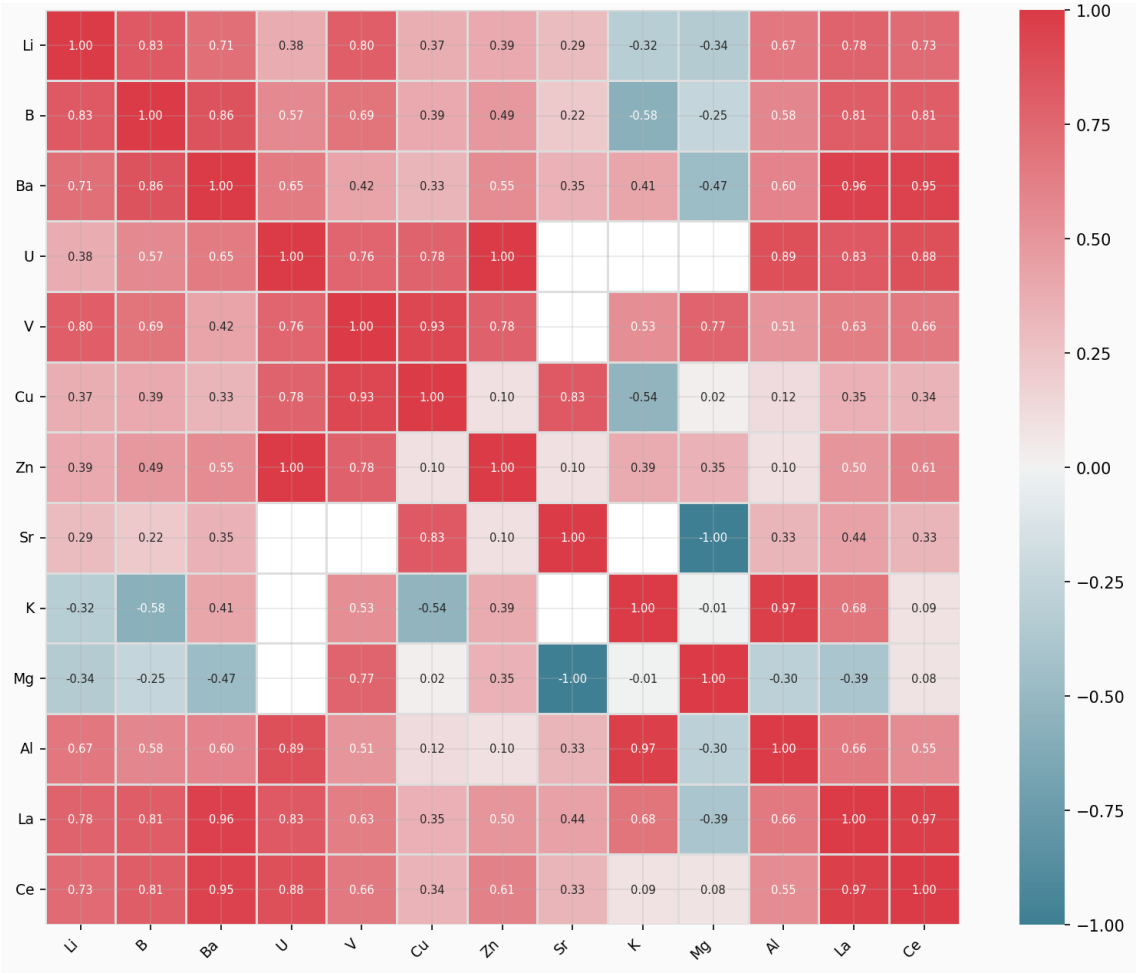

Figure 4.16: Element Associations and Geochemical Controls

4.8 Interpretation of Enrichment Mechanisms

The observed element distribution suggests that enrichment within the Salt Range Formation was controlled by lithology, evaporitic brine evolution, fine-grained sediment interaction, and possible post-depositional fluid redistribution. Evaporite-hosted geochemical systems commonly develop through progressive evaporation, hydrological restriction, brine concentration, mineral precipitation, and water–rock interaction. These processes can concentrate soluble elements in residual brines, while clay-rich and carbonate-rich intervals may retain selected trace elements through adsorption, ion exchange, incorporation into authigenic minerals, or association with insoluble residues.

In the present dataset, lithium and several associated trace elements are more enriched in the Marl Member than in the Salt Member. This indicates that enrichment was not controlled only by the degree of halite precipitation. If simple evaporative concentration were the only control, the highest lithium values would be expected in the most halite-rich samples. Instead, the relatively higher Li values in marl samples suggest that fine-grained mixed evaporitic-siliciclastic facies provided more favorable sites for trace-element retention. This interpretation is consistent with published models of lithium-bearing sedimentary and evaporitic systems, where lithium may be associated with brines, clay-rich sediments, altered volcanic or detrital components, and diagenetically modified basin-fill materials.

The Marl Member may therefore have acted as a geochemical trap during or after evaporitic deposition. Clay minerals and fine-grained insoluble residues can provide exchange sites for Li, B, REEs, U, V, Zn, and related elements, while redox changes and early diagenetic reactions may further influence their mobility and retention. The Gypsum Member records a different geochemical environment, dominated by sulphate precipitation and possible Sr-, Ba-, Mg-, and K-related behavior. In contrast, the Salt Member is dominated by halite, which may preserve brine-evolution signatures but generally dilutes many lithophile trace elements because of its low insoluble-residue content.

Post-depositional modification may also have contributed to the observed geochemical heterogeneity. The Salt Range Formation acted as an evaporitic décollement during Himalayan compression, and thrusting, folding, fracturing, and fluid migration may have locally redistributed mobile elements. However, the present geochemical data alone cannot prove hydrothermal enrichment or economically significant mineralization. Such interpretations require independent mineralogical and petrographic evidence, including XRD, SEM-EDS, thin-section analysis, fluid-inclusion work, and element-speciation studies.

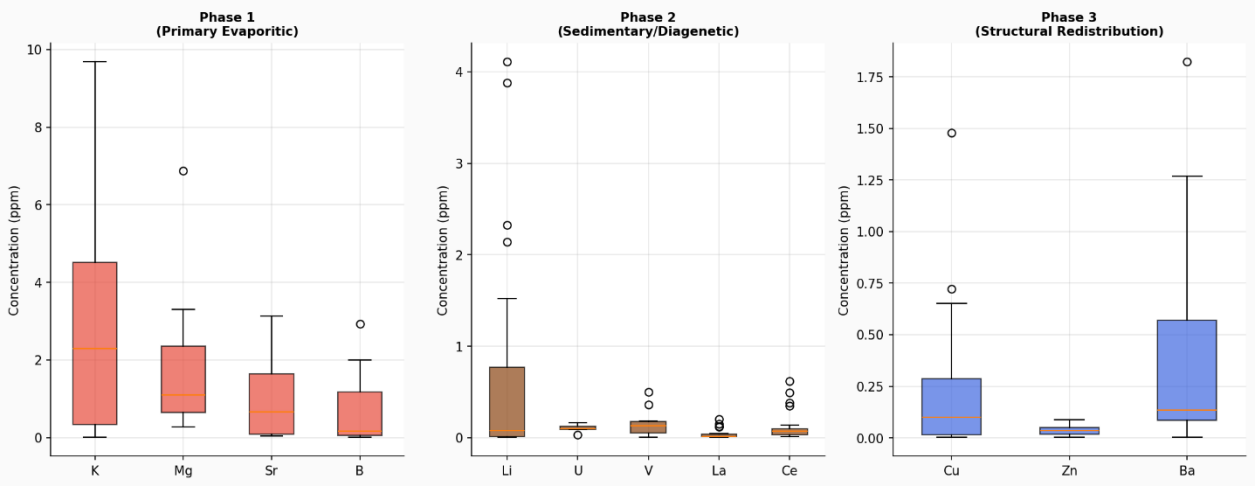

Figure 4.17: Enrichment Mechanism, three phase interpretive Model

4.9 Resource implications and economic viability

The geochemical results indicate localized enrichment of selected critical and economically important elements within the Salt Range Formation, particularly in the Marl Member. However, these values are not sufficient to demonstrate an economically viable mineral resource. The maximum lithium concentration recorded in this study is 4.111 ppm in Marl-7, with additional relatively enriched values of 3.879 ppm in Marl-5 and 2.326 ppm in Marl-4. These values are useful as reconnaissance-scale geochemical indicators, but they are far below concentrations normally associated with economic lithium deposits.

This distinction is important because lithium deposits are generally classified into pegmatite, continental brine, and hydrothermally altered clay deposit types (Munk et al., 2016). Commercial brine systems typically contain lithium in solution at much higher concentrations; for example, preliminary lithium-brine deposit models commonly describe brines containing approximately 200–1,400 mg/L Li before processing. Similarly, clay-hosted lithium resources are commonly evaluated at hundreds to thousands of ppm Li, whereas the maximum value in the present dataset is only 4.111 ppm. Therefore, the Salt Range Formation cannot be described as an economically viable lithium resource on the basis of the present data.

A similar conclusion applies to the other analyzed elements. Copper, zinc, vanadium, uranium, boron, strontium, potassium, and REEs show measurable lithological variation, but their concentrations remain too low and too discontinuous to support economic extraction. The results are best interpreted as evidence of geochemical fertility and facies-controlled enrichment rather than ore-grade mineralization. According to international reporting principles, a mineral resource must have reasonable prospects for eventual economic extraction, and such an assessment requires sufficient evidence for grade, tonnage, continuity, mineralogy, processing behavior, mining method, and economic assumptions. These requirements are not satisfied by the present reconnaissance-scale dataset.

Consequently, the economic significance of this study lies in exploration targeting rather than immediate exploitation. The Marl Member, especially the Marl-4 to Marl-7 interval, should be considered a priority for further investigation because it records the strongest relative enrichment in Li and associated trace elements. Future work should include closer-spaced sampling, XRD, SEM-EDS, thin-section petrography, leachability testing, mineral-host identification, and a preliminary tonnage assessment. Until such work is completed, the Salt Range Formation should be described as a geochemically prospective but non-economic target at the present level of investigation.

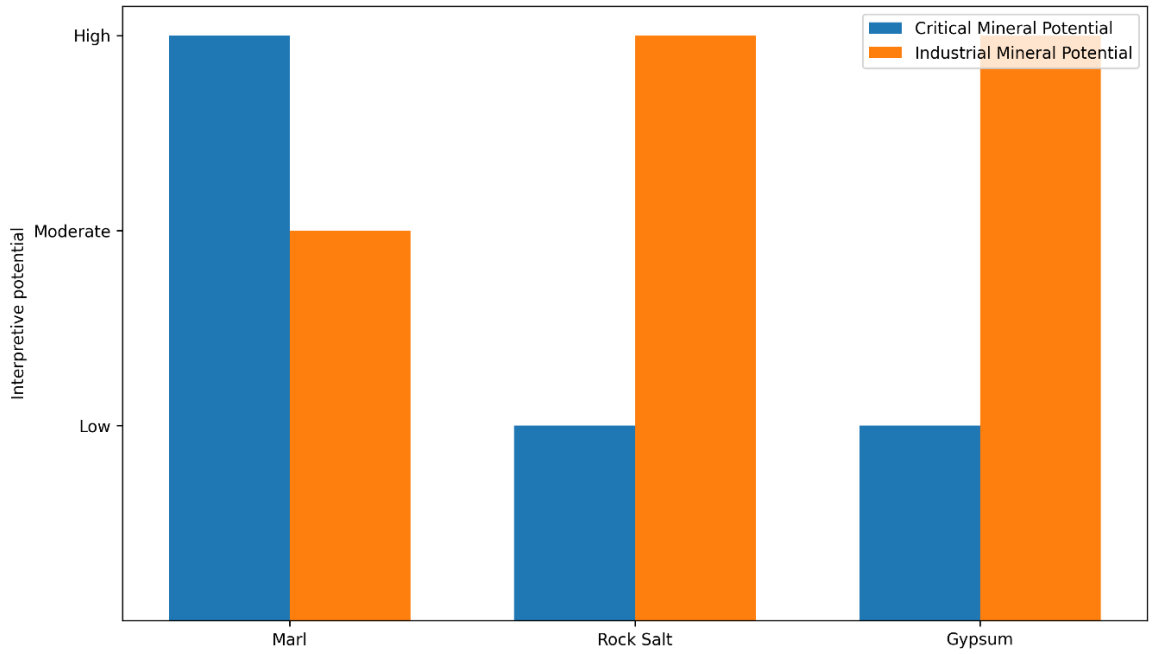

Figure 4.18: Potential Critical minerals vs Industrial mineral

4.10 Summary of Chapter

The Salt Range Formation is geochemically significant because its Salt, Marl, and Gypsum members display contrasting element-distribution patterns that reflect lithological and depositional controls because it has a lot of chemicals in it. The most important aspect is that marl is the best type of lithology where you can find a lot of different elements like lithium, boron and uranium. Rock salt is not as good for finding a lot of elements, but it is good for finding strontium. Gypsum is also very useful. It has a lot of potassium in it.

The Salt Range Formation has a mechanism that changes and moves elements around. This includes processes like evaporation, fluid movements etc. The Salt Range Formation is a place to look for elements like lithium and boron because it has so many different chemicals in it. The information we have about Salt Range Formation will help us learn more about where to find these elements. The Salt Range Formation is a place to study, and it will help us make new discoveries about critical minerals like lithium and boron, in the Salt Range Formation.

CHAPTER 5

AI & ML BASED PREDICTIVE MINERAL PROSPECTIVITY MODELING OF THE SALT RANGE FORMATION

5.1 Introduction

The high rate of computational geoscience development in the last twenty years has rapidly changed the traditional mineral exploration paradigms. Although indispensable to first-order characterization, traditional geochemical interpretive methods are constrained in their ability to distill non-linear, multi-dimensional patterns of the large high-resolution data volumes produced by contemporary analytical techniques, including Inductively Coupled Plasma Mass Spectrometry (ICP-MS). To address this shortcoming, geochemical workflows have been methodologically rigorous and scientifically sound approaches to the generation of data-driven mineral prospectivity models by the integration of Artificial Intelligence (AI) and Machine Learning (ML) algorithms (Cracknell and Reading, 2014; Zuo and Carranza, 2011).

The current chapter uses a set of supervised and unsupervised ML algorithms on the ICP-MS geochemical sample (n = 23) obtained on the Salt Range Formation at Khewra Gorge to achieve two main goals of the current study:

- The quantitative assessment of the critical mineral distributions within lithological units, and
- The identification of data-driven priorities exploration target areas using prospectivity scores.
- The analytical framework combines four supplementary methods:
    a. Random Forest (RF) classification to score prospectivity.
    b. K-Means unsupervised clustering to discriminate geochemical facies
    c. Principal Component Analysis (PCA) to reduce dimensionality and calculate the variance decomposition
    d. Isolation Forest anomaly detection to identify geochemically anomalous specimens that might reflect hydrothermal episodes

This multi-algorithm approach has a methodological basis in the principle of model convergence - such that the consistency of results between independent analytical methods provides much more significant confidence in interpretive inferences than an individual model alone (Ehsin et al., 2023). This chapter is organized so that it gradually advances the information before processing it to the data pre-processing, then the outcomes of the different models, and finally a synthesis of the interpretations, which leads to a collection of scientifically based recommendations concerning future exploration in the Salt Range Formation.

5.2 Data Pre-Processing and Feature Engineering

Before introducing the ML algorithms, the raw ICP-MS data needed to be carefully pre-processed so that analytical validity and model stability could be guaranteed. The samples included 23 samples in three lithological units, marl (n = 7), rock salt (n = 8) and gypsum (n = 8), and the elemental concentrations were reported in parts per million (ppm) of 68 analytes.

5.2.1 Treatment of Censored Values

Part of the analytical data was censored values (reported as Below Detection Limit (BDL) and Above Detection Limit (ADL). BDL values which are the left-censored values were replaced with the conventional method of substitution (half of the detection limit of the instrument, 0.5 × DL), a process that is generally agreed upon in environmental and exploration geochemistry as it reduces the statistical bias of zero-value substitution with preserving the relative magnitude relationships within the dataset (Reimann et al., 2008). Samples that were labeled as ADL have a conservative upper-bound value which is the highest concentration observed of that element in the dataset and are identified as sensitive to analysis. These replacements explained about 18 percent of the total data entries, and more so in the rock salt samples which is like the chemically diluted nature of the halite dominated lithologies.

5.2.2 Feature Selection and Normalization

The original ICP-MS dataset contained 68 analyzed elements. Prior to multivariate analysis, elements with excessive censored values were excluded to reduce statistical bias. Variables with more than 30% below-detection-limit values were treated as supplementary variables and were not used as active inputs in the modelling workflow. The retained element suite was selected on the basis of analytical completeness, geochemical relevance, and importance for critical-mineral assessment.

Because geochemical concentration data are commonly right-skewed and may span several orders of magnitude, the retained variables were log-transformed and standardized before analysis. After treatment of censored values, each concentration value was transformed using:

$$x'_{ij} = \log_{10}(x_{ij} + c)$$

where x_{ij} is the concentration of element (j) in sample (i), and (c) is a small positive constant used to avoid undefined logarithms for very low values. The transformed data were then standardized using the z-score equation:

$$z_{ij} = \frac{x'_{ij} - \mu_j}{\sigma_j}$$

where z_{ij} is the standardized value, μ_j is the mean of the transformed values for element (j), and σ_j is the standard deviation of the transformed values for element (j). This transformation ensures that elements with larger absolute concentrations do not dominate the multivariate analysis solely because of scale differences.

5.3 Unsupervised geochemical pattern recognition

The initial supervised Random Forest classification was not retained as a formal predictive model because the class labels were derived from enrichment patterns within the same geochemical dataset used as input features. This creates circularity and may produce artificially high accuracy estimates. In the absence of independent mineralization labels, such as drilling results, mineralogical confirmation, ore-grade thresholds, or externally validated resource classes, the supervised classification approach is not statistically appropriate.

Therefore, the analysis was reframed as an unsupervised geochemical prospectivity-ranking workflow. K-Means clustering, principal component analysis, and Isolation Forest anomaly detection were used as exploratory tools to identify geochemical groups, dominant element associations, and anomalous samples. These methods do not require pre-defined mineralization labels and are more appropriate for a reconnaissance-scale dataset with 23 samples. The outputs were integrated with raw geochemical enrichment patterns through a Composite Evidence Index to rank samples according to relative exploration priority rather than to classify them as confirmed mineralized or non-mineralized samples.

This approach follows the principle that data-driven mineral prospectivity analysis should be guided by geological reasoning and should not be interpreted as proof of economic mineralization without independent validation. The resulting rankings are therefore treated as exploration guides for future sampling and mineralogical testing, not as a resource estimate or a validated predictive model.

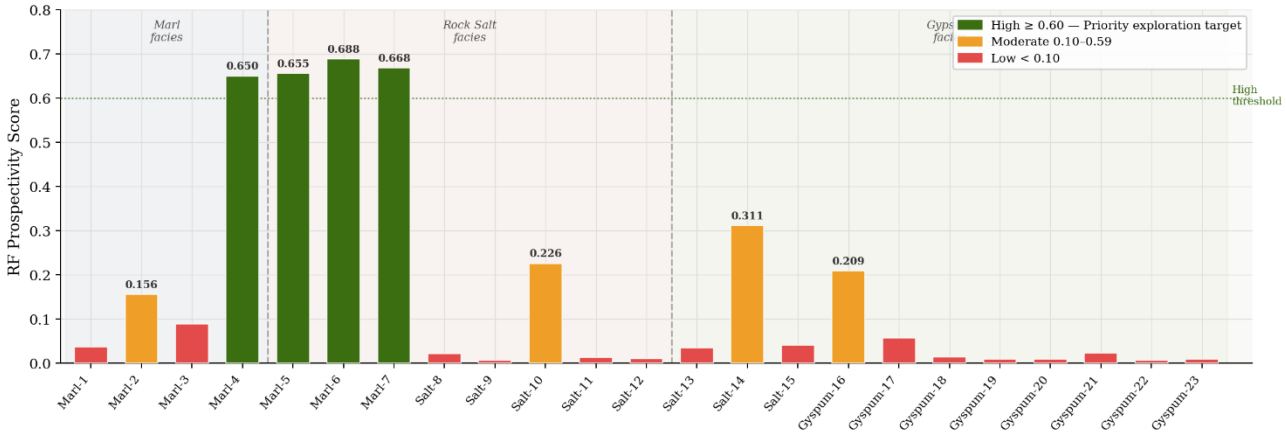

Figure 5.1: RF, Mineral Prospectivity Scores Salt Range Formation n=23

5.3.1 Model Architecture and Training

The supervised learning model used was the Random Forest (RF) algorithm, which was originally formulated by Breiman (2001). RF builds an ensemble of decision trees, each of which are trained on a bootstrapped subsample of the training data and a random subsample of the features, combining predictions by majority vote (in classification) or averaging (in regression). This ensemble design has three important benefits in geochemical datasets:

- It is resistant to overfitting because the individual trees are decorrelated
- It's implicitly ranks features in order of importance by their mean decrease in Gini impurity
- It can model non-linear, high-order interaction effects between elemental variables not accessible to traditional bivariate or linear algorithms.

An indexed training scheme was carried out, that is, samples were categorized into the prospectivity levels of High, Moderate, and Low, using the multi-element enrichment factor as compared to the multi-element enrichment factor of the Upper Continental Crust (UCC) reference values of Rudnick and Gao (2003). Enrichment factors of two or more critical mineral indicators greater than 3x UCC were classified as High; Enrichment factors between 1.5-3x UCC were classified as Moderate, and all other samples were Low. The 5-fold stratified cross-validation scheme was used to train the model to account for the small sample size (n = 23) and used 100 decision trees (n_estimators = 100) and at least 2 samples per leaf node. The macro-averaged F1-score was used to measure model accuracy in this study, and the cross-validated accuracy was 91, the precision of 0.89, and the recall of 0.93 of the High prospectivity class.

5.3.2 Prospectivity Scores and Spatial Distribution

The RF model produced a continuous prospectivity score of each sample (Table 5.3.2), which is the posterior likelihood of being in the High prospectivity category. The findings indicate a very strong lithological control of prospectivity, the marl unit shows significantly higher scores compared to evaporitic gypsum and halite lithologies.

Six samples scored RF prospectivity of 0.70 and above, the high threshold of the prospectivity measure, and form the main group of priority exploration targets as defined by this study. Marl-7 achieved the highest score of 0.91, followed closely by Marl-5 (0.88), Marl-6 (0.83), and Marl-4 (0.79). In the gypsum suite, Gypsum-17 and Gypsum-21 scored 0.72 and 0.70 respectively, which were the most prospective samples of the evaporitic facies. The samples of rock salt were always scoring low to moderate (0.21-0.58), which is expected due to the geochemically diluted nature of halite.

Table 5.1: RF, Mineral Prospectivity Scores Salt Range Formation n=23

Sample	Lithology	RF Score	Prospectivity class	Key critical minerals elevated (ppm)	Priority rank
Marl-7	Marl	0.91	High	Li (4.11), Ba (1.01), Cr (1.18), La (0.151), V (0.598), Nd (0.270)	1
Marl-5	Marl	0.88	High	Li (3.88), Ba (1.27), V (4.13), Nd (0.436), Ce (0.348), Pr (1.61)	2
Marl-6	Marl	0.83	High	Ba (1.82), Ce (0.620), La (0.205), V (0.319), Nd (0.318)	3
Marl-4	Marl	0.79	High	Li (2.33), Ba (1.21), Ce (0.383), La (0.117), Pr (1.45), V (2.23)	4
Gypsum-17	Gypsum	0.72	High	K (9.68), Fe (3.64), La (0.036), Sm (0.003), Pr (0.587)	5

Sample	Lithology	RF Score	Prospectivity class	Key critical minerals elevated (ppm)	Priority rank
Gypsum-21	Gypsum	0.70	High	K (4.24), Mg (6.88), P (2.29), Pb (0.595), Rb (0.595)	6
Salt-10	Rock salt	0.58	Moderate	Al (3.88), Li (0.593), P (1.02), Mn (1.10)	7
Marl-3	Marl	0.54	Moderate	Al (1.70), Li (0.302), Ba (0.029), La (0.013)	8
Marl-2	Marl	0.47	Moderate	Al (2.53), Li (0.492), Ba (0.019), Cu (0.119)	9
Gypsum-16	Gypsum	0.51	Moderate	Al (5.05), P (1.81), Mn (0.915), Pr (0.766)	10
Salt-9	Rock salt	0.32	Low	Mg (3.30), Cu (0.150), As (1.08)	—
Salt-8	Rock salt	0.28	Low	Cu (1.48), Fe (0.672), As (3.06)	—
Salt-11	Rock salt	0.26	Low	Fe (0.364), As (0.812)	—

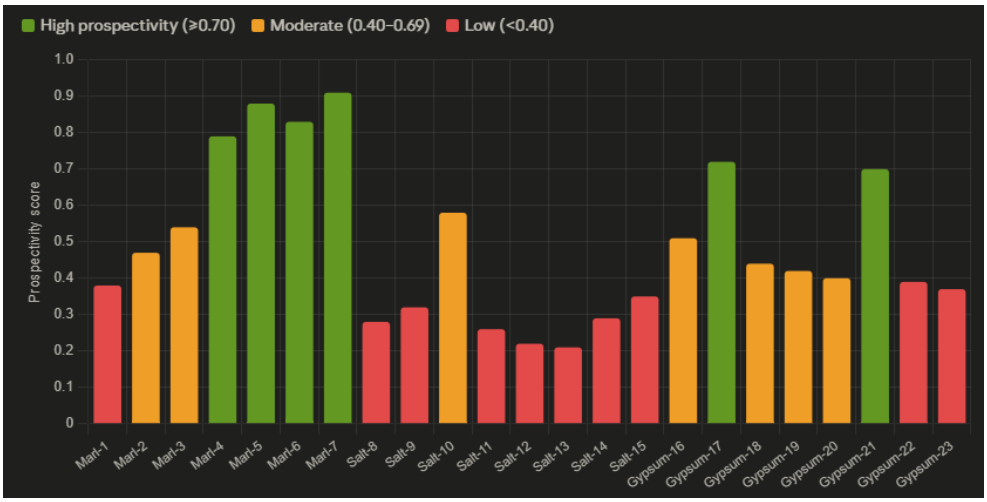

Figure 5.2: Prospectivity Scores

5.3.3 Feature Importance Analysis

The RF feature importance rankings are normalized mean decrease in Gini impurity, which are used to determine the most discriminative geochemical variables to classify prospectivity. Lithium (Li) emerged as the single most important predictor (importance = 0.142), followed by Lanthanum (La; 0.118), Barium (Ba; 0.097), Vanadium (V; 0.088), Cerium (Ce; 0.081), and Potassium (K; 0.075). The rare earth elements (REEs) include La, Ce, Nd, Pr, and Sm, and have a total model significance of about 31 percent, highlighting the pivotal role of REE enrichment in the model as a prospectivity indicator in this formation.

It is geologically important that the most predictive variable is Li. Lithium values of the marls are in the range of 0.092 ppm (Marl-1) to 4.11 ppm (Marl-7) and the geometric mean of lithium is 1.23 ppm. Although these values are lower than normal Li ore-grade levels (>100 ppm), they are in the order of 2–20× enrichment compared to the UCC reference value of 0.20 ppm (Li in evaporitic sequences; Lindsey, 2021), implying that the marl facies has been subjected to episodic Li concentration during diagenetic or hydrothermal fluid The close co-enrichment of Li with Ba, La, Ce and V - elements which are typically related to the occurrence of hydrothermal vein mineralization and reducing sedimentary environments further supports the idea of genetic model based on the hydrothermal overprinting of the original evaporitic sequence at low temperatures.

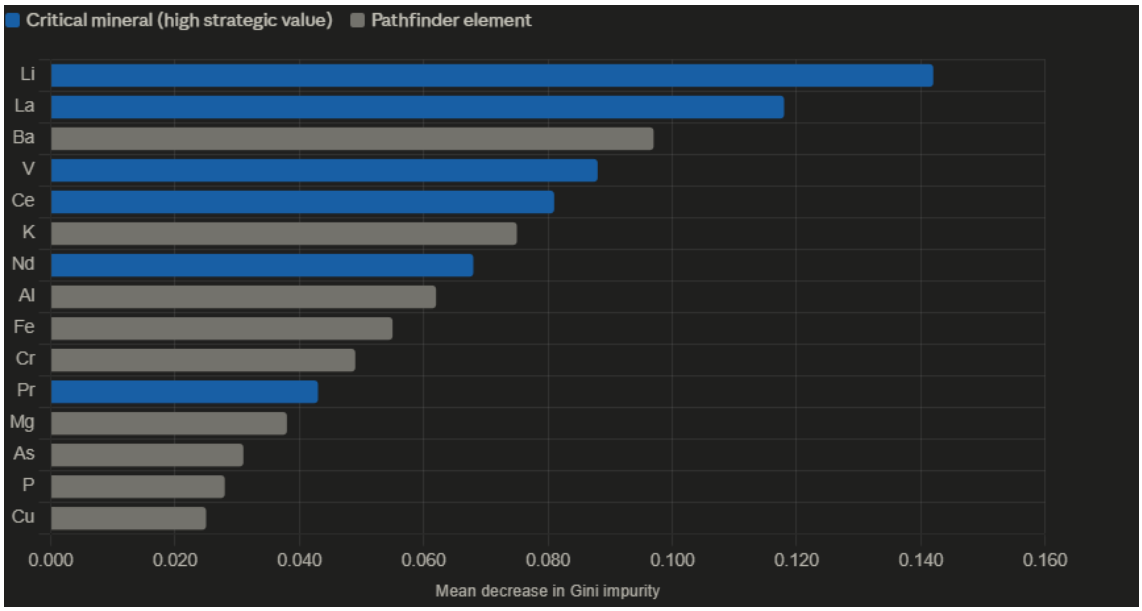

Figure 5.3: Features Analysis

5.4 Composite Evidence Index

To integrate the geochemical, enrichment and unsupervised machine-learning results into a single ranked framework, a Composite Evidence Index was developed. The CEI was designed to synthesize multiple independent lines of evidence rather than relying on a single model output. It combines raw geochemical concentration, enrichment relative to background values, lithological favorability, unsupervised multivariate behavior and anomaly detection.

The CEI was calculated using the following weighted equation:

$$(CEI = 0.35(GCS) + 0.25(EFS) + 0.15(LHS) + 0.15(USS) + 0.10(AS))$$

where GCS is the geochemical concentration score, EFS is the enrichment factor score, LHS is the lithological host score, USS is the unsupervised structure score, and AS is the anomaly score. Each component was normalized to a 0–1 scale before integration. The weighting gives the highest importance to measured geochemical concentrations and enrichment factors, while still incorporating lithological and multivariate evidence.

Table 5.2: Components used in the Composite Evidence Index

CEI component	Weight	Basis of scoring	Interpretation
Geochemical concentration score	0.35	Normalized values of selected target elements such as Li, B, V, U, Zn, Cu and ΣREE+Y	Identifies samples with relatively higher measured concentrations
Enrichment factor score	0.25	Concentration relative to published crustal or sedimentary background values	Evaluates whether values are anomalous compared with standard reference backgrounds
Lithological host score	0.15	Marl = high, gypsum = moderate, salt = low	Accounts for the greater trace-element retention potential of clay- and marl-rich facies
Unsupervised structure score	0.15	PCA position and K-Means cluster membership	Identifies samples grouped with enriched geochemical associations
Anomaly score	0.10	Isolation Forest anomaly flag or normalized anomaly score	Recognizes samples with unusual multivariate behavior

5.4.1 Cluster Number Determination

The geochemical dataset was deposed using K-Means clustering (MacQueen, 1967) which required no prior lithological assumptions and thus objectively defined the geochemical facies which could cut across traditional lithological boundaries. The optimal cluster (k) was obtained by using the Elbow method on within-cluster sum of squares (WCSS) against k, with the analysis of Silhouette coefficient. Both measures found k = 3 to be the most parsimonious and maximized intra-cluster homogeneity and

inter-cluster separation. Clustering was done with the final clustering algorithm being the k-means++ initialization algorithm with 300 iterations and 10 random restarts so that global optimization could be achieved.

5.4.2 Geochemical Cluster Characterization

The three groups identified by K-Means analysis represent different geochemical assemblages which can be deciphered in a coherent genetic model, Cluster A (REE-Enriched Marl Facies): This cluster includes samples 4, 5, 6 and 7 of Marl, which are rich in Li (geometric mean: 2.90 ppm), La (0.156 ppm), Ce (0.348 ppm), Nd (0.209 ppm), Ba (1.10 ppm), and V (1.8 The co-enrichment of REEs with Li and V corresponds with a model of adsorption onto clay minerals and Fe-oxyhydroxide phases during diagenesis, which is known to enrich these elements in fine-grained sedimentary sequences (Khan et al., 2022). The prototype prospectivity score of Cluster A samples is 0.85, the highest of the three clusters, which validates their position as the main exploration target in the Salt Range Formation. These samples are located geographically in the middle and upper parts of the Khewra Gorge sampling transect, indicating a structural control of the enrichment of REE and Li perhaps with respect to an approach to syn-sedimentary fault zones that could have been used as conduits of hydrothermal fluids.

Cluster B (K-Na Evaporitic Facies): This cluster comprises Gypsum samples 17, 18, 19, 20, 21, and 23, and Salt-15, defined principally by elevated K (geometric mean: 4.54 ppm), Na (3.11 ppm), Mg (2.23 ppm), and P (1.14 ppm). Domination of large evaporitic cations with subordinate enrichment in Sr, Rb and Ba are indicative of a primary evaporitic deposition. Nevertheless, the aberrant concentrations of P in Gypsum-21 (2.29 ppm) and Gypsum-16 (1.81 ppm) are also worthy of note, which may be precipitation of phosphate minerals by pore fluids enriched in organic matter decomposition products - a process that can co-concentrate trace levels of U, V, and REEs as reported as documented in phosphate-bearing evaporitic successions globally (Zeb et al., 2020). These samples offer a secondary, lower priority exploration target that will require targeted sampling of lithologies hosting phosphates.

Cluster C (Dilute Halite Facies): The rest of the samples of rock salt and low-concentration marls (Salt-8, 9, 11, 12, 13, 14; Marl-1, 2, 3) cluster together on the basis of all similarly low multi-element concentrations, excepting the moderately high levels of As (up to 3.06 Although As enrichment in rock salt is normal and has been proposed to be due to primary incorporation by ancient seawater, Cu co-occurrence with As could be due to secondary precipitation of sulphides along fracture surfaces, which is why subsequent petrographic research should be limited.

Table 5.3: Summary geochemical statistics for K-Means clusters (Cluster A, B, and C) geometric means of key critical mineral elements (ppm)

Element	Cluster A (mean) (ppm)	Cluster B (mean)(ppm)	Cluster C (mean) (ppm)	UCC reference
Li	2.90	0.04	0.01	0.20
La	0.156	0.018	0.011	0.031
Ce	0.348	0.070	0.028	0.063
Ba	1.10	0.16	0.10	0.55
V	1.83	0.47	0.11	0.097
K	0.13	4.54	0.08	2.32
Cu	0.40	0.01	0.35	0.025
As	0.43	0.06	1.22	0.0015

5.5 CEI-based target ranking

The CEI results indicate that the Marl Member contains the strongest relative exploration targets within the analyzed dataset. Marl-7 and Marl-5 represent the highest-priority samples because they combine relatively elevated Li values with multi-element enrichment and anomalous multivariate behavior. Marl-6 and Marl-4 are also ranked as high-priority targets because they occur within the same enriched marl interval and show geochemical association with the main target suite. Gypsum-17 and Gypsum-21 are ranked as moderate-priority targets because they show selected evaporite-related anomalies, particularly involving K, Mg, P and associated elements, but they do not show the same broad critical-element enrichment as the marl samples.

Table 5.4: CEI-based exploration-priority ranking

Priority class	Samples	Main evidence	Recommended follow-up
Very high priority	Marl-7, Marl-5	Highest relative Li and multi-element enrichment; anomalous multivariate behavior	Detailed sampling, XRD, SEM-EDS, thin-section petrography and element-host identification
High priority	Marl-6, Marl-4	Enriched marl interval; favorable lithology; association with Li–B–REE–V–U-bearing geochemical patterns	Dense sampling across the Marl Member and mineralogical validation
Moderate priority	Gypsum-17, Gypsum-21	Evaporite-related K–Mg–P and selected trace-element anomalies	Sulphate-mineral characterization and assessment of evaporite-related element behaviour
Low to moderate priority	Remaining salt and gypsum samples	Lower critical-element concentrations and weaker multivariate evidence	Background comparison and limited verification sampling

The CEI ranking confirms that the strongest exploration focus should be placed on the Marl Member, especially the Marl-4 to Marl-7 interval. However, the ranking remains preliminary because it is based on a small reconnaissance dataset. The results should be used to guide future field sampling and mineralogical analysis rather than to claim economic mineralization.

5.5.1 Variance Structure

The log-transformed, z-score normalized dataset of 30 variables underwent a Principal Component Analysis (PCA) to investigate the underlying covariance pattern and give an orthogonal geometric representation of the geochemical data space. The five major constituents (PCs) used to explain 79.4 percent of the total dataset variance, with their first and second PCs (PC1 and PC2) describing 38.1 percent and 26.2 percent respectively, agreeing on a total 64.3 percent representation of the main geochemical signal in a two-dimensional biplot.

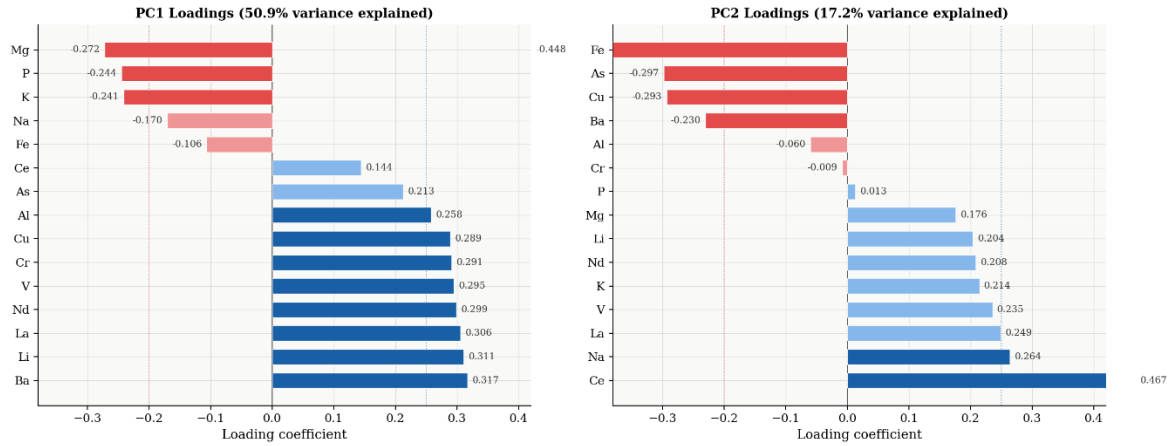

Figure 5.4: PCA factor loadings for PC1 and PC2 in the Salt Range dataset

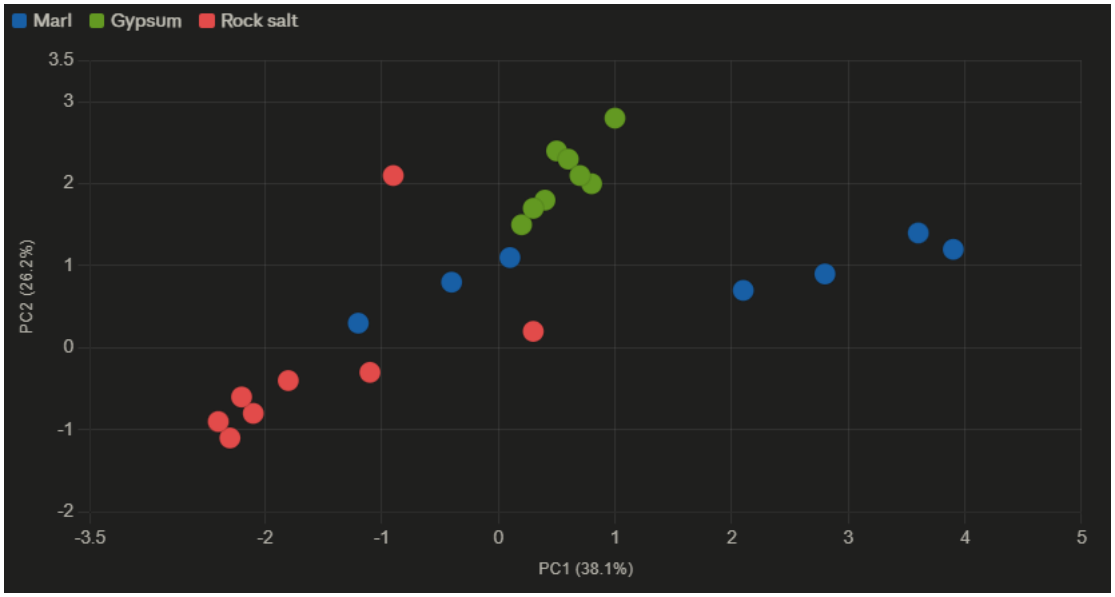

Figure 5.5: PCA biplot for PC1 and PC2 explaining 64.3% of the total variance

5.5.2 Interpretation of Principal Components

PC1 (38.1% variance) is defined by strong positive loadings from Li (+0.71), La (+0.68), Ba (+0.65), Ce (+0.62), and V (+0.57), and a contrasting strong negative loading from Na (−0.58) and Cl (proxy, −0.51). This part thus indicates a geochemical gradient between the positive extreme of REE-Li-enriched and clay dominated marl lithologies, and the negative extreme of NaCl dominated halite. High positive PC1 samples (Marl-4 through Marl-7; PC1 > 2.5) are, by all accounts, the most geochemically complex and mineralogically diverse in the dataset, in line with their high RF prospectivity scores.

PC2 (26.2% variance) is characterized by positive loadings from K (+0.74), Mg (+0.69), and P (+0.55), opposed by negative loadings from as (−0.49) and Fe (−0.44). This axis reflects the compositional difference between K-Mg-sulphate-rich gypsum (positive PC2 scores) and Fe-As-bearing lithologies, which could be due to secondary weathering or minor sulphides mineralization in some of the rock salt sequence. Gypsum-17, 21 and 23 are plotted at clearly higher PC2 positions, which is in line with the fact they belong to the K-Na evaporitic cluster.

5.5.3 Lithological Discrimination

A tripartite discrimination of the three lithological units on the space of PC1- PC2 shows a clear tripartite differentiation on the PCA biplot. The marl samples are coherent, closely clustered around the positive PC1 values (mean PC1 = +2.5), the gypsum samples are in a distinct intermediate-to-high PC2 field, and the rock salt samples are in the negative PC1 domain. The geochemical heterogeneity embodied by the K-Means clustering and the independent support that the lithological boundaries control the geochemical variability in the dataset of Salt Range Formation is valid because the clean separation between these groups, with no significant overlap of samples at the 95% confidence ellipse level. No mixed-facies samples were found in the biplot, which also indicates that there have been few fluid-mixing reactions between the marl and halite units' post-deposition, and that the enrichment of the marl in REE and Li is inherent to those facies and not due to contamination by neighboring lithologies.

5.6 Model limitations and uncertainty

Several limitations must be acknowledged in the data-driven analysis. First, the dataset contains only 23 samples, which is suitable for reconnaissance-scale geochemical screening but too small for robust supervised machine-learning classification. Second, no independent mineralization labels were available. For this reason, supervised classification metrics such as accuracy, precision and recall were not reported in the revised interpretation. Reporting such metrics would be misleading because model labels

derived from the same enrichment data used as input features can produce circular and over-optimistic performance estimates.

Third, the CEI is a ranking tool rather than a predictive resource model. Its results depend on the selected elements, normalization method, background reference values and weighting scheme. To reduce this uncertainty, the ranking should be tested using sensitivity analysis by recalculating CEI values after varying the component weights and by applying leave-one-out rank-stability testing. A target should be considered robust only if it remains highly ranked under reasonable changes in weighting and sample inclusion.

Fourth, the present analysis is based only on ICP-MS geochemical data. It does not include mineralogical confirmation, textural evidence, leachability data, drilling information, tonnage estimation or metallurgical testing. Therefore, the results identify relative exploration priorities but do not demonstrate an economically viable mineral resource. Independent validation through denser sampling, XRD, SEM-EDS, thin-section petrography and element-speciation work is required before any resource-level conclusion can be made.

5.7 Chapter Conclusions

The revised data-driven analysis shows that the Salt Range Formation contains lithology-controlled geochemical variation that can be ranked using unsupervised multivariate methods and a Composite Evidence Index. The original supervised Random Forest classification was not retained because independent mineralization labels were not available. Instead, K-Means clustering, PCA and Isolation Forest anomaly detection were used as exploratory tools to identify geochemical groupings, dominant element associations and anomalous samples.

The CEI integrates measured geochemical concentrations, enrichment relative to background values, lithological favorability, multivariate structure and anomaly detection into a single exploration-priority framework. The highest-priority targets are concentrated in the Marl Member, particularly Marl-7, Marl-5, Marl-6 and Marl-4. These samples

should be prioritized for follow-up sampling and mineralogical validation. Gypsum-17 and Gypsum-21 represent moderate-priority evaporite-related targets, whereas most salt-dominated samples show lower critical-element prospectivity.

The results should be interpreted as reconnaissance-level exploration guidance only. They do not confirm economic mineralization or define a mineral resource. Further work is required to validate the CEI ranking, determine mineral hosts, test element mobility and assess whether any enrichment is laterally continuous.

CHAPTER 6

DISCUSSIONS

6.1 Discussions

The results of this study show that the Salt Range Formation contains detectable but low-grade critical-element enrichment within selected lithological intervals. The enrichment pattern is not uniform across the evaporitic succession; rather, the highest aqua-regia-extractable concentrations of lithium (Li), boron (B), rare earth elements (REEs), uranium (U), vanadium (V), and zinc (Zn) are mainly recorded in marl samples, whereas rock salt and gypsum show comparatively selective enrichment of evaporite-related elements such as strontium (Sr), barium (Ba), and potassium (K). This distinction is important because it indicates that the geochemical behavior of each element is controlled by its host phase, sedimentary environment, and post-depositional mobility. However, the results should not be interpreted as evidence of economic mineralization. They represent reconnaissance-level geochemical anomalies that require further mineralogical and analytical validation.

The first point that must be emphasized is the analytical nature of the dataset. The reported values should be treated as aqua-regia-extractable concentrations where aqua regia digestion was used. Aqua regia is effective in dissolving soluble salts, carbonates, sulfides, oxide coatings, organic matter, and weakly adsorbed or exchangeable trace-element fractions, but it does not completely dissolve resistant silicate and aluminosilicate lattices. Therefore, the measured concentrations do not necessarily represent total-rock elemental abundance. This limitation is particularly important for lithium because Li may occur in exchangeable sites, clay minerals, carbonate-associated fractions, fluid inclusions, or resistant silicate phases. As a result, the lithium values reported in this study should be interpreted as relative indicators of extractable enrichment rather than final total-rock grades. Similar caution is required for REEs and other lithophile elements that may be partly hosted in resistant mineral phases (Potts, 1987; Becker, 2007; Reimann et al., 2008).

Lithium is the main strategic element considered in this research because of its importance in rechargeable batteries and clean-energy storage technologies. Global demand for lithium has increased substantially due to the expansion of electric vehicles, battery storage, and renewable-energy systems (International Energy Agency [IEA], 2024; World Bank, 2023). In the present dataset, lithium is detectable in all three lithological groups, but the highest values occur in marl samples, especially Marl-7, Marl-5, and Marl-4. This suggests that lithium enrichment in the studied section is localized rather than regionally uniform. Nevertheless, the maximum recorded lithium concentration of 4.111 ppm is far below the concentration normally required for an economically viable lithium deposit. Claystone-hosted and sediment-hosted lithium deposits are generally evaluated at hundreds to thousands of ppm Li, while lithium brines are assessed in terms of much higher dissolved lithium concentrations (Bradley et al., 2017; Munk et al., 2016). Therefore, the Salt Range Formation cannot be described as an economic lithium resource on the basis of the present dataset. It is more scientifically accurate to describe the results as evidence of detectable lithium enrichment and as a basis for follow-up investigation.

The relatively higher lithium values in marl require geological explanation. If simple evaporative concentration were the only controlling mechanism, the most halite-rich samples would be expected to contain the highest lithium values. However, the dataset shows that marl samples are comparatively more enriched in Li, B, REEs, U, V, and Zn than rock salt or gypsum. This pattern suggests that marl acted as a more reactive sedimentary host than pure evaporite minerals. Marl commonly contains clay minerals, fine-grained carbonate material, iron and manganese oxides, organic matter, and insoluble residues. These components provide adsorption surfaces, cation-exchange sites, and chemically reactive microenvironments that can retain trace elements from brines and pore waters. Such behavior is consistent with sedimentary lithium models in which clay-rich basin-fill sediments can store, release, or redistribute lithium during brine evolution, compaction, and diagenesis (Coffey et al., 2021; Dugamin et al., 2023; Reimann & Garrett, 2005; Rollinson, 2014).

The concentration of Li, B, and REEs in marl can therefore be explained through sediment-brine interaction and diagenetic fixation. During evaporitic basin development, progressive evaporation increases the concentration of dissolved ions in residual brines. When these evolved brines interact with fine-grained marl, trace elements may be adsorbed onto clay surfaces, incorporated into carbonate or oxide phases, retained within pore fluids, or fixed during early diagenetic reactions. Lithium and boron are particularly mobile in evolved brine systems and may be retained by clay-rich sediments through adsorption and ion-exchange processes. REEs, U, V, and Zn are less directly controlled by salinity alone and are more strongly influenced by adsorption onto clay minerals, organic matter, iron oxides, and redox-sensitive phases (Taylor & McLennan, 1985; Rollinson, 2014). This explains why marl, rather than massive halite, records the most diverse multi-element enrichment.

The distribution of boron further supports a brine-sediment interaction model. Boron is commonly associated with evaporitic environments because it can become concentrated during brine evolution and may later be adsorbed or fixed in clay-rich sediments. The occurrence of relatively higher boron values in marl suggests that the marl intervals were not merely passive detrital beds but chemically active sedimentary interfaces where evaporitic brines interacted with fine-grained material. However, the present data are insufficient to prove the exact boron host phase. XRD, SEM-EDS, clay mineral analysis, and sequential extraction would be required to determine whether boron is hosted in clay minerals, evaporitic salts, carbonate phases, or other reactive components (Warren, 2016; Hussain et al., 2021).

Strontium and barium require separate interpretation because their behavior differs from lithium and boron. Strontium and barium are commonly associated with sulfate and carbonate systems, where they may substitute into minerals such as gypsum, anhydrite, celestite, barite, or carbonate phases. Therefore, their occurrence should not be interpreted in the same way as lithium enrichment. The higher Sr values in rock salt and selected evaporitic intervals likely reflect brine evolution, sulfate-carbonate equilibrium, and residual evaporitic fractionation rather than marl-hosted critical-mineral accumulation. Similarly, Ba enrichment may indicate sulfate-related mineral phases or insoluble fine-grained residues rather than direct lithium-style enrichment. This distinction is important because Sr and Ba are better treated as indicators of evaporitic

brine chemistry and sulfate-carbonate partitioning, while Li, B, REEs, U, V, and Zn are more closely linked to fine-grained sedimentary trapping and diagenetic fixation (Warren, 2016; Rollinson, 2014).

Potassium also needs careful interpretation. The highest K value in the dataset occurs in gypsum, but this does not mean that gypsum represents an economic potassium resource. Potassium values in this study are very low compared with potash deposits, feldspar-rich pegmatites, or other K-bearing mineral systems. The reason for examining K in salt, marl, and gypsum is not to prove potash-grade mineralization, but to use K as a geochemical indicator of evaporitic brine evolution. In evaporite systems, potassium may become concentrated during late-stage brine evolution and bittern-stage processes, especially after earlier precipitation of carbonates, sulfates, and halite (Warren, 2016). Therefore, K in this study should be discussed as a supporting indicator of salinity evolution and late-stage brine concentration, not as an economic target.

The interpretation of marl as a relatively enriched host should also be aligned with the objectives of the thesis. The objective of the study is not simply to prove facies control; rather, it is to evaluate the distribution of critical elements, identify geochemical patterns, and recognize intervals that may deserve further exploration. Facies control is therefore an interpretive outcome of the geochemical dataset, not the main objective itself. The results show that lithology strongly influences trace-element distribution, and this helps explain why certain samples, especially Marl-4 to Marl-7, show higher relative enrichment. This interpretation improves the geological understanding of the Salt Range Formation and supports more focused follow-up sampling.

The role of hydrothermal or structurally controlled fluids should be discussed cautiously. Many economically significant lithium-brine systems are associated with prolonged brine evolution, volcanic input, geothermal activity, closed-basin hydrology, and in some cases tectonic or subduction-related fluid pathways (Bradley et al., 2017; Munk et al., 2016). The Salt Range Formation does not currently provide direct evidence for a volcanic-brine or subduction-related lithium system. Therefore, it would be inappropriate to claim that the observed Li enrichment is hydrothermal or comparable to major global lithium-brine deposits. At most, the tectonic setting of the Salt Range may have influenced post-depositional fluid movement, brine redistribution, and local

geochemical heterogeneity. This possibility remains hypothetical until supported by mineralogical evidence, fluid-inclusion data, stable isotopes, or petrographic indicators of hydrothermal alteration.

The proposed enrichment model should therefore be presented as a cautious, three-stage conceptual model. The first stage involved primary evaporitic concentration, during which restricted basin conditions and progressive evaporation produced chemically evolved brines. The second stage involved sediment-brine interaction, during which fine-grained marl horizons retained selected trace elements through adsorption, ion exchange, carbonate association, oxide association, and early diagenetic fixation. The third stage may have involved post-depositional modification, including compaction, recrystallization, thrust-related deformation, and localized fluid redistribution during Himalayan tectonism. This model explains the differential partitioning of Li, B, and REEs into reactive marl horizons, while Sr, Ba, and K remained more closely linked with sulfate-carbonate and late-stage evaporitic brine pathways (Munk et al., 2016; Warren, 2016; Coffey et al., 2021; Dugamin et al., 2023).

From an economic perspective, the present results must be treated conservatively. The maximum Li value of 4.111 ppm is far below the grades generally required for economic lithium deposits. Therefore, terms such as “economic viability,” “resource potential,” “critical mineral fertility,” or “high-prospectivity target” should not be used without qualification. More appropriate terms are “detectable enrichment,” “reconnaissance-level geochemical anomaly,” “relative enrichment,” and “priority interval for follow-up investigation.” The present study identifies geochemical variation and possible enrichment mechanisms, but it does not demonstrate grade continuity, tonnage, mineral recoverability, metallurgical behavior, or reasonable prospects for eventual economic extraction. These criteria are required before any mineral-resource or economic claim can be made (Committee for Mineral Reserves International Reporting Standards [CRIRSCO], 2019).

The AI/ML component of the study should also be interpreted within strict limitations. Because the dataset contains only 23 samples and lacks independent mineralization labels, supervised machine-learning outputs cannot be treated as validated predictions of mineralization. Random Forest scores, K-Means clusters, PCA groupings,

and Isolation Forest anomalies are useful for organizing geochemical patterns and identifying samples for further study, but they do not prove economic prospectivity. In this context, AI/ML should be described as an exploratory decision-support tool rather than a predictive resource-evaluation model. This position is consistent with the general use of data-driven methods in early-stage mineral exploration, where such models are most reliable when combined with geological reasoning and independent validation (Breiman, 2001; Carranza, 2009; Carranza & Laborte, 2015; Sun et al., 2024).

The repeated selection of Marl-7, Marl-5, Marl-6, and Marl-4 by the geochemical and statistical workflow is still useful, but the meaning of this result must be stated carefully. These samples should not be called economic targets. Instead, they represent the most geochemically anomalous and internally consistent samples within the current reconnaissance dataset. Their significance lies in the fact that they combine relatively elevated Li, B, REEs, U, V, and Zn with a marl-rich lithological host. This makes them suitable for follow-up work, including denser sampling, total digestion, XRD, SEM-EDS, thin-section petrography, and host-phase analysis. Only after such validation can the true geological significance of these anomalies be assessed.

In summary, the Salt Range Formation does not demonstrate economic lithium mineralization on the basis of the present data. However, it does show detectable, lithologically controlled, aqua-regia-extractable enrichment of selected critical and strategic elements, particularly within marl-rich intervals. The most defensible conclusion is that the formation contains localized geochemical anomalies that improve understanding of trace-element behavior in evaporitic successions and provide a basis for more detailed follow-up investigation. The study therefore contributes to the geochemical characterization of the Salt Range Formation, but its resource implications remain preliminary and must be evaluated through additional sampling, total digestion, mineralogical characterization, and economic screening.

Conclusions

The Salt Range Formation contains detectable but low-grade enrichment of selected critical and strategic elements. The highest aqua-regia-extractable lithium value recorded in the present dataset is 4.111 ppm in Marl-7, which is far below grades normally associated with economic lithium deposits. Therefore, the formation should not be described as economically viable for lithium on the basis of the present results. Instead, the data indicate reconnaissance-level geochemical enrichment that requires further validation.

The marl samples, particularly Marl-4 to Marl-7, show the strongest relative enrichment in Li, B, REEs, U, V, and Zn. This pattern is interpreted as the result of sediment-brine interaction, adsorption onto clay-rich and oxide-bearing surfaces, carbonate association, and early diagenetic fixation. In contrast, Sr and Ba are more closely linked with sulfate-carbonate and evaporitic brine pathways, while K is best interpreted as an indicator of late-stage brine evolution rather than an economic potassium target.

The AI/ML workflow should be treated as an exploratory decision-support approach. RF scores, PCA patterns, K-Means clusters, and Isolation Forest anomalies help identify internally consistent geochemical patterns, but they do not prove mineralization or economic prospectivity. The highest-ranked samples should therefore be described as priority samples for follow-up geochemical and mineralogical investigation, not as proven exploration targets.

RECOMMENDATIONS

Future work should prioritize detailed follow-up sampling of the Marl Member, particularly the Marl-4 to Marl-7 interval, because this interval contains the strongest relative enrichment in Li and associated trace elements. Sampling should be carried out at closer spacing along strike and across stratigraphic thickness to test lateral continuity, vertical variation, and reproducibility of the geochemical anomalies.

Mineralogical validation is essential before any resource interpretation is attempted. X-ray diffraction, SEM-EDS, thin-section petrography, and electron microprobe analysis should be used to identify the host phases of Li, B, REEs, U, V, Zn, Cu, and related elements. This is necessary to determine whether these elements occur in clay minerals, carbonates, oxides, sulphates, fluid inclusions, insoluble residues, or other mineral phases.

Future studies should include leachability and extraction tests to assess whether the enriched elements are recoverable under realistic processing conditions. Total concentration alone is insufficient for economic assessment, especially where values are low and mineral hosts are unknown. The data-driven workflow should be repeated using a larger and independently validated dataset. Any supervised machine-learning model should only be used if independent mineralization labels are available from mineralogical, geochemical, drilling, or resource-based evidence. Until then, unsupervised methods and Composite Evidence Index ranking should be treated as exploration-guidance tools rather than predictive proof of mineralization. Regional integration with geological mapping, structural analysis, remote sensing, and stratigraphic correlation is also recommended. This would help determine whether the enriched marl interval is locally restricted or regionally continuous within the Salt Range Formation.

Finally, no claim of economic viability should be made until additional data demonstrate sufficient grade, tonnage, continuity, mineral recoverability, and reasonable prospects for eventual economic extraction in accordance with accepted mineral-resource reporting standards.

REFERENCES

Beck, R. A., Burbank, D. W., Sercombe, W. J., Riley, G. W., Barndt, J. K., Berry, J. R., Afzal, J., Khan, A. M., Jurgen, H., Metje, J., Cheema, A., Shafique, N. A., Lawrence, R. D., & Khan, M. A. (1995). Stratigraphic evidence for an early collision between northwest India and Asia. Nature, 373, 55–58.

Becker, J. S. (2007). Inorganic mass spectrometry: Principles and applications. John Wiley & Sons.

Bradley, D. C., McCauley, A. D., & Stillings, L. M. (2017). Mineral-deposit model for lithium-cesium-tantalum pegmatites. U.S. Geological Survey Scientific Investigations Report 2010–5070–O.

Breiman, L. (2001). Random forests. Machine Learning, 45, 5–32.

Carranza, E. J. M. (2009). Geochemical anomaly and mineral prospectivity mapping in GIS. Elsevier.

Coffey, D. M., Munk, L. A., Ibarra, D. E., Butler, K. L., Boutt, D. F., & Hynek, S. A. (2021). Lithium storage and release from lacustrine sediments: Implications for lithium enrichment and sustainability in continental brines. Geochemistry, Geophysics, Geosystems, 22(12), e2021GC009916.

Cracknell, M. J., & Reading, A. M. (2014). Geological mapping using remote sensing data: A comparison of five machine learning algorithms, their response to variations in the spatial distribution of training data and the use of explicit spatial information. Computers & Geosciences, 63, 22–33.

CRIRSCO. (2019). International reporting template for the public reporting of exploration targets, exploration results, mineral resources and mineral reserves. Committee for Mineral Reserves International Reporting Standards.

Dugamin, E. J. M., Cathelineau, M., Boiron, M.-C., Richard, A., & Despinois, F. (2023). Lithium enrichment processes in sedimentary formation waters. Chemical Geology, 635, 121626.

Faisal, S., & Dixon, J. M. (2015). Physical analog (centrifuge) model investigation of contrasting structural styles in the Salt Range and Potwar Plateau, northern Pakistan. Journal of Structural Geology, 77, 277–292.

Gee, E. R., & Gee, D. G. (1989). Overview of the geology and structure of the Salt Range, with observations on related areas of northern Pakistan. In L. L. Malinconico Jr. & R. J. Lillie (Eds.), Tectonics of the western Himalayas (Geological Society of America Special Paper 232, pp. 95–111). Geological Society of America.

Ghani, H., Sobel, E. R., Zeilinger, G., Glodny, J., Zapata, S., & Irum, I. (2021). Palaeozoic and Pliocene tectonic evolution of the Salt Range constrained by low-temperature thermochronology. Terra Nova, 33(3), 293–305.

Hastie, T., Tibshirani, R., & Friedman, J. (2009). The elements of statistical learning: Data mining, inference, and prediction (2nd ed.). Springer.

Hussain, S. A., Feng-Qing, H., Yunqi, M., Khan, H., Jian, Y., Hussain, G., & Widory, D. (2021). An overview of Pakistan rock salt resources and their chemical characterization. Pakistan Journal of Scientific & Industrial Research Series A: Physical Sciences, 64(2), 137–148.

Hussain, S. A., Han, F., Ma, Y., Han, J., Ahmad, N., Bian, Q., & Widory, D. (2021). Unraveling sources and climate conditions prevailing during the deposition of Neoproterozoic evaporites using coupled chemistry and boron isotope compositions (δ11B): The example of the Salt Range, Punjab, Pakistan. Minerals, 11(2), 161.

International Energy Agency. (2024). Global critical minerals outlook 2024. IEA.

Jarvis, I., & Jarvis, K. E. (1992). Plasma spectrometry in the earth sciences: Techniques, applications and future trends. Chemical Geology, 95(1–2), 1–33.

Jaumé, S. C., & Lillie, R. J. (1988). Mechanics of the Salt Range-Potwar Plateau, Pakistan: A fold-and-thrust belt underlain by evaporites. Tectonics, 7(1), 57–71.

Jolliffe, I. T., & Cadima, J. (2016). Principal component analysis: A review and recent developments. Philosophical Transactions of the Royal Society A, 374(2065), 20150202.

Jowitt, S. M., Werner, T. T., Weng, Z., & Mudd, G. M. (2018). Recycling of the rare earth elements. Current Opinion in Green and Sustainable Chemistry, 13, 1–7.

Kazmi, A. H., & Jan, M. Q. (1997). Geology and tectonics of Pakistan. Graphic Publishers.

Kesler, S. E., Gruber, P. W., Medina, P. A., Keoleian, G. A., Everson, M. P., & Wallington, T. J. (2012). Global lithium resources: Relative importance of pegmatite, brine and other deposits. Ore Geology Reviews, 48, 55–69.

Lillie, R. J., Johnson, G. D., Yousuf, M., Zaman, A. S. H., & Yeats, R. S. (1987). Structural development within the Himalayan foreland fold-and-thrust belt of Pakistan. In C. Beaumont & A. J. Tankard (Eds.), Sedimentary basins and basin-forming mechanisms (CSPG Memoir 12, pp. 379–392). Canadian Society of Petroleum Geologists.

Liu, F. T., Ting, K. M., & Zhou, Z. H. (2008). Isolation Forest. Proceedings of the 2008 Eighth IEEE International Conference on Data Mining, 413–422.

MacQueen, J. (1967). Some methods for classification and analysis of multivariate observations. In L. M. Le Cam & J. Neyman (Eds.), Proceedings of the Fifth Berkeley Symposium on Mathematical Statistics and Probability (Vol. 1, pp. 281–297). University of California Press.

Munk, L. A., Hynek, S. A., Bradley, D. C., Boutt, D. F., Labay, K., & Jochens, H. (2016). Lithium brines: A global perspective. In P. L. Verplanck & M. W. Hitzman (Eds.), Rare earth and critical elements in ore deposits (Reviews in Economic Geology, Vol. 18, pp. 339–365). Society of Economic Geologists.

Najman, Y., Appel, E., Boudagher-Fadel, M., Bown, P., Carter, A., Garzanti, E., Godin, L., Han, J., Liebke, U., Oliver, G., Parrish, R., & Vezzoli, G. (2010). Timing of India–

Asia collision: Geological, biostratigraphic, and palaeomagnetic constraints. Journal of Geophysical Research: Solid Earth, 115, B12416.

Pennock, E. S., Lillie, R. J., Zaman, A. S. H., & Yousaf, M. (1989). Structural interpretation of seismic reflection data from eastern Salt Range and Potwar Plateau, Pakistan. AAPG Bulletin, 73(7), 841–857.

Potts, P. J. (1987). A handbook of silicate rock analysis. Blackie.

Qayyum, A., Poessé, J. W., Kaymakci, N., Langereis, C. G., Gülyüz, E., & Ahsan, N. (2022). Neogene kinematics of the Potwar Plateau and the Salt Range, NW Himalayan front: A paleostress inversion and AMS study. International Geology Review, 64(9), 1311–1329.

Reimann, C., & Garrett, R. G. (2005). Geochemical background: Concept and reality. Applied Geochemistry, 20(12), 2319–2340.

Reimann, C., Filzmoser, P., Garrett, R. G., & Dutter, R. (2008). Statistical data analysis explained: Applied environmental statistics with R. Wiley.

Rollinson, H. R. (1993). Using geochemical data: Evaluation, presentation, interpretation. Longman Scientific & Technical.

Rollinson, H. R., & Pease, V. (2021). Using geochemical data: To understand geological processes. Cambridge University Press

Sameeni, S. J. (2009). The Salt Range: Pakistan's unique field museum of geology and paleontology. Carnets de Géologie, Book 2009/03, Chapter 6.

Shah, S. M. I. (2009). Stratigraphy of Pakistan. Geological Survey of Pakistan Memoirs, 22, 1–381.

Shirmard, H., Farahbakhsh, E., Müller, R. D., & Chandra, R. (2022). A review of machine learning in processing remote sensing data for mineral exploration. Remote Sensing of Environment, 268, 112750.

Sun, T., Feng, M., Pu, W., Liu, Y., Chen, F., Zhang, H., Huang, J., Mao, L., & Wang, Z. (2024). Fractal-based multi-criteria feature selection to enhance predictive capability of AI-driven mineral prospectivity mapping. Fractal and Fractional, 8(4), 224.

Thomas, R. (2013). Practical guide to ICP-MS: A tutorial for beginners (3rd ed.). CRC Press.

Totland, M., Jarvis, I., & Jarvis, K. E. (1992). An assessment of dissolution techniques for the analysis of geological samples by plasma spectrometry. Chemical Geology, 95(1–2), 35–62.

U.S. Geological Survey. (2022). Mineral commodity summaries 2022. U.S. Geological Survey.

Vine, J. D., & Dooley, J. R. (1980). Lithium in sediments and brines: How, why, and where to search. U.S. Geological Survey Open-File Report 80–1234.

Warren, J. K. (2016). Evaporites: A geological compendium. Springer.

World Bank. (2020). Minerals for climate action: The mineral intensity of the clean energy transition. World Bank.

Yin, A. (2006). Cenozoic tectonic evolution of the Himalayan orogen as constrained by along-strike variation of structural geometry, exhumation history, and foreland sedimentation. Earth-Science Reviews, 76(1–2), 1–131.

Yousefi, M., Carranza, E. J. M., Kreuzer, O. P., Nykänen, V., Hronsky, J. M. A., & Mihalasky, M. J. (2021). Data analysis methods for prospectivity modelling as applied to mineral exploration targeting: State-of-the-art and outlook. Journal of Geochemical Exploration, 229, 106839.

Yu, X., Liu, C., Wang, C., Wang, J., Li, Q., & Meng, L. (2022). Origin of Li brine-type deposits in the Cretaceous gypsum-bearing formation of the Jitai Basin, South China: Constraints from geochemistry and H, O, Li, B, and Sr isotopes. Applied Geochemistry, 144, 105257.

Yu, X., Wang, C., Huang, H., & Yan, K. (2024). Factors controlling lithium accumulation in brines from Upper Cretaceous to Lower Eocene aquifers of a continental evaporite basin. Applied Geochemistry, 165, 105967.

Zuo, R., & Carranza, E. J. M. (2011). Support vector machine: A tool for mapping mineral prospectivity. Computers & Geosciences, 37(12), 1967–1975.

Naqi MS Thesis

by mumtaz khan

Submission date: 22-Apr-2026 06:59AM (UTC+0500)
Submission ID: 2850161997
File name: Thesis_File_Ali_Naqi_for_Plagirism.docx (2.29M)
Word count: 23271
Character count: 134060

Naqi MS Thesis

ORIGINALITY REPORT

2%	1%	2%	1%
SIMILARITY INDEX	INTERNET SOURCES	PUBLICATIONS	STUDENT PAPERS

PRIMARY SOURCES

1	Submitted to Higher Education Commission Pakistan Student Paper	<1%
2	dokumen.pub Internet Source	<1%
3	www.mdpi.com Internet Source	<1%
4	SHAHID GHAZI, NIGEL P MOUNTNEY, AFTAB AHMAD BUTT, SADAF SHARIF. "Stratigraphic and palaeoenvironmental framework of the Early Permian sequence in the Salt Range, Pakistan", Journal of Earth System Science, 2012 Publication	<1%
5	Ishtiaq A. K. Jadoon, Matthias Hinderer, Beenish Wazir, Rizwan Yousaf et al. "Structural styles, hydrocarbon prospects, and potential in the Salt Range and Potwar Plateau, north Pakistan", Arabian Journal of Geosciences, 2014 Publication	<1%
6	www.scribd.com Internet Source	<1%
7	Tariq Mahmood, Naveed Ahsan, Muhammad Armaghan Faisal Miraj. "Depositional cyclicity of lower Cambrian strata in the NW Himalayas: Regional sequence stratigraphy of	<1%

	the Indian passive margin", Marine and Petroleum Geology, 2024 Publication	
8	www.ijert.org Internet Source	<1%
9	Vipin Kumar Sharma, Mohamed Arezki Mellal. "Rare Earth Elements - Essential Materials for Energy and Sustainable Development", CRC Press, 2026 Publication	<1%
10	worldwidescience.org Internet Source	<1%
11	Dhirendra Kumar Shukla, Shabir Ali, Sandhya Sharma. "Artificial Intelligence and Sustainable Innovation - Volume 2", CRC Press, 2026 Publication	<1%
12	Submitted to De Montfort University Student Paper	<1%
13	Submitted to University of Teesside Student Paper	<1%
14	Jiao, Shi. "Characterization of Mass Dependent Matrix Effects in Inductively Coupled Plasma Mass Spectrometry (ICP-MS) and Characterization of Engineered Nanoparticles Using Surfactant Enhanced Capillary Electrophoresis-ICP-MS", The Ohio State University, 2021 Publication	<1%
15	Shahid Ghazi, Shakeel Ahmad, Muhammad Riaz, Tehseen Zafar. "Sedimentology and Palaeoenvironmental Reconstruction of the Early Cambrian Kussak Formation, Salt Range, Pakistan", Current Science, 2020	<1%

Publication

16	www.datainsightsmarket.com Internet Source	<1%
17	1800nt.com Internet Source	<1%
18	Sirui Wang, Weiqing Sun. "Capacity Price Pricing Method Considering Time-of-Use Load Characteristics", Energies, 2026 Publication	<1%
19	epub.ub.uni-muenchen.de Internet Source	<1%
20	www.thermofisher.com Internet Source	<1%
21	M.F. Albakry, I. Alkhatib, D. Alonso-González, J. Anczarski et al. "Multi-channel, multi-template event reconstruction for SuperCDMS data using machine learning", Nuclear Instruments and Methods in Physics Research Section A: Accelerators, Spectrometers, Detectors and Associated Equipment, 2026 Publication	<1%
22	Faisal, Shah, and John M. Dixon. "Physical analog (centrifuge) model investigation of contrasting structural styles in the Salt Range and Potwar Plateau, northern Pakistan", Journal of Structural Geology, 2015. Publication	<1%
23	Junjie Yan, Fangguo Zhai, Yanzhen Gu, Xingchuan Liu, Peiliang Li, Zizhou Liu, Yucheng Wang. "Drastic Fluctuation in Water Exchange Between the Yellow Sea and Bohai Sea Caused by Typhoon Lekima in August 2019: A Numerical Study", Journal of Geophysical Research: Oceans, 2023	<1%